Dissertation
submitted to the
Combined Faculties of the Natural Sciences and Mathematics
of the Ruperto-Carola-University of Heidelberg. Germany
for the degree of
Doctor of Natural Sciences

put forward by

Dipl.-Phys. Norman Neitz

born in Zeitz, Germany

Oral examination: July 24th, 2014

Radiation-Reaction Effects in the Quantum Regime

Referees: PD Dr. Antonino Di Piazza
Prof. Dr. Joerg Jaeckel

Zusammenfassung
In dieser Arbeit wird der Einfluss von Strahlungsdämpfungseffekten auf die Wechselwirkung eines Elektronenbündels mit einem starken Laserfeld untersucht, unter Einbeziehung nichtlinearer sowie quantenmechanischer Effekte. Dieses Vorhaben ist durch zweierlei technologische Entwicklungen begründet: Zum einen durch die erhebliche Zunahme experimentell verfügbarer Laserintensitäten sowie zum anderen durch die bedeutenden Fortschritte in der Elektronenbeschleunigung. In einem Parameterbereich, in dem Strahlungsdämpfung durch die inkohärente Emission mehrerer Photonen verursacht wird, wird ein kinetischer Ansatz entwickelt, um die Dynamik von Elektronen sowie Photonen mittels Verteilungsfunktionen zu beschreiben. Während klassische Elektrodynamik, ausgehend von der Landau-Lifshitz Gleichung, eine Abnahme der Breite der Energieverteilung des Elektronenbündels vorhersagt, zeigt die Analyse in dieser Arbeit den gegenteiligen Effekt, sobald Quanteneffekte bedeutsam werden. Wie gezeigt wird, wird die Verbreiterung der Elektronenenergieverteilung durch die intrinsich stochastische Natur der Photonemission verursacht. Um den Unterschied zwischen klassischer und quantentheoretischer Strahlungsdämpfung quantitativ zu erklären, wird gezeigt, dass die Energieverteilung des Elektronenbündels nach der Streuung bei gegebener Laserfluenz von der Form des Laserpulses und seiner Dauer abhängt. Im Gegensatz dazu zeigt die klassische Analyse keine derartige Abhängigkeit. Schließlich wird der kinetische Ansatz verallgemeinert, um die Erzeugung von Elektron-Positron-Paaren durch Photonen, welche während der Wechselwirkung emittiert wurden, miteinzubeziehen. Dies erlaubt eine abschließende Untersuchung der nichtlinearen, gekoppelten Dynamik aller an der Wechselwirkung beteiligten Teilchen, d.h. anfänglich vorhandener Elektronen, emittierter Photonen sowie während der Wechselwirkung erzeugter Elektron-Positron-Paare.

Abstract
In this work the influence of radiation reaction on the interaction of an electron bunch with a strong laser field is studied including nonlinear and quantum effects. This venture is motivated by two technological developments: On the one hand, the tremendous increase in available laser intensities and, on the other hand, the significant advancements in electron acceleration technology. Considering a regime where radiation reaction effects are caused by the incoherent emission of several photons, a kinetic approach is developed to describe the dynamics of electrons and photons via distribution functions. Whereas classical electrodynamics, employing the Landau-Lifshitz equation, predicts a narrowing of the energy distribution of the electron beam, the analysis in this work reveals the opposite effect in case that quantum effects become significant. The spreading of the electrons' energy distribution is shown to be caused by the intrinsic stochastic nature of photon emission. In order to explain quantitatively the discrepancy between classical and quantum radiation reaction, the final electron distribution as computed in our quantum treatment is demonstrated to depend on the laser's envelope shape and its duration at a given total laser fluence. On the contrary, the classical analysis does not exhibit such a dependency. Finally, the kinetic approach is extended to allow for the inclusion of pair creation by photons emitted during the scattering. This facilitates a conclusive investigation of the nonlinear coupled dynamics of all particles involved in the interaction, i.e., electrons in the initial bunch, photons and electron-positron pairs produced during the scattering.

In connection with the work on this thesis, the following articles were published in refereed journals:

- N. Neitz and A. Di Piazza,
  Stochasticity Effects in Quantum Radiation Reaction,
  Physical Review Letters **111**, 054802 (2013).
- F. Mackenroth, N. Neitz, and A. Di Piazza,
  Novel aspects of radiation reaction in the ultrarelativistic quantum regime,
  Plasma Physics and Controlled Fusion **55**, 124018 (2013).
- N. Neitz, N. Kumar, F. Mackenroth, K. Z. Hatsagortsyan, C. H. Keitel, and A. Di Piazza,
  Novel aspects of radiation reaction in the classical and the quantum regime ,
  Journal of Physics: Conference Series **497**, 012015 (2014).

In connection with the work on this thesis, the following preprint was submitted:

- N. Neitz, and A. Di Piazza,
  Electron-beam dynamics in a strong laser field including quantum radiation reaction,
  submitted 2014, arXiv:1403.2450.

Contents

1 Introduction **11**
1.1 Notations and units 15

2 Theoretical background **17**
2.1 Radiation reaction in classical and quantum electrodynamics 18
2.1.1 Classical electrodynamics 18
2.1.2 Quantum electrodynamics 20
2.2 Kinetic theory 25

3 Kinetic approach (1): Photon emission **29**
3.1 Derivation and properties of the kinetic equations for photon emission 29
3.2 Comparison of the classical and the nonlinear moderately quantum regime 36
3.2.1 Classical dynamics 37
3.2.2 Replacement of the classical intensity $\boldsymbol{I_{cl}}$ by the quantum intensity $\boldsymbol{I_q}$ 39
3.2.3 Stochastic nature of photon emission 40
3.3 Pulse-shape effects 43
3.3.1 Influence of the laser pulse shape 43
3.3.2 Influence of the laser pulse duration 45

4 Kinetic approach (2): Pair production **49**
4.1 Derivation of the kinetic equations including pair creation 49
4.2 The coupled dynamics of photon emission and pair production 51
4.3 Dependence on the laser pulse shape and the initial electron energy . 54

5 Numerical treatment of the kinetic equations **59**

6 Summary and outlook **65**

Appendices

A Modified Bessel functions **71**

B Calculation of the expansion of eq. (3.17) **73**

C Connection between the Fokker-Planck and the Langevin equation **77**
C.1 From the Langevin to the Fokker-Planck equation 77

C.2 Interpretation of $\boldsymbol{A}(\boldsymbol{\varphi}, \boldsymbol{p}_-)$ and $\boldsymbol{B}(\boldsymbol{\varphi}, \boldsymbol{p}_-)$ 79

D Approximated solution of eq. (3.27) **81**

E Microscopic approach **85**

Bibliography **87**

1 Introduction

In a recent experiment the mass of the electron was measured with an unprecedented relative precision [Stur 14]. Not only does this measurement constitute a remarkable experimental result but it is also in perfect agreement with the theoretical predictions made by quantum electrodynamics (QED). In general, the formidable predictive power of this latter theory has been tested in numerous experimental studies: Prime examples of such investigations include the determination of the electron's g-factor both in a free state [Hann] and bound states of hydrogen-like atoms [Haff 00, Verd 04, Stur 11]. The extraordinarily good agreement of experimentally determined quantities and the corresponding theoretical calculations led to the conclusion that QED is the "best tested" existing physical theory.

This assertion is noteworthy inasmuch as the fully developed theory of QED has only been available for some 60 years [Nobe 65]. The theory of classical electrodynamics, on the other hand, was developed already in the 1860s. Thus, it was subjected to far more experimental tests all confirming its validity in a parameter regime where quantum effects are negligible. However, even this uncountably often tested theory exhibits an unresolved issue even in its realm of applicability. The problem is encountered in the calculation of an electron's (in fact any charged particle's) trajectory in the presence of an external electromagnetic field, taking into account the energy-momentum loss of the particle due to the emission of electromagnetic radiation [Land 75, Spoh 04, Rohr 07] (see sec. 2.1.1). The effect of this energy-momentum loss on the electron's trajectory is commonly referred to as radiation reaction (RR). Conventionally a particle's trajectory is calculated by means of the Lorentz force equation and its emission employing Maxwell's equations. By solving the coupled system of these latter equations, the so-called Lorentz-Abraham-Dirac (LAD) equation can be obtained containing terms apart from the Lorentz-force, which describe RR [Rohr 07]. This equation, however, features several physical problems (see sec. 2.1.1). However, it has been pointed out [Land 75] that in the classical domain, where quantum effects such as recoil in photon emission are negligible, the LAD equation can be approximated in a theoretical consistent fashion. This approximated equation is known as the Landau-Lifshitz (LL) equation and it does not exhibit the shortcomings of the former [Spoh 00, Rohr 02, Di P 12]. In addition, alternative equations have been proposed as a description of RR [Hamm 10], which are not pursued in this work. In any case, in external fields strong enough to cause an electron to emit an average energy comparable to its initial one within only one laser period, the electron dynamics is clearly dominated by RR effects [Koga 05, Di P 08].

Nevertheless, nowadays an experimental realization of the accordingly required very strong fields is rather complicated, which explains the lack of an experimental test of the LL equation. However, employing an analytical solution of the LL equation in an arbitrary plane-wave field [Di P 08], it was shown that RR effects should be detectable also at lower field strengths [Di P 09]. Moreover, various recent theoretical studies pointed out possible detection schemes of signatures of RR in the classical regime [Harv 11, Thom 12, Hein 13, Tamb 14, Gree 14].

It is commonly believed that in order to meaningfully judge upon the validity of either description of RR in the classical domain it is necessary to go to the underlying theoretical framework of QED which includes classical electrodynamics as a limiting case as soon as quantum effects are negligible. However, recalling the previously mentioned lack of an agreement on the proper classical description of RR, it is not surprising that there is much less consensus on an according quantum description of RR. One may approach an according theoretical framework, however, following a simple consideration: In classical electrodynamics the description of RR requires the solution of the fully self-coupled dynamics of an external-field-driven electron, clearly going beyond the Lorentz force formalism. An according quantum description would consequently call for the inclusion of all processes that may occur from an initial electron accelerated in an external electromagnetic field [Di P 10, Di P 12, Ilde 13b, Ilde 13a] (see sec. 2.1.2). Thus, obviously a full quantum picture of RR would require the incorporation of effects such as multiple photon emission and radiative corrections. In the case of sufficiently strong electromagnetic fields, however, even further effects such as the process of pair production have to be taken into account. The produced electrons and positrons, in turn, are accelerated by the background field and will emit further photons and, for certain conditions, even facilitate the formation of the so-called QED cascades [Bell 08, Fedo 10, Elki 11, Soko 10, Neru 11]. Hence it is obvious that solving the intrinsically multiparticle problem of quantum RR is a formidable theoretical task. Moreover, already in a parameter regime where pair production is still negligible, the quantum and RR effects dominate the electron dynamics if the recoil of the emitted becomes substantial. Beyond the just outlined theoretical interest in developing a concise understanding of RR, there also exists a technologically motivated need for a reliable framework of describing RR. Since the onset of RR effects signifies the regime in which a charged particle's dynamics is substantially altered, due to its inevitable emission of electromagnetic radiation, understanding it most profoundly is also vitally essential for experimental applications as, e.g., accelerator and plasma physics. This urge even translates to the construction of novel experimental devices, e.g., quantum x-free electron lasers [Boni 84, Boni 85]. In particular, there is a strong demand of further theoretical studies of RR effects in the interaction of electrons with ultra-intense laser pulses, as the latter are generic sources of ultra-high electromagnetic fields in laboratories around the world nowadays.

In addition to RR, however, in the interaction of electrons with strong laser pulses there occurs another class of novel effects, namely nonlinear dynamics. Since the groundbreaking invention of the laser [Maim 60], lasers have become powerful experimental tools for the investigations of various physical phenomena. Already shortly after the first realization of the laser, sufficiently high intensities to cause nonlinear optical effects could be produced. These nonlinear effects include, e.g., second-harmonic generation first demonstrated in [Fran 61]. A significant breakthrough in the generation of intense laser pulses has been achieved by the so-called chirped

pulse amplification technique [Stri 85]. This facilitated the production of pulses with intensities beyond 10^{14}-$10^{15}\,\mathrm{W/cm^2}$ at which the dynamics of an electron in an atom or molecule is substantially modified, since the corresponding electron field strengths become comparable to the Coulomb field in atoms. Such high intensities trigger high-order harmonic generation (HHG) resulting in the creation of extreme-ultraviolet and soft x-ray radiation [Prot 97, Agos 04]. Considering even higher optical laser intensities of the order $10^{18}\,\mathrm{W/cm^2}$, an electron in a laser field is accelerated to relativistic velocities within only one laser wavelength. Thus, this regime is known as the relativistic regime. In order to quantify the interaction with such relativistic intense fields, it is convenient to introduce the so-called classical nonlinearity parameter [Brow 64]

$$\xi = \frac{|e|E_0}{\omega_0 mc}, \tag{1.1}$$

with the peak electric field strength E_0, the speed of light c, and the central angular frequency ω_0. The charge and the mass of an electron are indicated by $e < 0$ and m, respectively. The absence of Planck's constant $\hbar$ in this Lorentz-invariant parameter demonstrates its purely classical nature. It can be interpreted as the work in units of the electron mass performed on the electron by the laser field in one laser period. Since consequently beyond the threshold $\xi = 1$ the electron is accelerated to relativistic velocities within one laser cycle, its dynamics in this regime depends nonlinearly on the laser field amplitude. This nonlinearity induces various new effects as, e.g., a longitudinal electron drift and the appearance of higher harmonics in the emission spectrum. Furthermore, also in the relativistic regime a novel technique labeled laser wakefield acceleration was developed [Muls 10]. Such acceleration mechanisms can be exploited in so-called plasma-based laser-electron accelerators [Esar 09, Malk 12] and allow already for the production of electron beams with an energy in the GeV range [Wang 13].

So far, the highest laser peak intensity realized in a laboratory is roughly $2 \times 10^{22}\,\mathrm{W/cm^2}$ [Yano 08]. In general, the question arises which is the highest laser intensity that can be generated. As theoretical investigations have shown a laser field reaching the value of the critical field of QED

$$F_{\mathrm{cr}} = \frac{m^2c^3}{|e|\hbar} \approx 1.3 \times 10^{16}\frac{\mathrm{V}}{\mathrm{cm}} \tag{1.2}$$

would result in the creation of electron-positron pairs directly from the vacuum [Saut 31a, Saut 31b, Heis 36, Schw 51]. Hence, a laser field with the corresponding critical intensity of $I_{\mathrm{cr}} = cF_{\mathrm{cr}}^2/4\pi \approx 4.6 \times 10^{29}\,\mathrm{W/cm^2}$ would be rapidly depleted by the production of pairs. However, it was pointed out [Fedo 10] that the attainable laser intensities might be drastically reduced due to the formation of QED cascades even if only one electron-positron pair is created. The production of such an "initial" electron-positron pair can originate from the presence of a photon in the laser field, which itself may have been emitted by an accelerated electron originally stemming from residual gas in the interaction region. In the case of an electron or a photon propagating in a laser pulse, it is useful to introduce two additional Lorentz-invariant expressions. Considering the motion of an electron with four-momentum p_μ in a laser field with wave vector k_0^μ, the so-called nonlinear quantum parameter is given by [Ritu 85]

$$\chi = \frac{|e|\hbar\sqrt{|(F^{\mu\nu}(\varphi)p_\nu)^2|}}{m^3c^3} = \frac{(k_0^\mu p_\mu)}{\omega_0 mc}\frac{E(\varphi)}{F_{\mathrm{cr}}}, \tag{1.3}$$

where $F^{\mu\nu}(\varphi)$ is the electromagnetic field strength tensor depending on the laser phase $\varphi = k_0^\mu x_\mu$ and $E(\varphi)$ the corresponding phase-dependent electric field. This quantity can be interpreted as the electric field amplitude in units of the critical field experienced by the electron in its initial rest frame and it measures the importance of quantum effects, e.g., the photon recoil in multiphoton Compton scattering. Analogously, for a photon with wave vector k_μ propagating through the laser field the parameter

$$\varkappa = \frac{|e|\hbar\sqrt{|(F^{\mu\nu}(\varphi)k_\nu)^2|}}{m^3c^3} = \frac{(k_0^\mu k_\mu)}{\omega_0 mc}\frac{E(\varphi)}{F_{\mathrm{cr}}} \tag{1.4}$$

can be constructed in complete accordance to the parameter χ. In case that the single photon upon the collision with the laser field creates a pair, $\varkappa$ can be interpreted as the electric field amplitude in units of the critical field in the center-of-mass system of the produced electron and positron [Ritu 85]. It was shown that the increase of the laser intensity not only results in the occurrence of nonlinear effects but also quantum effects become substantial if the parameters χ and $\varkappa$ reach the order of unity [Ritu 85].

Following these technical progresses, the main goal of this thesis is to further elucidate the characteristics of RR effects in the nonlinear quantum regime. To this end, the impact of RR on the dynamics of an ultrarelativistic electron beam colliding with an intense laser pulse will be investigated.

The remainder of this thesis is organized in the following way: In chapter 2 the theoretical background of radiation reaction is presented. To this end, the classical interaction of a charged particle with an external field is recapitulated, with a special emphasis on the possible classical description of radiation reaction via the Landau-Lifshitz equation. This discussion is then transferred to the framework of QED. Employing the solutions of the Dirac equation in the presence of a plane-wave field, the photon emission probability is examined and the notion of the nonlinear moderately quantum regime is introduced, in which radiation reaction effects mainly stem from multiple incoherent photon emission and pair creation is negligible. Subsequently, the process of pair production is studied in order to allow for investigations beyond the nonlinear moderately quantum regime. Finally, some of the key aspects of the kinetic theory are recapitulated and the necessary assumptions for the employment of a kinetic approach are discussed.

Chapter 3 is then dedicated to the development and thorough examination of a kinetic approach describing the collision of an intense laser pulse with an ultrarelativistic electron beam. Restricting to the nonlinear moderately quantum regime, the general three-dimensional kinetic approach, based on the Vlasov equation, is simplified to one dimension, where the evolution of electrons and photons is investigated in terms of distribution functions. Within this regime, however, RR is shown to have an unconventional effect on the evolution of the electron distribution function. Specifically, in case of non-negligible quantum effects RR leads to a spreading of the energy distribution of the electrons, whereas classical electrodynamics employing the LL equation predicts a narrowing. In order to explain this, the classical limit of the kinetic equations is derived via an expansion in the quantum nonlinearity parameter χ. After proving the numerical validity of our approach in the limit $\chi \to 0$, we discuss the effects of the leading order quantum corrections. These quantum corrections modify the structure of the kinetic equation in such a way that the corresponding single-particle equation is a stochastic differential equation. Considering an approximate solution of the kinetic equations, the leading-order quantum

corrections are shown to induce a broadening of the electron distribution function. Thus, the stochasticity of photon emission can clearly be identified as the source of the broadening feature of RR in the quantum case. To further clarify the different properties of RR in the classical and the nonlinear moderately quantum regime, we investigate the influence of the laser pulse shape and duration on the dynamics of electrons and photons. Whereas the LL equation indicates no dependency on the pulse shape and duration at a given total laser fluence, the numerical simulations of RR exhibit a dependency in both cases.

In chapter 4, we drop the condition that pair creation is excluded and amend the kinetic approach by the dominating pair production process. The resulting set of equations is then solved numerically and the coupled dynamics of the distribution functions is investigated. To this end, the evolution of the fully coupled system is compared to those cases, where either pair production is neglected or the radiation of the created positrons is artificially excluded. Furthermore, the dependency on the laser pulse duration at a given fluence of the laser field is studied for different initial electron beam energies. Finally, we give estimates on the necessary laser intensities for an experimental observation of pair production by considering electron bunches with energies achievable nowadays.

In chapter 5, the numerical evaluation of the kinetic equations is discussed. With emphasis on rewriting the kinetic equations into a form convenient for a numerical treatment, we explain the applied numerical methods and the employed approximations.

In the final chapter 6, the findings of this thesis are summarized and an outlook is given.

The details of the expansion of the kinetic equation in χ are given in app. B. In app. C it is shown how a stochastic differential equation can be related to this expanded kinetic equation. An approximate solution to the latter is derived in app. D. In addition, app. E shows the numerical equivalence of our approach with the microscopic approach employed in [Di P 10].

1.1 Notations and units

Throughout the remainder of the work, we will make use of natural units defined by the conditions

$$\hbar = c = 1, \tag{1.5}$$

with $\hbar$ indicating Planck's constant and c the speed of light. We further assume the charge of an elementary particle to include its sign, i.e., for an electron $e = -|e|$, and employ the Gaussian unit convention

$$4\pi\varepsilon_0 = 1, \tag{1.6}$$

where ε_0 indicates the vacuum permittivity[I], leading to the connection of the fine structure constant α with the unit charge

$$e^2 = \alpha \approx \frac{1}{137}. \tag{1.7}$$

[I] Note that in the remaining part of the thesis ε_0 always indicates the initial energy.

Finally, the following table displays a summary of the notations employed in this work.

Notations	
$a^\mu = (a_0, \mathbf{a})$	four-vector with the spatial components $\mathbf{a}$
x^μ, p^μ	space-time coordinates and momentum four-vector
$v^\mu = p^\mu/m$	four-velocity
k_0^μ, ϵ_0^μ	four-wave vector and polarization four vector of the laser
$\mathbf{a}_\perp$	spatial components of four-vector a perpendicular to the spatial laser wave vector $\boldsymbol{k}_0$
$a_\parallel$	spatial component of four-vector a parallel to the spatial laser wave vector $\boldsymbol{k}_0$
$\phi, T, \mathbf{x}_\perp$	light-cone coordinates for the space-time vector x
$p_-, p_+, \mathbf{p}_\perp$	light-cone coordinates for the four-momentum p
$f(\mathbf{x})$	function depending on the spatial coordinates
x^*	typical value of the quantity x
σ	standard deviation of a distribution function
$\partial_x f(x)$	partial derivative with respect to x
$\mathrm{d}f(x)/\mathrm{d}x$	total derivative with respect to x
$\partial_\mu = (\partial_t, \nabla)$	four-derivative
$\mathrm{d}^4 a$	volume element of the four components of a four-vector a
$\mathrm{d}\mathbf{a}$	volume element of the 3 spatial components of a four-vector a
γ^μ	vector of Dirac matrices
$a_\mu b^\mu$	four-product employing the Einstein sum convention
$\not{a} = \gamma_\mu a^\mu$	Feynman slash notation

2 Theoretical background

In order to describe the effects of radiation reaction, it is necessary to define the term in the classical as well as in the quantum framework. Therefore, the interaction of a charged particle with an external electromagnetic field is discussed in the first section of this chapter, with special emphasis on the radiation emitted by the accelerated particle. This, however, leads immediately to the problem that the loss of energy and momentum is not taken into account in the calculation of the charged particle's trajectory by the common treatment employing the Lorentz equation. This issue is known as radiation reaction. Thus, a self-consistent solution of the Maxwell equations and the Lorentz equation is introduced, which, however, exhibits several unphysical drawbacks. Finally, an approximated equation, the so-called Landau-Lifshitz equation, is presented avoiding these shortcomings. In addition, the analytical solution in case of a plane-wave background field is given for this equation.

In the second part of the first section, the previous analysis is reapplied in the framework of quantum electrodynamics. To this end, the wave functions are introduced describing a charged particle in the presence of an external plane-wave field. Focusing on the case of strong external fields, the properties of the probability of photon emission are discussed. In analogy to the classical case, radiation reaction is identified with the dynamical processes beyond Lorentz dynamics. In this context, the notion of the so-called nonlinear moderately quantum regime is introduced. After that, the first section is concluded by a brief discussion of the pair-creation process.

The second section is devoted to a brief overview of the kinetic theory, in which an ensemble of particles is described statistically by employing a distribution function. Thus, the fundamental Vlasov equation is introduced describing the evolution of a charged particle distribution in the presence of an electromagnetic field. This equation is then amended by the inclusion of collision terms and transformed into a general transport equation. Finally, the kinetic approach as a semi-classical method is demonstrated to be an adequate description of the collision of an ultrarelativistic electron beam and a strong plane-wave laser field.

This chapter mainly contains a summary of discussions made in standard textbooks such as [Jack 75, Land 75, Bere 82, Pita 81].

2.1 Radiation reaction in classical and quantum electrodynamics

2.1.1 Classical electrodynamics

In the framework of classical electrodynamics, the motion of a charged particle, an electron for definiteness (with electric charge $e < 0$ and mass m), is described by the Lorentz force equation [Land 75]

$$m\frac{\mathrm{d}v^\mu}{\mathrm{d}s} = eF^{\mu\nu}v_\nu, \tag{2.1}$$

where $v^\mu = (v_0, \boldsymbol{v}) = \mathrm{d}x^\mu/\mathrm{d}s$ indicates the four-velocity of the electron and s is its proper time. An arbitrary electromagnetic field can be expressed by the four-potential $A^\mu(x) = (\Phi(x), \boldsymbol{A}(x))$, with the scalar potential $\Phi(x)$ and the vector potential $\boldsymbol{A}(x)$, which constitutes the antisymmetric field strength tensor $F^{\mu\nu}(x) = \partial^\mu A^\nu(x) - \partial^\nu A^\mu(x)$ employed in eq. (2.1). In turn, in the presence of a four-current $j^\mu = (\rho, \boldsymbol{j})$, with the charge density ρ and the spatial charge current $\boldsymbol{j}$, the field strength tensor is defined by the Maxwell equations [Land 75]

$$\partial_\mu F^{\mu\nu}(x) = 4\pi j^\nu(x). \tag{2.2}$$

From the definition of the field strength tensor, however, it is apparent that there is no unique choice of the four-potential $A^\mu(x)$ and the application of a gauge transformation does not alter the corresponding expression of the field strength tensor. Thus, the four-potential itself cannot be a measurable quantity and the actual physical quantities uniquely defined by eq. (2.2) are the electric and the magnetic field $\boldsymbol{E}(x)$ and $\boldsymbol{B}(x)$, respectively. These fields can be obtained from the four-potential via the formulas

$$\boldsymbol{E}(x) = -\nabla\Phi(x) - \frac{\partial \boldsymbol{A}(x)}{\partial t} \tag{2.3}$$

$$\boldsymbol{B}(x) = \nabla \times \boldsymbol{A}(x). \tag{2.4}$$

In the case of a vanishing four-current $j^\mu \equiv 0$ and by choosing the Lorenz gauge condition $\partial_\mu A^\mu(x) = \partial_t \Phi(x) + \nabla \boldsymbol{A}(x) = 0$, eq. (2.2) is reduced to the wave equation

$$\Box A^\mu(x) = 0, \tag{2.5}$$

where we introduced the D'Alembert operator $\Box = \partial_\mu \partial^\mu = \partial_t^2 - \nabla^2$. Eq. (2.5) determines the propagation of an electromagnetic wave in free space. Early on it was discovered that functions depending on the space-time coordinates only via the phase $\varphi = k_0^\mu x_\mu$ are solutions to eq. (2.5). These are the so-called plane-wave solutions. The corresponding wave vector is then given by $k_0^\mu = (\omega_0, \boldsymbol{k}_0)$, where $\omega_0 = |\boldsymbol{k}_0|$ indicates the central angular frequency and $\boldsymbol{k}_0$ is the spatial wave vector. Since we will focus on the case of a linearly polarized plane-wave, the four-potential can be written as $A^\mu = A_0 \epsilon^\mu \mathfrak{f}(\varphi)$, with the constant amplitude A_0, the plane-wave's polarization four-vector ϵ^μ, and the shape function $\mathfrak{f}(\varphi)$ determining the temporal variation of the potential. Considering the reference frame of a vanishing scalar potential $\Phi(x) \equiv 0$, the four- potential has the form $A^\mu(\varphi) = (0, \boldsymbol{A}(\varphi))$, corresponding to a purely spatial polarization vector $\epsilon^\mu = (0, \boldsymbol{\epsilon})$ fulfilling $\boldsymbol{k}_0 \cdot \boldsymbol{\epsilon} = 0$. In order to describe the sojourn of an electron in a plane-wave field, it is convenient to introduce for an arbitrary four-vector $a^\mu = (a_0, \boldsymbol{a})$ the expressions $a_\parallel = \boldsymbol{k}_0 \cdot \boldsymbol{a}/\omega_0$, $\boldsymbol{a}_\perp = \boldsymbol{a} - \boldsymbol{k}_0 a_\parallel/\omega_0$,

and $a_- = a_0 - a_\parallel$. Since the plane-wave only depends on the phase, $\boldsymbol{x}_\perp$ and $t + x_\parallel$ are cyclic coordinates in the corresponding Lagrange formulation of the problem. Thus the conjugated momenta $\boldsymbol{p}_\perp(\varphi) + e\boldsymbol{A}(\varphi)$ and $p_-(\varphi)$ have to be conserved, where we introduced the electron momentum $p^\mu = (\varepsilon, \boldsymbol{p}) = mv^\mu$. Employing the initial condition $p^\mu(\varphi_0) = (\varepsilon_0, \boldsymbol{p}_0)$ for an initial phase φ_0, the evolution of the electron's four-momentum is determined by [Land 75]

$$\varepsilon(\varphi) = \varepsilon_0 - e\,\frac{\boldsymbol{p}_{0,\perp}\cdot[\boldsymbol{A}(\varphi)-\boldsymbol{A}(\varphi_0)]}{p_{0,-}} + \frac{e^2}{2}\frac{[\boldsymbol{A}(\varphi)-\boldsymbol{A}(\varphi_0)]^2}{p_{0,-}}, \tag{2.6}$$

$$\boldsymbol{p}_\perp(\varphi) = \boldsymbol{p}_{0,\perp} - e\,[\boldsymbol{A}(\varphi)-\boldsymbol{A}(\varphi_0)]\,, \tag{2.7}$$

$$p_\parallel(\varphi) = p_{0,\parallel} - e\,\frac{\boldsymbol{p}_{0,\perp}\cdot[\boldsymbol{A}(\varphi)-\boldsymbol{A}(\varphi_0)]}{p_{0,-}} + \frac{e^2}{2}\frac{[\boldsymbol{A}(\varphi)-\boldsymbol{A}(\varphi_0)]^2}{p_{0,-}}. \tag{2.8}$$

However, these formulas do not take into account that an accelerated electron emits radiation, which in turn modifies the electron's trajectory due to the loss of energy and momentum. This backreaction of the self-generated electromagnetic field on the electron dynamics is known as radiation reaction (RR). The motion of a point charge constitutes a charge current and its emission can be calculated by employing the Liénard-Wiechert potentials [Jack 75,Land 75]. Analyzing the angular distribution of the emitted radiation in the case of an ultrarelativistic electron, one obtains that the opening angle of the emission cone is $\Delta\vartheta \sim m/\varepsilon$, where ϑ indicates the angle between the instantaneous propagation direction of the electron and the direction in which radiation is emitted [Jack 75,Land 75]. Thus in this work, the emission is considered to occur mainly in the instantaneous forward direction. Considering now the emitted power $\mathcal{P}$ which is given by the relativistic Larmor formula [Land 75]

$$\mathcal{P} = -\frac{2}{3}e^2\frac{\mathrm{d}v^\mu}{\mathrm{d}s}\frac{\mathrm{d}v_\mu}{\mathrm{d}s}, \tag{2.9}$$

where $\mathrm{d}v^\mu/\mathrm{d}s$ indicates the acceleration, an additional damping force can be introduced into the common Lorentz force equation. In [Abra 04] the generalized form of this damping force was suggested to be

$$F_R^\mu = \frac{2}{3}e^2\left(\frac{\mathrm{d}^2v^\mu}{\mathrm{d}s^2} + \frac{\mathrm{d}v^\nu}{\mathrm{d}s}\frac{\mathrm{d}v_\nu}{\mathrm{d}s}v^\mu\right). \tag{2.10}$$

The inclusion of this expression in eq. (2.1), is known as the Lorentz-Abraham-Dirac (LAD) equation

$$m\frac{\mathrm{d}v^\mu}{\mathrm{d}s} = eF^{\mu\nu}v_\nu + \frac{2}{3}e^2\left(\frac{\mathrm{d}^2v^\mu}{\mathrm{d}s^2} + \frac{\mathrm{d}v^\nu}{\mathrm{d}s}\frac{\mathrm{d}v_\nu}{\mathrm{d}s}v^\mu\right). \tag{2.11}$$

However, this equation exhibits several unphysical properties. For instance, it allows for so-called runaway solutions, where even in the absence of an accelerating field the acceleration of the electron diverges exponentially [Rohr 07, Hart 10].

As it was pointed out in [Land 75], the Lorentz force is much larger than F_R^μ in the instantaneous rest-frame of the electron if the conditions

$$\lambda^* \gg \alpha\lambda_C \qquad \text{and} \qquad F^* \ll \frac{F_{\mathrm{cr}}}{\alpha} \tag{2.12}$$

are fulfilled. Here, we introduced the typical wavelength λ^* and typical field amplitude F^* for the external electromagnetic field and the Compton wavelength $\lambda_C = 1/m \approx 3.9 \times 10^{-11}\,\mathrm{cm}$. The conditions (2.12) are always fulfilled in the framework of classical electrodynamics. Indeed, quantum effects like photon recoil are negligible and the wave function of the electron remains well localized, if the more restrictive conditions $F^* \ll F_{\mathrm{cr}}$ and $\lambda^* \gg \lambda_C$ are fulfilled. If the conditions in eq. (2.12) are also fulfilled in the instantaneous rest frame of the electron, the order of the LAD equation can be reduced by replacing the electron acceleration occurring in eq. (2.11) by means of eq. (2.1). Following this procedure, one obtains the Landau-Lifshitz (LL) equation

$$m\frac{\mathrm{d}v^\mu}{\mathrm{d}s} = eF^{\mu\nu}v_\nu + \frac{2}{3}\alpha\left[\frac{e}{m}(\partial_\alpha F^{\mu\nu})v^\alpha v_\nu - \frac{e^2}{m^2}F^{\mu\nu}F_{\alpha\nu}v^\alpha + \frac{e^2}{m^2}(F^{\alpha\nu}v_\nu)(F_{\alpha\lambda}v^\lambda)v^\mu\right]. \tag{2.13}$$

This equation does no longer have the drawbacks of the LAD equation. In fact, the investigations in [Spoh 00, Rohr 08] further corroborate that the LL equation is the correct description of classical RR. Nonetheless, the LL equation does not represent the only equation that has been proposed to describe RR in classical electrodynamics without the shortcomings of the LAD equation, see the recent review [Hamm 10]. The LL equation can be solved analytically for several external field configurations, e.g., a constant electromagnetic field [Sen 71a, Sen 71b, Gupt 72, Sen 73, Herr 73, Kazi 11] and a monochromatic plane-wave [Niki 96]. In addition, the LL equation allows for an analytical solution also in the case of an arbitrary plane-wave [Di P 08]. As only the quantity $v_-(\varphi)$ will be of interest in the following chapters, we cite here only the equation for $v_-(\varphi)$ [Di P 08]

$$v_-(\varphi) = \frac{v_{0,-}}{h(\varphi)}, \tag{2.14}$$

where we introduced the function

$$h(\varphi) = 1 + \frac{2}{3}R_C\int_{\varphi_0}^{\varphi}\mathrm{d}\varphi'\,\mathfrak{f}^2(\varphi'), \tag{2.15}$$

$v_{0,-}$ indicates the initial value, and we made use of the quantity $R_C = \alpha\xi\chi$. Furthermore, if $R_C \approx 1$ and $\chi \ll 1$, i.e., quantum effects like photon recoil are negligible, the interaction of the electron and the plane-wave field occurs in the so-called classical radiation dominated regime. This regime has been studied in [Shen 70, Koga 05] and it is characterized by the fact that some components of the RR force (see eq. (2.10)) can be of the same order as the Lorentz force in the laboratory frame. Therefore, in this parameter regime the RR force can lead to strongly altered dynamics of the electron in comparison to the one expected from only considering Lorentz dynamics.

2.1.2 Quantum electrodynamics

So far the electron has been described as a point charge. In the framework of a quantum theory, however, electrons are rather described by wave functions. Considering only a single-particle quantum theory, the Dirac equation [Dira 28]

$$\left\{\gamma^\mu\left[i\partial_\mu - eA_\mu(x)\right] - m\right\}\psi(x) = 0 \tag{2.16}$$

determines the evolution of a four-component electron bispinor $\psi(x)$ in the presence of an external electromagnetic field $A^\mu(x)$. γ^μ indicate the Dirac matrices. In the

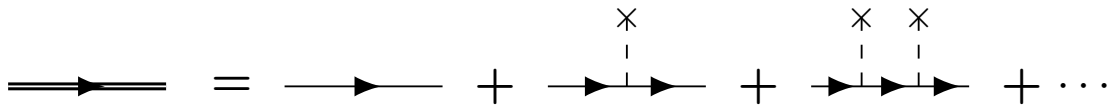

Figure 2.1: Symbolical depiction of the Furry picture, where the interaction of the electron with the unquantized external field (dashed lines) is taken into account exactly.

special case of a plane-wave field, the Dirac equation permits an analytical solution. Assuming that in the limit $\varphi \to -\infty$, the four-potential vanishes, $A^\mu(-\infty) = 0$, and that the electron momentum and spin are given by $p_0^\mu = (\varepsilon_0, \boldsymbol{p}_0)$ and $\sigma_0/2 = \pm 1/2$, respectively, we obtain the positive energy ($\varepsilon_0 > 0$) solutions [Volk 35, Bere 82]

$$\psi_{p_0,\sigma_0}(x) = \left[1 + \frac{e}{2(k_{0,\mu}p_0^\mu)} \not{k}_0 \not{A}(\varphi)\right] \frac{u_{p_0,\sigma_0}}{\sqrt{2V\varepsilon_0}} \exp(iS_{p_0}) \tag{2.17}$$

with the quantization volume V and the free positive-energy bispinor u_{p_0,σ_0} [Bere 82]. We further employed the Feynman slash notation $\not{a} = \gamma_\mu a^\mu$ for an arbitrary four-vector a^μ. The quantity

$$S_{p_0}(x) = -(p_0^\mu x_\mu) - \int_{-\infty}^{\varphi} \mathrm{d}\varphi' \left\{ \frac{e[p_0^\mu A_\mu(\varphi')]}{(k_{0,\mu}p_0^\mu)} - \frac{e^2 A^2(\varphi')}{2(k_{0,\mu}p_0^\mu)} \right\} \tag{2.18}$$

expresses the classical action of an electron propagating in a plane-wave field. The states $\psi_{p_0,\sigma_0}(x)$ are known as Volkov states and they constitute a complete set of orthogonal states [Ritu 85, Zako 05, Boca 10], i.e., the Volkov states can be employed as a basis to study the evolution of electron wave packets. In order to understand the importance of these solutions, we recall the classical nonlinearity parameter ξ which can be understood as the work performed by the external field over one Compton wavelength λ_C in units of the wave's photon energy ω_0. From this one can conclude that at $\xi \gtrsim 1$, multiphoton effects will become important in QED processes and in turn the plane-wave field cannot be taken into account perturbatively [Ritu 85]. Therefore, the Volkov states will be employed instead of the free particle states in the QED calculations. These calculations employ the so-called Furry picture [Furr 51], wherein the interaction of $\psi(x)$ and the radiation field described by $\mathcal{A}^\mu(x)$ is treated by means of perturbation theory, whereas the interaction with the external field is accounted for exactly. Hence, the dynamics of the electron-positron field and the radiation field is determined by the S-matrix [Bere 82]

$$S = \mathcal{T}\left\{\exp\left[-ie\int \mathrm{d}^4x\, \overline{\psi}(x)\gamma^\mu\psi(x)\mathcal{A}_\mu(x)\right]\right\}, \tag{2.19}$$

where $\mathcal{T}$ indicates the time-ordering operator and $\overline{\psi}(x) = \psi^\dagger(x)\gamma^0$ is the adjoint spinor to $\psi(x)$. Graphically this can be depicted in terms of the common Feynman diagrams, only with double lines indicating electron (or positron) states that take the unquantized external field into account exactly.

We now turn to one particular QED process, namely the emission of a single-photon by an electron in a plane-wave field. The emission of a photon with wave vector k^μ changes the electron's initial momentum p_i^μ to the final momentum p_f^μ, where the absorption of ℓ plane-wave photons with wave vector k_0^μ is assumed. Note

that in the case of a vanishing external field, the conservation law $p_i^\mu = p_f^\mu + k^\mu$ has to be fulfilled, which is kinematically forbidden. The S matrix element corresponding to single-photon emission can be written as [Ritu 85]

$$S_{fi} = -ie \int \mathrm{d}^4x\, \overline{\psi}_{p_f,\sigma_f}(x) \not{A}^*_{em}(x) \psi_{p_i,\sigma_i}(x), \tag{2.20}$$

where $\overline{\psi}_{p_f,\sigma_f}(x)$ and $\psi_{p_i,\sigma_i}(x)$ are the Volkov states according to eq. (2.17) and

$$A^\mu_{em}(x) = \sqrt{\frac{2\pi}{\omega V}} \epsilon^\mu_k \exp\left(ik_\nu x^\nu\right) \tag{2.21}$$

is the wave function of the emitted free photon. Since we are not interested in the polarization characteristics of this process, we can average over the initial electron spin and sum over the final electron spin and the photon polarization. The corresponding emission probability has been evaluated in [Boca 09, Mack 11, Seip 11] and [Niki 64] in the case of a pulsed plane-wave and a monochromatic plane-wave field, respectively. However, it was pointed out [Ritu 85] that the emission probability is a gauge- and Lorentz-invariant quantity and in turn can only depend on quantities that are gauge- and Lorentz-invariant themselves. In the case of an electron moving in an arbitrary electromagnetic field ($F^{\mu\nu}(x) = (E(x), B(x))$) the probability can generally depend on the quantities ξ and $\chi(x)$ depending on the local field amplitude as well as on the field invariants

$$\mathcal{F}(x) = \frac{1}{4} F^{\mu\nu}(x) F_{\mu\nu}(x) = -\frac{1}{2}\left[E^2(x) - B^2(x)\right], \tag{2.22}$$

$$\mathcal{G}(x) = \frac{1}{4} F^{\mu\nu}(x) \tilde{F}_{\mu\nu}(x) = -\boldsymbol{E}(x) \cdot \boldsymbol{B}(x), \tag{2.23}$$

where $\tilde{F}_{\mu\nu}(x) = \epsilon_{\mu\nu\rho\sigma} F^{\rho\sigma}(x)/2$ is the dual field of $F^{\mu\nu}(x)$ and $\epsilon^{\mu\nu\rho\sigma}$ is the four-dimensional completely antisymmetric tensor with $\epsilon^{0123} = 1$. If the external fields now fulfill the conditions

$$|\mathcal{F}(x)|, |\mathcal{G}(x)| \ll F^2_{\mathrm{cr}}, \qquad |\mathcal{F}(x)|, |\mathcal{G}(x)| \ll \chi^2(x) F^2_{\mathrm{cr}}, \tag{2.24}$$

we are allowed to neglect the dependencies on the quantities $\mathcal{F}(x)$ and $\mathcal{G}(x)$ [Ritu 85]. In turn, the probability of photon emission practically coincides with the one obtained in the case of a constant crossed field. This justifies the employment of the constant crossed field probability, with the replacements $E \to E(x)$ and $B \to B(x)$. Since $\mathcal{F}(x)$ and $\mathcal{G}(x)$ vanish identically for a plane-wave field, the probability always depends on $\chi(x)$ and ξ exclusively and the constant field probability can be employed if $\xi \gg 1$. In fact, in the case of $\xi \gg 1$, the region in which the radiation is formed l_0, the so-called radiation formation length, is $l_0 = \lambda_0/\xi \ll \lambda_0$, where λ_0 is the central wavelength [Ritu 85]. This illustrates that the region in which the radiation is formed is much smaller than the distance over which the plane-wave field varies. In order to describe the photon emission process, it is convenient to introduce the expression $u = k_-/(p_- - k_-)$. Finally, the single-photon emission probability per unit phase φ and per unit u in the ultrarelativistic regime $\xi \gg 1$ reads [Ritu 85]

$$\begin{aligned} \frac{\mathrm{d}P_{p_-}}{\mathrm{d}\varphi \mathrm{d}u} =& \frac{\alpha}{\sqrt{3}\pi} \frac{m^2}{\omega_0 p_-} \frac{1}{(1+u)^2} \left[\left(1 + u + \frac{1}{1+u}\right) \right. \\ & \left. \times \mathrm{K}_{\frac{2}{3}}\left(\frac{2u}{3\chi(\varphi, p_-)}\right) - \int_{\frac{2u}{3\chi(\varphi,p_-)}}^{\infty} \mathrm{d}x\, \mathrm{K}_{\frac{1}{3}}(x) \right] \end{aligned} \tag{2.25}$$

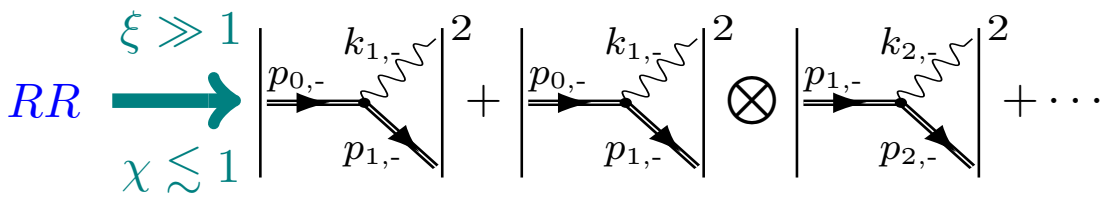

Figure 2.2: Schematic depiction of the nonlinear moderately quantum regime, where RR stems from the incoherent emission of multiple photons.

for an electron with initial momentum value p_- and an emitted photon with momentum value k_- and with $\chi(\varphi, p_-) = (p_-/m)|E(\varphi)|/F_{\mathrm{cr}}$. The functions $\mathrm{K}_\nu(x)$ are the modified Bessel functions of the second kind and of νth order (see app. A). In addition, we mention here that for $\xi \gg 1$ the number of absorbed laser photons ℓ scales like $\ell \sim \xi^3$ [Ritu 85]. Furthermore, from eq. (2.25) we can derive the total quantum radiation intensity [Ritu 85, Baie 94]

$$\begin{aligned} I_q &= \frac{\alpha m^2}{3\sqrt{3}\pi} \int_0^\infty \mathrm{d}u \, \frac{4u^3 + 5u^2 + 4u}{(1+u)^4} \mathrm{K}_{\frac{2}{3}}\left(\frac{2u}{3\chi}\right), \\ &= \frac{2}{3}\alpha m^2 \chi^2 \left(1 - \frac{55\sqrt{3}}{16}\chi + 48\chi^2\right) + \mathcal{O}\left(\chi^5\right). \end{aligned} \tag{2.26}$$

Note that the leading order term is exactly the classical radiation intensity $I_{cl} = (2/3)\alpha m^2 \chi^2$ corresponding to classically emitted power in eq. (2.9).

Returning to the issues of RR, it has to be clarified what RR effects actually are in the framework of quantum electrodynamics. In the case of classical electrodynamics we identified RR as all the effects which are not included in the Lorentz dynamics and arise due to the interaction of the electromagnetic field emitted by an electron with the electron itself. By transferring this definition to the realm of QED, RR in principle incorporates all possible quantum processes originating from an initial single electron propagating in an external field. The possibly occurring quantum processes include multiple photon emission, pair creation by previously emitted photons and higher-order radiative corrections. Hence, a full description of quantum RR would require not only a full evaluation of the S-matrix in eq. (2.19) but also the inclusion of all possible final states.

However, in [Di P 10] the so-called nonlinear moderately quantum regime was introduced, which is constituted by the conditions $\xi \gg 1$ and $\chi \lesssim 1$. Since the probability of pair creation by a photon with light cone momentum k_- is approximately suppressed by the exponential factor $\eta(k_-) = \exp(-8/3\varkappa)$, with $\varkappa = k_-\chi/p_-$, the condition $\chi \lesssim 1$ allows to neglect electron-positron pair production. In addition, the emission of j photons within one radiation formation length is roughly α^{j-1} times the emission probability of one photon for $\chi \lesssim 1$ [Ritu 85] and in turn only the emission of one photon per radiation formation length can be taken into account. As radiative corrections also give rise to additional factors of α, these contributions can be neglected as well. Thus, we can conclude that in the nonlinear moderately quantum regime RR is due to multiple incoherent photon emissions [Di P 10], as is graphically shown in fig. 2.2.

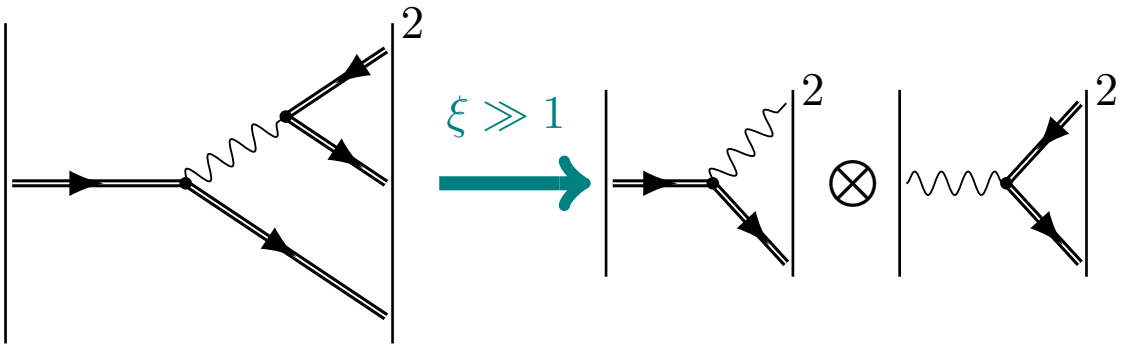

Figure 2.3: In the case of $\xi \gg 1$, the trident process is dominated by the consecutive processes of photon emission and laser assisted pair production by the emitted photon [Hu 10, Ilde 11].

Under these assumptions the single-photon emission probability is approximately $P_{p_-} \sim R_Q \Delta\varphi$, with $R_Q = \alpha\xi$ and the phase interval $\Delta\varphi$ corresponding to the pulse duration. These considerations lead to the introduction of the so-called quantum radiation dominated regime, which is characterized by $R_Q \approx 1$ and $\chi \gtrsim 1$. As long as $\chi \ll 1/\alpha^{3/2}$ and pair creation is still negligible, the above description of RR remains valid in the case $\chi \gtrsim 1$, since for $\chi \gg 1$ the emission of j photons within one radiation formation length is roughly $(\alpha\chi^{2/3})^{j-1}$ times the emission probability of one photon [Ritu 85]. In the quantum radiation dominated regime the emission of multiple photons occurs already in one laser period. We note that the obtained spectrum of single-photon emission in the classical limit $\chi \to 0$ coincides with the one obtained for multiphoton Thomson scattering based on the trajectory calculated by employing the Lorentz equation [Mack 11]. This corroborates the idea that RR can be related to the radiation processes that go beyond single-photon emission.

In the regime described above, pair production has always been neglected. However, with increasing values of χ, RR effects will also include the effect of creating electron-positron pairs. As in the framework of QED only vertices connecting two fermion lines and one photon line are allowed, the production of a pair from an electron requires at least two vertices. In the co-called trident process an electron emits a photon, which in turn splits into an electron and a positron (see fig. 2.3). The trident process consists of two physically distinct channels. In the first case, pair production is a two-step process, where the initial electron emits a real photon which subsequently transforms into a pair of charged particles. In the second case, the emitted photon is virtual and pair production is a one-step process, i.e., photon emission and pair creation occur in the same formation region. In [Hu 10, Ilde 11] (see also [King 13]) the trident process has been studied and pair production via the two-step process was found to be dominant in the presence of a strong laser plane-wave ($\xi \gg 1$). In fig. 2.3 it is shown that the trident process can then be separated into two processes. The probability of a photon creating an electron-positron pair can be calculated analogously to the probability of photon emission. Since $\xi \gg 1$, the probability in the case of a constant crossed field can be employed. In addition, we average over the initial photon polarization and sum over the spins of the electron and the positron. Finally, for a photon with momentum k_- creating an electron with momentum p_- and a positron with momentum $k_- - p_-$, the probability per

unit phase and unit p_- reads (see [Ritu 85])

$$\frac{\mathrm{d}P_{k_-}}{\mathrm{d}\varphi \mathrm{d}p_-} = \frac{\alpha}{\sqrt{3}\pi}\frac{m^2}{\omega_0 k_-^2}\left[\frac{k_-^2}{p_-(k_- - p_-)}\,\mathrm{K}_{\frac{2}{3}}\left(\kappa(\varphi, k_-, p_-)\right) - \int_{\kappa(\varphi,k_-,p_-)}^{\infty} dx\,\mathrm{K}_{\frac{5}{3}}(x)\right], \tag{2.27}$$

where we introduced the function $\kappa(\varphi, k_-, p_-) = 2k_-^2/[3p_-(k_- - p_-)\varkappa(\varphi, k_-)]$, with $\varkappa(\varphi, k_-) = (k_-/m)|E(\varphi)|/F_{\mathrm{cr}}$.

2.2 Kinetic theory

The main idea of the kinetic theory is to avoid the microscopic description of each particle in a physical ensemble, e.g., a plasma or a gas, and rather describe the evolution of the entire system statistically by means of distribution functions (see, e.g., [Pita 81]). This is motivated by the fact that a system of N particles in principle requires the solution of 6^N coupled equations in order to define the particles' evolution in phase space spanned by the spatial coordinates $\boldsymbol{r}$ and the particles' momenta $\boldsymbol{p}$. In fact, the number of equations is even larger if the constituting particles of the system feature additional degrees of freedom, e.g., vibrational and rotational in the case of non-monoatomic molecules. Since the particles under consideration in the main part of this thesis are electrons, photons and positrons, and we are not investigating the influence of spin and polarization on the dynamics, there are no additional internal degrees of freedom that have to be taken into account. Therefore, the evolution of an ensemble of particles can be described by the distribution functions $f_{\mathfrak{p}}(t, \boldsymbol{r}, \boldsymbol{p})$, where the index $\mathfrak{p}$ indicates the particle type, limited here to electrons, positrons and photons. The distribution function is considered to be normalized in such a way that the integral over the spatial coordinates and the momenta components results in the total number of particles. By neglecting internal interactions such as collisions of the particles, the distribution functions obey Liouville's theorem [Pita 81]

$$\frac{\mathrm{d}f_{\mathfrak{p}}(t, \boldsymbol{r}, \boldsymbol{p})}{\mathrm{d}t} = 0. \tag{2.28}$$

Assuming an external potential $U(\boldsymbol{r})$, eq. (2.28) can be rewritten as

$$\frac{\mathrm{d}f_{\mathfrak{p}}(t, \boldsymbol{r}, \boldsymbol{p})}{\mathrm{d}t} = \frac{\partial f_{\mathfrak{p}}(t, \boldsymbol{r}, \boldsymbol{p})}{\partial t} + \underbrace{\frac{\mathrm{d}\boldsymbol{r}}{\mathrm{d}t}}_{=\boldsymbol{v}} \cdot \frac{\partial f_{\mathfrak{p}}(t, \boldsymbol{r}, \boldsymbol{p})}{\partial \boldsymbol{r}} + \underbrace{\frac{\mathrm{d}\boldsymbol{p}}{\mathrm{d}t}}_{=\boldsymbol{F}} \cdot \frac{\partial f_{\mathfrak{p}}(t, \boldsymbol{r}, \boldsymbol{p})}{\partial \boldsymbol{p}} = 0, \tag{2.29}$$

where we introduced the external force $\boldsymbol{F}$. In the case of an electron propagating in an electromagnetic field and neglecting other forces with respect to the Lorentz force, the corresponding equation reads [Pita 81]

$$\frac{\partial f_{e^-}(t, \boldsymbol{r}, \boldsymbol{p})}{\partial t} + \boldsymbol{v} \cdot \frac{\partial f_{e^-}(t, \boldsymbol{r}, \boldsymbol{p})}{\partial \boldsymbol{r}} + e\left[\boldsymbol{E} + \boldsymbol{v} \times \boldsymbol{B}\right] \cdot \frac{\partial f_{e^-}(t, \boldsymbol{r}, \boldsymbol{p})}{\partial \boldsymbol{p}} = 0. \tag{2.30}$$

This equation is the well-known Vlasov equation. The according equation for a positron can be achieved by the replacement of the subscript $e^- \to e^+$ and $e \to |e|$.[I]

[I] Recall that we included the sign of the charge in the definition of e, i.e., for an electron the last term on the right hand side of eq. (2.30) implies a negative sing, whereas a positive sign is implied in the case of a positron.

As the photon is not a charged particle, it is not affected by the Lorentz force and the equation for the photon distribution is simplified to

$$\frac{\partial f_\gamma(t,\boldsymbol{r},\boldsymbol{k})}{\partial t} + \frac{\boldsymbol{k}}{\omega}\cdot\frac{\partial f_\gamma(t,\boldsymbol{r},\boldsymbol{k})}{\partial \boldsymbol{r}} = 0, \tag{2.31}$$

where we made use of the common notation $\boldsymbol{k}$ as the wave vector of a photon instead of $\boldsymbol{p}$ to indicate its momentum. If also collisions of the particles are taken into account, eq. (2.28) becomes the more general transport equation [Pita 81]

$$\frac{\mathrm{d}f_{\mathfrak{p}}(t,\boldsymbol{r},\boldsymbol{p})}{\mathrm{d}t} = \mathcal{C}[f_{\mathfrak{p}}(t,\boldsymbol{r},\boldsymbol{p})], \tag{2.32}$$

where $\mathcal{C}[f_{\mathfrak{p}}(t,\boldsymbol{r},\boldsymbol{p})]$ is the so-called collision integral. The collisional processes in the system under consideration will be the emission of photons and the creation of electron-positron pairs. We note here that for the photon emission the transport equation has the form of a so-called diffusion equation. Introducing the momentum distribution, e.g., for an electron,

$$f_{e^-}(t,\boldsymbol{p}) = \int \mathrm{d}^3\boldsymbol{r}\, f_{e^-}(t,\boldsymbol{r},\boldsymbol{p}) \tag{2.33}$$

the diffusion equation reads [Pita 81]

$$\frac{\partial f_{e^-}(t,\boldsymbol{p})}{\partial t} = \int \mathrm{d}^3\boldsymbol{p}'\, \left[P(\boldsymbol{p}+\boldsymbol{p}',\boldsymbol{p}')f_{e^-}(t,\boldsymbol{p}+\boldsymbol{p}') - P(\boldsymbol{p},\boldsymbol{p}')f_{e^-}(t,\boldsymbol{p})\right], \tag{2.34}$$

where $P(\boldsymbol{p},\boldsymbol{p}')$ indicates the probability per unit time for an electron to emit a photon resulting in the change $\boldsymbol{p}\to\boldsymbol{p}'$ in the electron momentum. Apparently, the number of particles in a certain phase space volume is changed via two events. On the one hand, an electron with initially higher momentum can emit a photon in such a way that the final electron is in the considered phase space volume. On the other hand, an electron initially in this phase space volume can leave this volume due to the emission of a photon. In addition to the distribution function we define the corresponding entropy [Pita 81], again in the case of an electron,

$$S = \int \mathrm{d}^3\boldsymbol{r}\,\mathrm{d}^3\boldsymbol{p}\, f_{e^-}(t,\boldsymbol{r},\boldsymbol{p}) \ln\left[\frac{k_B}{f_{e^-}(t,\boldsymbol{r},\boldsymbol{p})}\right], \tag{2.35}$$

with the Boltzmann constant k_B. Considering now the time evolution of the entropy, we obtain

$$\begin{aligned}\frac{\mathrm{d}S}{\mathrm{d}t} &= \int \mathrm{d}^3\boldsymbol{r}\,\mathrm{d}^3\boldsymbol{p}\,\frac{\partial}{\partial t}\left\{f_{e^-}(t,\boldsymbol{r},\boldsymbol{p})\ln\left[\frac{k_B}{f_{e^-}(t,\boldsymbol{r},\boldsymbol{p})}\right]\right\}\\ &= -\int \mathrm{d}^3\boldsymbol{r}\,\mathrm{d}^3\boldsymbol{p}\,\ln\left[f_{e^-}(t,\boldsymbol{r},\boldsymbol{p})\right]\frac{\partial f_{e^-}(t,\boldsymbol{r},\boldsymbol{p})}{\partial t}.\end{aligned} \tag{2.36}$$

Applying eq. (2.29) and eq. (2.32), the terms involving derivatives with respect to $\boldsymbol{r}$ and $\boldsymbol{p}$ can be shown to vanish by employing Gauss's theorem. This simplifies the above equation to

$$\frac{\mathrm{d}S}{\mathrm{d}t} = -\int \mathrm{d}^3\boldsymbol{r}\,\mathrm{d}^3\boldsymbol{p}\,\ln\left[f_{e^-}(t,\boldsymbol{r},\boldsymbol{p})\right]\mathcal{C}[f_{e^-}(t,\boldsymbol{r},\boldsymbol{p})], \tag{2.37}$$

indicating that the evolution of the entropy is exclusively determined by the collision integral.

So far we did not take into account the fact that electrons, positrons and photons in general require a description via quantum wave functions. In principle, this leads to an analogously defined transport equation, where the canonical variables $\boldsymbol{r}$ and $\boldsymbol{p}$ are operators and the observables are calculated as expectation values employing a quantum density matrix (see, e.g., [Vask 05]). However, it was pointed out in [Baie 94] that, e.g., photon emission from a high-energetic charge in the presence of an external field exhibits two different kinds of quantum effects. The first type concerns the quantization of the particle's dynamic variables and their non commutativity, which can be shown, e.g., in the case of a charged particle in a magnetic field B, to be of the order of $B/(F_{\mathrm{cr}}\gamma^2)$, with the relativistic gamma factor $\gamma = \varepsilon/m$. Therefore, the motion of the particle becomes classical at relativistic energies and thus can be described without the use of quantum states. However, the second type of quantum effect concerns the recoil experienced by the emitting particle upon the emission of a photon which cannot be neglected at $\chi \lesssim 1$, i.e., the actual process of photon emission has to be treated in the framework of strong-field QED. This permits a semi-classical investigation, where the electrons in the beam and the emitted photons are described by distribution functions in phase space obeying kinetic equations and the radiation process is characterized by the quantum emission probability. Analogously, the quantum effects accompanying pair creation are only taken into account via the pair production probability in the kinetic equation of the photons.

3 Kinetic approach (1): Photon emission

In this chapter, the collision of an ultrarelativistic electron beam with an intense laser pulse is considered and a theoretical model describing the effects of RR on the dynamics is developed in the so-called nonlinear moderately quantum regime. Starting from the general Vlasov equation including terms corresponding to the incoherent emission of single photons by the electron beam, the simplified one-dimensional kinetic equations describing the evolution of electrons and photons by means of distribution functions are derived by employing their kinematic properties within this regime. Subsequently, this approach is proven analytically and numerically to coincide with the results obtained by the LL equation in the parameter region where quantum effects like photon recoil are known to be negligible. However, while the LL equation predicts a narrowing of the electron distribution function, the numerical simulations exhibit the opposite tendency in the case where the neglect of quantum effects is no longer justified. By expanding the kinetic equation of the electrons for small quantum corrections, the approximated evolution of a single electron is shown to be described by a Langevin equation, i.e., the dynamics of the electron is no longer deterministic as soon as quantum effects become important. In fact, the stochastic nature of photon emission is demonstrated to induce a broadening mechanism in the evolution of the electron distribution. Finally, the influence of the laser pulse shape and duration on the dynamics of electrons and photons is investigated. Parts of this chapter have been presented in [Neit 13] and [Neit 14].

3.1 Derivation and properties of the kinetic equations for photon emission

In order to achieve a complete description of RR in the full strong-field QED regime, the problem arises to determine the full S-matrix including effects as radiative corrections, multiple photon emission as well as subsequent pair creation by simultaneously taking into account exactly all interactions with the strong external field. Since there is no solution at hand to this highly demanding task, it is favorable to examine a concrete scenario allowing for several restrictions to the full process. Motivated by the recent developments in the creation of intense laser pulses [Yano 08] and the production of high-energy electron bunches [Wang 13], the head-on collision of an ultrarelativistic electron beam with a strong plane-wave field is considered in the nonlinear moderately quantum regime [Di P 10] (see sec. 2.1.2). On the

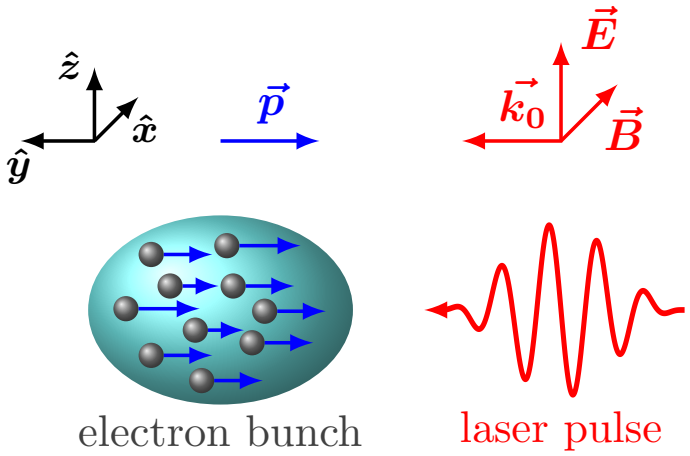

Figure 3.1: Generic choice of the coordinate frame for the collision of the electron bunch and the laser pulse.

one hand, this implies a large relativistic nonlinearity parameter, $\xi \gg 1$, indicating strongly nonlinear dependency on the laser field amplitude. On the other hand, the condition $\chi \lesssim 1$ ensures that, while nonlinear QED effects become significant, electron-positron pair creation and higher-order radiative corrections can still be neglected. Within this regime, the effect of RR can be understood as the consecutive incoherent emission of multiple photons by the beam electrons [Di P 10]. Further, it was pointed out in [Baie 94] (see sec. 2.2) that photon emission by an ultrarelativistic charge permits a semi-classical investigation, where the electrons in the beam and the emitted photons are described by distribution functions in phase space obeying kinetic equations, and the radiation process is characterized by the quantum emission probability. Hence, in the nonlinear moderately quantum regime, RR can be studied by means of a kinetic approach [Baie 94, Khok 04, Soko 10, Elki 11]. An alternative, microscopic approach has been examined in [Di P 10] leading to equivalent results (see app. E). As for $\chi \lesssim 1$ pair creation is negligible, the set of kinetic equations is further simplified since the distribution function of the positrons is expected to vanish throughout the whole interaction time and the electron distribution function is decoupled from the one for the photons.

Turning now to the specific scenario under consideration, as depicted in fig. 3.1, we assume the plane-wave to propagate along the positive y direction, to be linearly polarized along the z direction and to have the wave vector $k_0^\mu = (\omega_0, \boldsymbol{k}_0)$, with ω_0 being the laser central angular frequency. In this case, the electric field can be written as $\boldsymbol{E}(\varphi) = E_0 f(\varphi)\hat{\boldsymbol{z}}$, where $\varphi = \omega_0(t - y)$ indicates the laser phase and we introduced an arbitrary pulse shape function $f(\varphi)$ fulfilling $|f(\varphi)|_{\max} = 1$. On the other hand, the electrons are assumed to propagate along the negative y direction with initial four-momentum $p^\mu = (\varepsilon, \boldsymbol{p})$, with $\varepsilon = \sqrt{m^2 + \boldsymbol{p}^2}$. We start the derivation of the kinetic equations at the general three-dimensional Vlasov equation (see, e.g., [Pita 81] and sec. 2.2) for an electron distribution function $f_{e^-}(t, \boldsymbol{r}, \boldsymbol{p})$ depending on the spacetime variables as well as the momenta of the electrons

$$\frac{\mathrm{d}f_{e^-}(t, \boldsymbol{r}, \boldsymbol{p})}{\mathrm{d}t} = \left[\frac{\partial}{\partial t} + \frac{\mathrm{d}\boldsymbol{r}}{\mathrm{d}t} \cdot \frac{\partial}{\partial \boldsymbol{r}} + \frac{\mathrm{d}\boldsymbol{p}}{\mathrm{d}t} \cdot \frac{\partial}{\partial \boldsymbol{p}}\right] f_{e^-}(t, \boldsymbol{r}, \boldsymbol{p}) = \text{collision terms}, \tag{3.1}$$

where the collision terms indicate the terms corresponding to the occurrence of pho-

ton emission that are proportional to the emission probabilities per unit time $\mathrm{d}P/\mathrm{d}t$. In the case of a plane-wave electromagnetic field $(\boldsymbol{E}(\phi), \boldsymbol{B}(\phi))$, the expression $\mathrm{d}\boldsymbol{p}/\mathrm{d}t$ is given by the Lorentz force $\boldsymbol{F}_L(\phi, \boldsymbol{p}) = e[\boldsymbol{E}(\phi) + (\boldsymbol{p}/\varepsilon) \times \boldsymbol{B}(\phi)]$.[I] This allows us to rewrite eq. (3.1) as

$$\begin{aligned}\left[\frac{\partial}{\partial t} + \frac{\boldsymbol{p}}{\varepsilon}\cdot\frac{\partial}{\partial \boldsymbol{r}} + \boldsymbol{F}_L(\phi,\boldsymbol{p})\cdot\frac{\partial}{\partial \boldsymbol{p}}\right] f_{e^-}(t\boldsymbol{r},\boldsymbol{p}) = \\ \int \mathrm{d}\boldsymbol{k}\,\frac{\mathrm{d}P(\phi;\boldsymbol{p}_\perp+\boldsymbol{k}_\perp\to\boldsymbol{p}_\perp, p_-+k_-\to p_-)}{\mathrm{d}t\mathrm{d}\boldsymbol{k}} f_{e^-}(t,\boldsymbol{r},\boldsymbol{p}+\boldsymbol{k}) \\ - f_{e^-}(t,\boldsymbol{r},\boldsymbol{p})\int \mathrm{d}\boldsymbol{k}\,\frac{\mathrm{d}P(\phi;\boldsymbol{p}_\perp\to\boldsymbol{p}_\perp-\boldsymbol{k}_\perp, p_-\to p_- - k_-)}{\mathrm{d}t\mathrm{d}\boldsymbol{k}},\end{aligned} \tag{3.2}$$

where $[\mathrm{d}P(\phi;\boldsymbol{p}_\perp \to \boldsymbol{p}_\perp - \boldsymbol{k}_\perp, p_- \to p_- - k_-)/\mathrm{d}t\mathrm{d}\boldsymbol{k}]\mathrm{d}\boldsymbol{k}$ indicates the probability per unit time that a photon with a momentum ranging between $\boldsymbol{k}$ and $\boldsymbol{k} + \mathrm{d}\boldsymbol{k}$ is emitted by an electron with momentum $\boldsymbol{p}$. As pointed out in sec. 2.1.2, the radiation formation length $l_0 = \lambda_0/\xi$ is much smaller than the central wavelength if $\xi \gg 1$ and in turn the background field can be assumed to be uniform and constant within a radiation formation length. Hence, the expression $\mathrm{d}P(\phi;\boldsymbol{p}_\perp \to \boldsymbol{p}_\perp - \boldsymbol{k}_\perp, p_- \to p_- - k_-)/\mathrm{d}t\mathrm{d}\boldsymbol{k}$ can be replaced by the corresponding expression obtained when considering a constant crossed field $(\boldsymbol{E}, \boldsymbol{B})$, with the substitution $(\boldsymbol{E}, \boldsymbol{B}) \to (\boldsymbol{E}(\phi), \boldsymbol{B}(\phi))$ [Ritu 85]. In addition, in case of a plane-wave background field the notation apparently displays the conservation of the transverse momentum in the photon emission [Bere 82]. Furthermore, the canonical momenta $p_-(\phi)$ and $\boldsymbol{p}_\perp + e\boldsymbol{A}(\phi)$ are conserved during the sojourn of the electron in the laser field [Land 75]. Considering this aspect, it is convenient to perform a change of variables from the common spacetime coordinates to the light-cone coordinates $\phi = t - y$, $T = (t+y)/2$ and $\boldsymbol{r}_\perp = (x, z)$, and the corresponding quantities $p_- = \varepsilon - p_y$ (which will be called the minus momentum in the following), $p_+ = (\varepsilon + p_y)/2$ and $\boldsymbol{p}_\perp = (p_x, p_z)$, which obey the formulas (see eq. (2.6)-eq. (2.8))

$$p_-(\phi) \equiv p_{0,-}, \tag{3.3}$$

$$\boldsymbol{p}_\perp(\phi) = \boldsymbol{p}_{0,\perp} - e\boldsymbol{A}(\phi), \tag{3.4}$$

$$p_+(\phi) = \frac{m^2 + \boldsymbol{p}_\perp^2(\phi)}{2p_{0,-}}, \tag{3.5}$$

where we introduced the four-vector potential in Lorentz gauge $A^\mu(\phi) = (0, \boldsymbol{A}(\phi)) = (0, -E_0\mathfrak{f}(\phi)\hat{\boldsymbol{z}})$, with $\mathfrak{f}(\phi) = \int_0^\phi d\phi'\, f(\phi')$, and $\boldsymbol{p}_{0,\perp}$ and $p_{0,-}$ indicate the initial transverse and minus momentum, respectively. Thus, we obtain for the expression on the left-hand side of eq. (3.2)

$$\begin{aligned}\frac{\partial}{\partial t} + \frac{\boldsymbol{p}}{\varepsilon}\cdot\frac{\partial}{\partial \boldsymbol{r}} + \boldsymbol{F}_L(\phi,\boldsymbol{p})\cdot\frac{\partial}{\partial \boldsymbol{p}} = \frac{p_-}{\varepsilon}\frac{\partial}{\partial\phi} + \frac{p_+}{\varepsilon}\frac{\partial}{\partial T} + \frac{\boldsymbol{p}_\perp}{\varepsilon}\cdot\frac{\partial}{\partial \boldsymbol{r}_\perp} \\ + eE(\phi)\left(\frac{p_-}{\varepsilon}\frac{\partial}{\partial p_z} + \frac{p_z}{\varepsilon}\frac{\partial}{\partial p_y}\right),\end{aligned} \tag{3.6}$$

with $E(\phi) = E_0 f(\phi)$. In the following, we will continue to explicitly write all the dependencies of the distribution function by $f_{e^-}(\phi, T, \boldsymbol{r}_\perp, p_-, \boldsymbol{p}_\perp)$. Note that there

[I] In order to avoid additional factors of ω_0 throughout the derivation, we make use of the phase variable $\phi = t - y$ instead of φ, but will return to the latter notation at the end of the derivation.

exists a one-to-one relation between the quantity $p_- = \sqrt{m^2 + \boldsymbol{p}_\perp^2 + p_y^2} - p_y$ and p_y at a given value $\boldsymbol{p}_\perp$. As mentioned before, we consider the electron bunch to be ultrarelativistic, and the kinetic equation permits further simplification if the condition $\varepsilon^* \gg m\xi$ is fulfilled. The quantity ε^* indicates a typical energy of an electron in the beam and can be expressed as $\varepsilon^* \approx p_-^*/2$. In the realistic situation, for example, of an electron bunch with typical energy $\varepsilon^* = 1$ GeV colliding head-on with a laser field of intensity 10^{22} W/cm^2 [Yano 08] with an optical frequency $\omega_0 = 1.55$ eV, the condition $\varepsilon^* \gg m\xi = 24$ MeV is fairly well fulfilled. As can be seen from eq. (3.4), this condition ensures that the electron is barely deflected by the laser field and that the transverse momentum remains negligible in comparison to p_-. Moreover, if the electrons are ultrarelativistic, the electromagnetic radiation is mainly directed along the instantaneous propagation direction of the electrons [Ritu 85].

Finally, the energy loss due to photon emission is presumed to be sufficiently small, in order to grant the validity of the condition $\varepsilon^* \gg m\xi$ for the entire interaction between the laser pulse and the electron bunch. This implies that the electrons are not reflected by the pulse at any time, as $p_y^* \approx -\varepsilon^*$ [Di P 09]. For the purpose of estimation, a sine pulse with N_L cycles is considered and we calculate the final value $p_{-,f}^* \approx 2\varepsilon_f^* \approx 2|p_{y,f}^*|$ employing the classical exact solution of the LL equation [Di P 08],

$$p_{-,f}^* = \frac{p_-^*}{1 + \frac{2}{3}\alpha\chi^*\xi\pi N_L}, \tag{3.7}$$

and presume that the condition $p_{-,f}^* = p_-^*/[1 + (2/3)\alpha\chi^*\xi\pi N_L] \gg m\xi$ is fulfilled. Note that the latter condition is also fulfilled for the average momentum in the quantum regime, as the average energy emitted in the quantum case is overestimated by the classical formulas [Ritu 85]. Under the aforementioned conditions, the electron distribution function will remain well-peaked in the region of momenta where $|\boldsymbol{p}_\perp| \ll \varepsilon$, $p_- \approx 2\varepsilon$ and $p_+ = (m^2 + \boldsymbol{p}_\perp^2)/2p_- \ll \varepsilon$ during the collision and we can seek for a solution of the form $f_{e^-}(\phi, T, \boldsymbol{r}_\perp, p_-, \boldsymbol{p}_\perp) = g_{e^-}(\phi, \boldsymbol{p}_\perp)\rho_{e^-}(\phi, T, \boldsymbol{r}_\perp, p_-)$, where the dependency on the transverse momentum was separated. The introduction of the function $g_{e^-}(\phi, \boldsymbol{p}_\perp)$ allows for a treatment of the phase evolution of a finite transverse momentum. By applying the adopted structure of the electron distribution function, the left-hand side of eq. (3.6) can be approximated as

$$\frac{\partial}{\partial t} + \frac{\boldsymbol{p}}{\varepsilon} \cdot \frac{\partial}{\partial \boldsymbol{r}} + \boldsymbol{F}_L(\phi, \boldsymbol{p}) \cdot \frac{\partial}{\partial \boldsymbol{p}} \approx \frac{p_-}{\varepsilon}\left[\frac{\partial}{\partial \phi} + eE(\phi)\frac{\partial}{\partial p_z}\right], \tag{3.8}$$

where the ratio p_-/ε was kept for the moment, anticipating the subsequent derivation.

Now, as the emission probabilities do not depend on T and on $\boldsymbol{r}_\perp$, we are allowed to factorize these dependencies and rewrite the distribution function $\rho_{e^-}(\phi, T, \boldsymbol{r}_\perp, p_-) = f_T(T) f_\perp(\boldsymbol{r}_\perp) n_{e^-}(\phi, p_-)$ and the functions $f_T(T)$ and $f_\perp(\boldsymbol{r}_\perp)$ can be assumed to be well-peaked in the spatial region at the values $T = 0$ and $\boldsymbol{r}_\perp = \boldsymbol{0}$, respectively, by assigning initial conditions for the electron beam accordingly. Furthermore, as it was already pointed out, the photons will be emitted mainly in the negative y direction in case of ultrarelativistic electrons and in turn, the differential probability

$[\mathrm{d}P(\phi;\boldsymbol{p}_\perp \to \boldsymbol{p}_\perp - \boldsymbol{k}_\perp, p_- \to p_- - k_-)/\mathrm{d}t\mathrm{d}\boldsymbol{k}]\mathrm{d}\boldsymbol{k}$ can be approximated by

$$\begin{aligned}\frac{\mathrm{d}P(\phi;\boldsymbol{p}_\perp \to \boldsymbol{p}_\perp - \boldsymbol{k}_\perp, p_- \to p_- - k_-)}{\mathrm{d}t\mathrm{d}\boldsymbol{k}}\mathrm{d}\boldsymbol{k} &\approx \frac{\mathrm{d}P(\phi;p_- \to p_- - k_-)}{\mathrm{d}t\mathrm{d}k_y}\delta(\boldsymbol{k}_\perp)\mathrm{d}\boldsymbol{k} \\ &= \frac{\mathrm{d}P(\phi;p_- \to p_- - k_-)}{\mathrm{d}t\mathrm{d}k_-}\mathrm{d}k_- \\ &= \frac{p_-}{\varepsilon}\frac{\mathrm{d}P(\phi;p_- \to p_- - k_-)}{\mathrm{d}\phi\mathrm{d}k_-}\mathrm{d}k_-.\end{aligned} \tag{3.9}$$

We emphasize here that the electron and photon momenta only appear as p_- and k_- in the expression $\mathrm{d}P(\phi;p_- \to p_- - k_-)/d\phi\mathrm{d}k_-$ [Ritu 85]. Utilizing the approximated expressions in eq. (3.8) and in eq. (3.9) derived above, the initial kinetic equation (3.2) is turned into

$$\begin{aligned}\left[\frac{\partial}{\partial\phi} + eE(\phi)\frac{\partial}{\partial p_z}\right] g_{e^-}(\phi,\boldsymbol{p}_\perp)n_{e^-}(\phi,p_-) = \\ g_{e^-}(\phi,\boldsymbol{p}_\perp)\left[\int_0^\infty dk_-\,\frac{dP(\phi;p_- + k_- \to p_-)}{d\phi dk_-}n_{e^-}(\phi,p_- + k_-)\right. \\ \left. -n_{e^-}(\phi,p_-)\int_0^\infty dk_-\,\frac{dP(\phi;p_- \to p_- - k_-)}{d\phi dk_-}\right].\end{aligned} \tag{3.10}$$

At this point, the function $g_{e^-}(\phi,\boldsymbol{p}_\perp)$ can be chosen to fulfill the Liouville-like equation

$$\left[\frac{\partial}{\partial\phi} + eE(\phi)\frac{\partial}{\partial p_z}\right] g_{e^-}(\phi,\boldsymbol{p}_\perp) = 0. \tag{3.11}$$

Considering $g_{e^-}(0,\boldsymbol{p}_\perp)$ to be a function $\tilde{g}_{e^-}(\boldsymbol{p}_\perp)$ well-peaked in the region $\boldsymbol{p}_\perp \approx \boldsymbol{0}$, the solution of eq. (3.11) reads $g_{e^-}(\phi,\boldsymbol{p}_\perp) = \tilde{g}_{e^-}(\boldsymbol{p}_\perp + e\boldsymbol{A}(\phi))$, with $\boldsymbol{A}(\phi) = (0,0,-\int_0^\phi d\phi' E(\phi'))$ (see also eq. (3.4)), leading to a decoupling of the evolution of the transverse and the longitudinal momenta. Note that also the initial function $\tilde{g}_{e^-}(\boldsymbol{p}_\perp) = \delta(\boldsymbol{p}_\perp)$ is a valid choice in the limiting case. This reduces eq. (3.10) to

$$\begin{aligned}\frac{\partial n_{e^-}(\phi,p_-)}{\partial\phi} = \int_0^\infty \mathrm{d}k_-\,\frac{\mathrm{d}P(\phi;p_- + k_- \to p_-)}{\mathrm{d}\phi\mathrm{d}k_-}n_{e^-}(\phi,p_- + k_-) \\ - n_{e^-}(\phi,p_-)\int_0^\infty \mathrm{d}k_-\,\frac{\mathrm{d}P(\phi;p_- \to p_- - k_-)}{\mathrm{d}\phi\mathrm{d}k_-},\end{aligned} \tag{3.12}$$

and we stress the fact that there are no terms arising from the Lorentz force, since p_- is a constant of motion in the presence of a plane-wave background field. In fact, this indicates that without the occurrence of photon emission the electron distribution function cannot depend on the laser phase but only on p_-. By recalling the complete electron distribution function $f_{e^-}(t,\boldsymbol{r},\boldsymbol{p}) = f_T(T)f_\perp(\boldsymbol{r}_\perp)g_{e^-}(\phi,\boldsymbol{p}_\perp)n_{e^-}(\phi,p_-)$ and employing a particular well-peaked function $g_{e^-}(\phi,\boldsymbol{p}_\perp)$, e.g., a Gaussian, the electron distribution function $F_{e^-}(t,\boldsymbol{r})$ in the configuration space can be approximated as

$$\begin{aligned}F_{e^-}(t,\boldsymbol{r}) &= \int \mathrm{d}\boldsymbol{p}\, f_{e^-}(t,\boldsymbol{r},\boldsymbol{p}) \\ &\approx f_T(T)f_\perp(\boldsymbol{r}_\perp)\int_0^\infty \frac{\mathrm{d}p_-}{2}\, n_{e^-}(\phi,p_-),\end{aligned} \tag{3.13}$$

where the additional factor 1/2 origins from the change of variable from p_y to p_-. Note that the function $n_{e^-}(\phi, p_-)$ is presumed to be peaked in the region of p_- such that $p_- \approx 2\varepsilon$. It can be easily derived that the expression $\int_0^\infty \mathrm{d}p_- n_{e^-}(\phi, p_-)$ is actually independent of ϕ by integrating eq. (3.12) with respect to p_-. Hence, we can conclude from eq. (3.13) that the spatial shape of the electron bunch remains unchanged throughout the collision, whereas the movement of its center is determined by $y \approx -t$ and $\boldsymbol{r}_\perp \approx \boldsymbol{0}$.

Before coming to the final form of the kinetic equation for the electrons, we turn to the full kinetic equation for the photon distribution $f_\gamma(t, \boldsymbol{r}, \boldsymbol{k})$,

$$\left[\frac{\partial}{\partial t} + \frac{\boldsymbol{k}}{\omega} \cdot \frac{\partial}{\partial \boldsymbol{r}}\right] f_\gamma(t, \boldsymbol{r}, \boldsymbol{k}) = \int \mathrm{d}\boldsymbol{p} \, \frac{\mathrm{d}P(\phi; \boldsymbol{p}_\perp \to \boldsymbol{p}_\perp - \boldsymbol{k}_\perp, p_- \to p_- - k_-)}{\mathrm{d}t \mathrm{d}\boldsymbol{k}} f_{e^-}(t, \boldsymbol{r}, \boldsymbol{p}). \tag{3.14}$$

By following the same course of derivation as in the case of the electron distribution, we can simplify the kinetic equation and obtain

$$\frac{\partial n_\gamma(\phi, k_-)}{\partial \phi} = \int_0^\infty \mathrm{d}p_- \, \frac{\mathrm{d}P(\phi; p_- \to p_- - k_-)}{\mathrm{d}\phi \mathrm{d}k_-} n_{e^-}(\phi, p_-), \tag{3.15}$$

where we defined $n_\gamma(\phi, k_-)$ analogously to $n_{e^-}(\phi, p_-)$. We will now return to the original notation $\varphi = \omega_0 \phi$ and introduce $p_{i,-} = p_- + k_-$ as the initial momentum of the electron. In the last step, we adopt the single-photon emission probability averaged over the initial electron spin and summed over the final electron spin and photon polarization per unit phase φ and per unit $u = k_-/(p_- - k_-)$ (see [Ritu 85] and eq. (2.25)),

$$\begin{aligned} \frac{\mathrm{d}P_{p_-}}{\mathrm{d}\varphi \mathrm{d}u} =& \frac{\alpha}{\sqrt{3}\pi} \frac{m^2}{\omega_0 p_-} \frac{1}{(1+u)^2} \left[\left(1 + u + \frac{1}{1+u}\right)\right. \\ & \left. \times \mathrm{K}_{\frac{2}{3}}\left(\frac{2u}{3\chi(\varphi, p_-)}\right) - \int_{\frac{2u}{3\chi(\varphi,p_-)}}^\infty \mathrm{d}x \, \mathrm{K}_{\frac{1}{3}}(x)\right], \end{aligned} \tag{3.16}$$

where $\mathrm{K}_\nu(x)$ is the modified Bessel function of the second kind of νth order and $\chi(\varphi, p_-) = (p_-/m)|E(\varphi)|/F_{\mathrm{cr}}$. This probability has actually been derived for the case of a constant crossed field but, as mentioned before, can be applied here since the variation of the field within one radiation formation length is negligible due to $\xi \gg 1$. Together with the identification $\omega_0^{-1} \mathrm{d}P(\phi; p_{i,-} \to p_{i,-} - k_-)/\mathrm{d}\phi \mathrm{d}k_- \mapsto \mathrm{d}P_{p_{i,-}}/\mathrm{d}\varphi \mathrm{d}k_-$ (note that, as $p_{i,-} = p_- + k_-$, where p_- refers to the final electron, $\mathrm{d}P_{p_{i,-}}/\mathrm{d}\varphi \mathrm{d}k_- = \mathrm{d}P_{p_{i,-}}/\mathrm{d}\varphi \mathrm{d}p_-$), the result of our derivation is the set of kinetic equations (see [Baie 94])

$$\frac{\partial n_{e^-}(\varphi, p_-)}{\partial \varphi} = \int_{p_-}^\infty \mathrm{d}p_{i,-} \, n_{e^-}(\varphi, p_{i,-}) \frac{\mathrm{d}P_{p_{i,-}}}{\mathrm{d}\varphi \mathrm{d}p_-} - n_{e^-}(\varphi, p_-) \int_0^{p_-} \mathrm{d}k_- \frac{\mathrm{d}P_{p_-}}{\mathrm{d}\varphi \mathrm{d}k_-}, \tag{3.17}$$

$$\frac{\partial n_\gamma(\varphi, k_-)}{\partial \varphi} = \int_{k_-}^\infty \mathrm{d}p_{i,-} \, n_{e^-}(\varphi, p_{i,-}) \frac{\mathrm{d}P_{p_{i,-}}}{\mathrm{d}\varphi \mathrm{d}k_-}, \tag{3.18}$$

with

$$\frac{\mathrm{d}P_{p_{i,-}}}{\mathrm{d}\varphi \mathrm{d}p_-} = \left|\frac{\mathrm{d}u}{\mathrm{d}p_-}\right| \left.\frac{\mathrm{d}P_{p_{i,-}}}{\mathrm{d}\varphi \mathrm{d}u}\right|_{u=(p_{i,-}-p_-)/p_-} = \frac{p_{i,-}}{p_-^2} \left.\frac{\mathrm{d}P_{p_{i,-}}}{\mathrm{d}\varphi \mathrm{d}u}\right|_{u=(p_{i,-}-p_-)/p_-}, \tag{3.19}$$

$$\frac{\mathrm{d}P_{p_-}}{\mathrm{d}\varphi \mathrm{d}k_-} = \frac{\mathrm{d}u}{\mathrm{d}k_-}\left.\frac{\mathrm{d}P_{p_-}}{\mathrm{d}\varphi \mathrm{d}u}\right|_{u=k_-/(p_- - k_-)} = \frac{p_-}{(p_- - k_-)^2}\left.\frac{\mathrm{d}P_{p_-}}{\mathrm{d}\varphi \mathrm{d}u}\right|_{u=k_-/(p_- - k_-)}, \tag{3.20}$$

$$\frac{\mathrm{d}P_{p_{i,-}}}{\mathrm{d}\varphi \mathrm{d}k_-} = \frac{\mathrm{d}u}{\mathrm{d}k_-}\left.\frac{\mathrm{d}P_{p_{i,-}}}{\mathrm{d}\varphi \mathrm{d}u}\right|_{u=k_-/(p_{i,-} - k_-)} = \frac{p_{i,-}}{(p_{i,-} - k_-)^2}\left.\frac{\mathrm{d}P_{p_{i,-}}}{\mathrm{d}\varphi \mathrm{d}u}\right|_{u=k_-/(p_{i,-} - k_-)}. \tag{3.21}$$

Note that equation (3.17) is an integro-differential equation, i.e., it is non-local in the momentum p_-. This fact is deeply related to the quantum nature of the emission of radiation, which is quantum mechanically described as the emission of photons which carry energy and momentum. Through this emission process the initial momentum $p_{0,-}$ of an electron emitting a photon with momentum k_- will be coupled to that with momentum $p_{0,-} - k_-$, where k_- spans from 0 to $p_{0,-}$.

Integrating eq. (3.17) over p_- yields after a short calculation

$$\frac{\partial}{\partial \varphi}\int_0^\infty \mathrm{d}p_-\, n_{e^-}(\varphi, p_-) = \frac{\partial N_{e^-}}{\partial \varphi} = 0, \tag{3.22}$$

which expresses the conservation of the total number of electrons N_{e^-}. Furthermore, by multiplying the kinetic equation of the electron and the photon distributions by p_- and k_-, respectively, and in turn integrating over all p_- and k_-, we achieve

$$\frac{\partial}{\partial \varphi}\left[\int_0^\infty \mathrm{d}p_-\, n_{e^-}(\varphi, p_-)p_- + \int_0^\infty \mathrm{d}k_-\, n_\gamma(\varphi, k_-)k_-\right] = 0, \tag{3.23}$$

implying that the total energy minus the total longitudinal momentum is conserved. As the total number of electrons is conserved, equation (3.17) must be expressible by means of a continuity equation

$$\frac{\partial n_{e^-}(\varphi, p_-)}{\partial \varphi} + \frac{\partial j(\varphi, p_-, n_{e^-}(\varphi, p_-))}{\partial p_-} = 0, \tag{3.24}$$

where $j(\varphi, p_-, n_{e^-}(\varphi, p_-))$ indicates the current density that in principle can depend on phase and momentum as well as on the distribution function itself. In fact, after some algebra we find

$$\begin{aligned} j(\varphi, p_-, n_{e^-}(\varphi, p_-)) = &-\frac{\alpha m^2}{\sqrt{3}\pi\omega_0}\int_{p_-}^\infty \mathrm{d}p'_-\, n_{e^-}(\varphi, p'_-)\left\{\int_0^{p_-}\frac{\mathrm{d}p''_-}{p'^2_-}\right. \\ &\left.\times\left[\left(\frac{p'_-}{p''_-} + \frac{p''_-}{p'_-}\right)\mathrm{K}_{\frac{2}{3}}\left(Y(\varphi, p'_-, p''_-)\right) - \int_{Y(\varphi, p'_-, p''_-)}^\infty \mathrm{d}x\, \mathrm{K}_{\frac{1}{3}}(x)\right]\right\}, \end{aligned} \tag{3.25}$$

with

$$Y(\varphi, p'_-, p''_-) = \frac{2mF_{\mathrm{cr}}}{3p'_-|E(\varphi)|}\left(\frac{p'_-}{p''_-} - 1\right). \tag{3.26}$$

Once more the structure of the current density in eq. (3.25) emphasizes the non-locality in the electron momentum, since it is not possible to separate the distribution function from the current density.

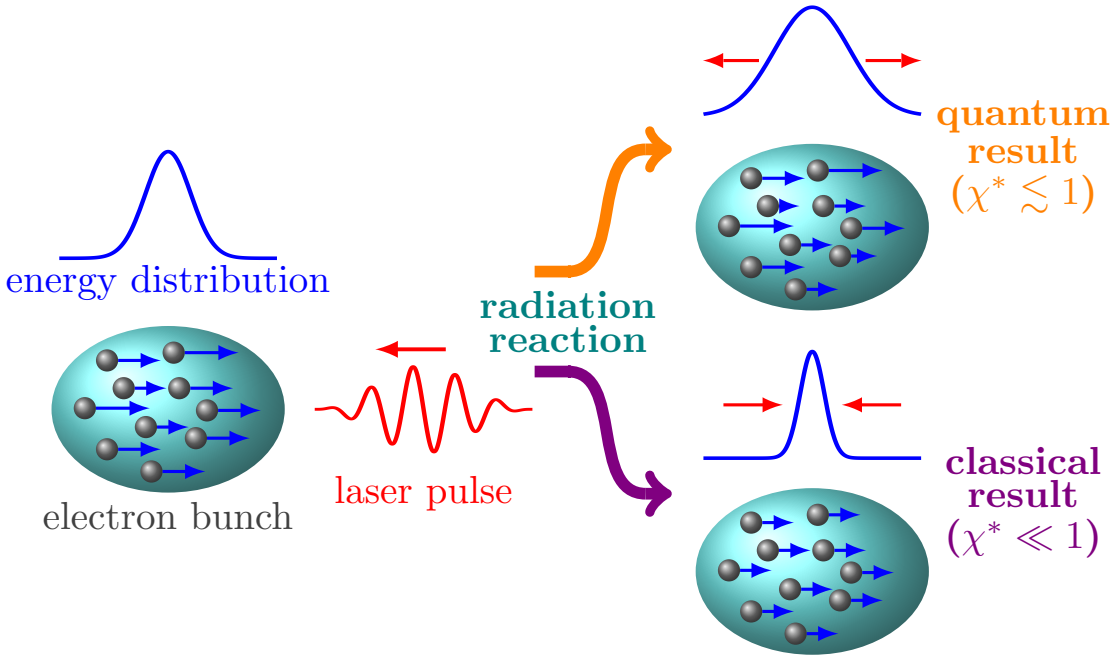

Figure 3.2: Schematic depiction of the effect of RR in the classical and the nonlinear moderately quantum regime.

3.2 Comparison of the classical and the nonlinear moderately quantum regime

After the derivation of the kinetic equations, we now turn to the predictions they make about the phase evolution of the electron and photon distributions especially for the nonlinear moderately quantum regime. The numerical evaluation of eq. (3.17), however, immediately leads to a contradiction to the results obtained in classical electrodynamics by employing the LL equation. The different impact of including RR in the classical and the quantum regime is schematically depicted in fig. 3.2. It was shown that in the framework of classical electrodynamics the energy distribution of particles interacting with strong laser fields is narrowed by the effects of RR [Zhid 02, Naum 09, Chen 11, Tamb 10, Tamb 11]. On the other hand, the numerical investigation of eq. (3.17) reveals an opposite effect, namely an increase in the energy width of the electron beam. In order to understand this striking difference in the consequences of RR in both regimes, we investigate the classical limit of eq. (3.17) for $\chi(\varphi, p_-) \ll 1$ (the derivation of the analytical expansion of eq. (3.17) can be found in app. B). To this purpose, it is favorable to perform the changes of variables $\mathrm{v} = (p_{i,-} - p_-)/p_-\chi(\varphi, p_-)$ and $\mathrm{v} = k_-/(p_- - k_-)\chi(\varphi, p_-))$ in the first and second integral in eq. (3.17), respectively. Expanding the resulting equation in $\chi(\varphi, p_-)$ up to the order $\chi^3(\varphi, p_-)$ yields the Fokker-Planck-like equation [Gard 09] (see also [Pita 81, Soko 10])

$$\frac{\partial n_{e^-}(\varphi, p_-)}{\partial \varphi} = -\frac{\partial}{\partial p_-}\left[A(\varphi, p_-) n_{e^-}(\varphi, p_-)\right] + \frac{1}{2}\frac{\partial^2}{\partial p_-^2}\left[B(\varphi, p_-) n_{e^-}(\varphi, p_-)\right] \tag{3.27}$$

with a "drift" coefficient $A(\varphi, p_-)$ and a "diffusion" coefficient $B(\varphi, p_-)$ given by

$$A(\varphi, p_-) = -\frac{2\alpha m^2}{3\omega_0}\chi^2(\varphi, p_-)\left[1 - \frac{55\sqrt{3}}{16}\chi(\varphi, p_-)\right] \tag{3.28}$$

$$B(\varphi, p_-) = \frac{\alpha m^2}{3\omega_0}\frac{55}{8\sqrt{3}}p_-\chi^3(\varphi, p_-), \tag{3.29}$$

respectively (see also sec. C.2). Note that this expansion transformed eq. (3.17) from an integro-differential equation into a partial differential equation, i.e., for small quantum photon-recoil effects the evolution of the electron distribution function with momentum p_- is essentially determined by values in the vicinity of p_-, rendering its dynamics local. Finally, we mention that in an expansion up to higher orders in $\chi(\varphi, p_-)$, terms proportional to higher-order derivatives of $n_{e^-}(\varphi, p_-)$ with respect to p_- would arise.

3.2.1 Classical dynamics

At first, we only consider the terms proportional to $\chi^2(\varphi, p_-)$ in eq. (3.27), resulting in a Liouville-type equation:

$$\frac{\partial n_{e^-}(\varphi, p_-)}{\partial \varphi} = -\frac{\partial}{\partial p_-}\left(n_{e^-}(\varphi, p_-)\frac{\mathrm{d}p_-^{(c)}}{\mathrm{d}\varphi}\right) \tag{3.30}$$

with

$$\frac{\mathrm{d}p_-^{(c)}}{\mathrm{d}\varphi} = -\frac{I_{cl}(\varphi, p_-)}{\omega_0}, \tag{3.31}$$

where $I_{cl}(\varphi, p_-) = (2/3)\alpha m^2\chi^2(\varphi, p_-)$ indicates the classical radiation intensity [Land 75]. Employing the LL equation, one obtains exactly the classical single-particle equation for p_- in eq. (3.31) [Di P 08] (see also [Elki 11]). This implies that the classical dynamics of the electron distribution including RR is characterized precisely by the terms proportional to $\chi^2(\varphi, p_-)$ in eq. (3.27). In addition, eq. (3.30) being of the Liouville type indicates that the evolution of the electron distribution is deterministic in classical electrodynamics, as it has to be [Gard 09]. Moreover, the single-particle equation in eq. (3.31) allows for an analytical solution for $p_-^{(c)}(\varphi, p_{0,-})$ [Di P 08],

$$p_-^{(c)}(\varphi, p_{0,-}) = \frac{p_{0,-}}{h^{(c)}(\varphi, p_{0,-})} \tag{3.32}$$

with

$$h^{(c)}(\varphi, p_{0,-}) = 1 + \frac{2}{3}\alpha\frac{p_{0,-}}{\omega_0}\frac{E_0^2}{F_{\mathrm{cr}}^2}\int_0^\varphi \mathrm{d}\varphi' f^2(\varphi'), \tag{3.33}$$

for an electron with initial momentum $p^\mu(0) = p_0^\mu = (\epsilon_0, \boldsymbol{p}_0)$ ($p_{0,-} = \epsilon_0 - p_{0,y}$) at the initial phase $\varphi_i = 0$. As $0 < \partial p_-^{(c)}(\varphi, p_{0,-})/\partial p_{0,-} < 1$ for $\varphi > 0$, we can immediately observe that the difference $\Delta p_-^{(c)}(\varphi)$ between the momenta of two electrons decreases for increasing values of φ, which is due to the nonlinearity of I_{cl} in the parameter $\chi(\varphi, p_-)$. Explicitly, the difference between the two momenta $p_-^{(a)}$ and $p_-^{(b)}$ with initial values $p_{0,-}^{(a)}$ and $p_{0,-}^{(b)}$, respectively, evolves like (w.l.o.g. $p_-^{(a)} > p_-^{(b)}$)

$$\Delta^c p_-(\varphi) = p_-^{(a)}(\varphi) - p_-^{(b)}(\varphi) = \frac{p_{0,-}^{(a)} - p_{0,-}^{(b)}}{h^{(c)}\left(\varphi, p_{0,-}^{(a)}\right)h^{(c)}\left(\varphi, p_{0,-}^{(b)}\right)} \leq p_{0,-}^{(a)} - p_{0,-}^{(b)}. \tag{3.34}$$

Since we have the analytical solution (refLLansol) at hand, the exact analytical solution of eq. (3.30) can be derived by means of the method of characteristics. Considering as initial distribution $n_{e^-}(0, p_-)$, e.g., a Gaussian

$$n_{e^-}(0, p_-) = \frac{N_{e^-}}{\sqrt{\frac{\pi}{2}}\sigma_{p_-}\left[1 + \mathrm{erf}\left(\frac{p_-^*}{\sqrt{2}\sigma_{p_-}}\right)\right]} \exp\left[-\frac{(p_- - p_-^*)^2}{2\sigma_{p_-}^2}\right], \tag{3.35}$$

where N_{e^-} is again the total number of electrons, p_-^* is the average value of p_- and σ_{p_-} is the standard deviation[II], the solution of eq. (3.30) can be written as

$$n_{e^-}(\varphi, p_-) = \frac{N_{e^-}}{\sqrt{\frac{\pi}{2}}\sigma_{p_-}\left[1 + \mathrm{erf}\left(\frac{p_-^*}{\sqrt{2}\sigma_{p_-}}\right)\right] g^2(\varphi, p_-)} \exp\left\{-\frac{1}{2\sigma_{p_-}^2}\left[\frac{p_-}{g(\varphi, p_-)} - p_-^*\right]^2\right\}, \tag{3.36}$$

where we introduced the function

$$g(\varphi, p_-) = 1 - \frac{2}{3}\alpha\frac{p_-}{\omega_0}\frac{E_0^2}{F_{\mathrm{cr}}^2}\int_0^\varphi d\phi f^2(\phi). \tag{3.37}$$

Note that $g(\varphi, p_-) = h^{(c)}(\varphi, -p_-)$. As $p_{0,-}$ is positive for finite values of $p_{0,y}$ and $p_{0,-} \to 0$ only at $p_y \to +\infty$ and as $p_{0,-} = p_-^{(c)}(\varphi, p_{0,-})g(\varphi, p_-^{(c)}(\varphi, p_{0,-}))$, the function $g(\varphi, p_-)$ has to be strictly positive for all values of φ. This implies that at each φ there is a maximum value $p_{-,\max} = p_{-,\max}(\varphi)$ for p_- fixed by the equation $g(\varphi, p_{-,\max}) = 0$. The appearance of $g(\varphi, p_-)$ in the exponent of eq. (3.36) indicates again that classical RR effects tend to decrease the energy width of the electron distribution, which is in accordance with results obtained in previous studies of the production of particle beams via laser-plasma interaction [Zhid 02,Naum 09,Chen 11,Tamb 10,Tamb 11]. In addition, in case of $\sigma_{p_-} \ll p_-^*$ in eq. (3.36), it can be shown that the distribution $n_{e^-}(\varphi, p_-)$ is approximately a Gaussian centered at $p_-^{(c)}(\varphi, p_-^*)$ and has approximately an effective width of

$$\sigma_{p_-}^{(c)}(\varphi, p_-^*) \approx \frac{\sigma_{p_-}}{h^2(\varphi, p_-^*)}, \tag{3.38}$$

which decreases with increasing φ.

Finally, we also want to test the numerical coincidence of eq. (3.17) and eq. (3.30) in a situation where quantum effects are negligible but RR effects are large. Therefore, a 1600-cycle optical laser pulse (corresponding to a final phase of $\varphi_f = 3200\pi$), i.e., $f(\varphi) = f_1(\varphi) = \sin(\varphi)\sin^2(\varphi/3200)$ (corresponding to a pulse duration τ of about 4 ps) with peak intensity $I_{0,1} = 4.3 \times 10^{20}$ W/cm^2 and central angular frequency $\omega_0 = 1.55$ eV ($\xi_1 = 10$) is considered to collide with an initially Gaussian electron beam centered at $p_-^* = 84$ MeV ($\varepsilon^* \approx p_-^*/2 = 42$ MeV) such that $\chi_1^* = (p_-^*/m)(E_0/F_{\mathrm{cr}}) \approx 5 \times 10^{-3}$ with width $\sigma_{p_-} = 8.4$ MeV and $N_{e^-} = 1000$ the total number of electrons. The results for the initial and final distributions are shown in fig. 3.3. Corroborating the discussion above, the final distribution $n_{e^-}(\varphi_f, p_-)$, obtained by numerically solving eq. (3.17) (solid, red line), and the classical analytical solution $n_{e^-}^{\mathrm{LL}}(\varphi_f, p_-)$ (see eq. (3.36)) are very similar and both display a

[II] This is strictly only true if the variable p_- spans from $-\infty$ to $+\infty$. However, the momentum p_- allows only for positive values, and in the case where $p_-^* \gg \sigma_{p_-}$ (which will be fulfilled in all our numerical examples), p_-^* and σ_{p_-} are good approximations of the average value and of the standard deviation of the distribution, respectively.

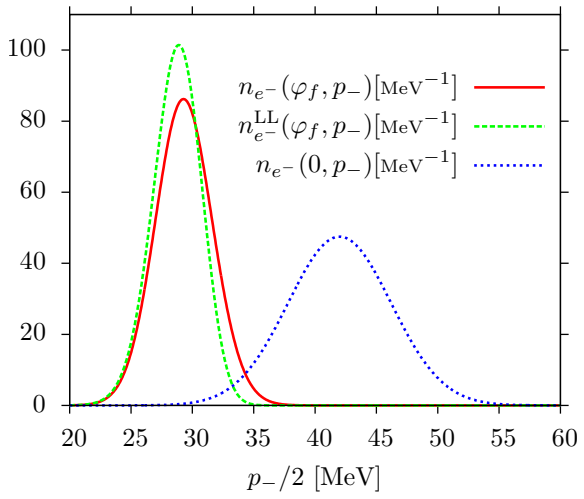

Figure 3.3: Comparison of the initial electron distribution (dotted, blue line) and the final electron distribution according to eq. (3.17) (solid, red line) and to eq. (3.36) (dashed, green line), as functions of $p_-/2 \approx \varepsilon$. The laser and the electron distribution parameters are given in the text [Neit 13].

decrease of the width from 8.4 MeV to 4.7 MeV. Note that for an average energy of $\varepsilon_f^* = 30$ MeV of the final distribution, the condition $\varepsilon_f^* \gg m\xi_1 = 5$ MeV ensuring the validity of our approach is fairly well-fulfilled.

3.2.2 Replacement of the classical intensity I_{cl} by the quantum intensity I_q

An examination of the structure of eq. (3.30) and eq. (3.31) seems to suggest that the quantum description of RR effects would be incorporated in the evolution of the electron distribution function by the replacement of the classical radiation intensity $I_{cl}(\varphi, p_-)$ by the corresponding quantum one $I_q(\varphi, p_-)$ (see eq. (2.26)). And, in fact, we observe that the leading quantum correction proportional to $\chi^3(\varphi, p_-)$ in the drift coefficient $A(\varphi, p_-)$ (see eq. (3.28)) is exactly the term one achieves by the substitution $I_{cl}(\varphi, p_-) \to I_q(\varphi, p_-)$ [Baie 94, Ritu 85]. The replacement of the intensity and the subsequent modification of the drift coefficient, however, does not alter the Liouville-like structure of the approximated kinetic equation, whereas the momentum change per unit phase is "effectively" changed. In particular, the single-particle equation corresponding to the modified kinetic equation is still a deterministic differential equation. As we find the leading quantum correction to be negative, it is expectable that the classically predicted narrowing of the energy width is reduced or even overcome. In order to investigate whether the replacement of the intensities would lead to a broadening in the energy width, we return to the evolution of the difference between two momenta $p_-^{(a)}$ and $p_-^{(b)}$ with initial values $p_{0,-}^{(a)}$ and $p_{0,-}^{(b)}$, respectively (w.l.o.g. $p_-^{(a)} > p_-^{(b)}$). Taking into account the full expression

for the quantum intensity given in eq. (2.26), one obtains

$$\begin{aligned}\frac{\mathrm{d}\Delta^q p_-(\varphi)}{\mathrm{d}\varphi} &= \frac{\mathrm{d}p_-^{(a)}(\varphi)}{\mathrm{d}\varphi} - \frac{\mathrm{d}p_-^{(b)}(\varphi)}{\mathrm{d}\varphi} = -\frac{1}{\omega_0}\left[I_q\left(\varphi, p_-^{(a)}\right) - I_q\left(\varphi, p_-^{(b)}\right)\right] \\ &= -\frac{\alpha m^2}{3\sqrt{3}\pi\omega_0}\int_0^\infty \mathrm{d}u\, \frac{4u^3+5u^2+4u}{(1+u)^4}\left[\mathrm{K}_{\frac{2}{3}}\left(\frac{2u}{3\chi\left(\varphi, p_-^{(a)}\right)}\right) - \mathrm{K}_{\frac{2}{3}}\left(\frac{2u}{3\chi\left(\varphi, p_-^{(b)}\right)}\right)\right] \\ &\leq 0,\end{aligned} \tag{3.39}$$

where we made use of the fact that the modified Bessel function of the second kind is strictly decreasing. Thus, although the substitution $I_{cl}(\varphi, p_-) \to I_q(\varphi, p_-)$ might extenuate the reduction of the energy width, the incorporation of the quantum intensity would still predict a narrowing of the energy distribution. This can also be understood intuitively, since quantum mechanically, electrons with higher energy will *on average* emit more radiation. Therefore, we can conclude that the broadening of the electron distribution must be due to another reason than the modification of the drift coefficient $A(\varphi, p_-)$ and we will see in the next section that it is caused by the appearance of the diffusion term $B(\varphi, p_-)$.

3.2.3 Stochastic nature of photon emission

Recalling the approximated Fokker-Planck-like equation (3.27), we identify another quantum correction that is of the same order as the one in the function $A(\varphi, p_-)$. This second quantum correction manifests itself in the occurrence of the diffusion coefficient $B(\varphi, p_-)$, which is also multiplied by a second -order derivative of $n_{e^-}(\varphi, p_-)$ with respect to p_-. In turn, the Liouville-like structure of the classical kinetic equation (3.30) is substantially altered and this structural change is closely related to the stochastic nature of the quantum emission of photons. In accordance with the theory of stochastic differential equations, the Fokker-Planck-like equation (3.27) describing the evolution of the electron distribution can be connected with a single-particle stochastic equation

$$\mathrm{d}p_- = A(\varphi, p_-)\mathrm{d}\varphi + \sqrt{B(\varphi, p_-)}\mathrm{d}W, \tag{3.40}$$

where $\mathrm{d}W$ represents an infinitesimal stochastic function [Gard 09] (see app. C), i.e., the trajectory of a single beam electron is no longer deterministic as in the framework of classical electrodynamics. In fact, the diffusion term in eq. (3.27) tends to increase in the energy width of the distribution [Gard 09] (see also sec. C.2) and, as we will see in our numerical simulations below, it is causing the broadening of the electron distribution function. In app. D, an approximated solution of the Fokker-Planck-like equation (3.27) is derived assuming that a Gaussian distribution centered at p_-^* and with width $\sigma_{p_-} \ll p_-^*$ at $\varphi_i = 0$ will keep its Gaussian shape and be well-peaked throughout the whole interaction. The movement of the center of the Gaussian can then be approximately described by (see eq. (D.9) and eq. (D.10))

$$p_-^{(q)}(\varphi, p_-^*) \approx p_-^{(c)}(\varphi, p_-^*)[1 + \delta h(\varphi, p_-^*)], \tag{3.41}$$

where we introduced the correction to $h^{(c)}(\varphi, p_-^*)$ introduced above (see eq. (D.10))

$$\delta h^{(c)}(\varphi, p_-^*) = \frac{55\sqrt{3}}{16 h^{(c)}(\varphi, p_-^*)}\int_0^\varphi \mathrm{d}\varphi' \chi(\varphi', p_-^*)\frac{\partial}{\partial\varphi'}\left\{\ln\left[h^{(c)}(\varphi', p_-^*)\right]\right\}. \tag{3.42}$$

Note that the expression $\delta h^{(c)}(\varphi, p_-^*)$ originates from the quantum correction to the drift function $A(\varphi, p_-)$ and that it is non-negative for all phases $\varphi > 0$. Furthermore, the evolution of the width of the distribution is given by

$$\sigma_{p_-}^{(q)}(\varphi, p_-^*) \approx \sigma_{p_-}^{(c)}(\varphi, p_-^*) \left[1 + 2\delta h(\varphi, p_-^*) + \frac{1}{2\sigma_{p_-}^2} \int_0^\varphi \mathrm{d}\varphi' B(\varphi', p_-^*) \right], \tag{3.43}$$

making apparent that both quantum corrections discussed above tend to increase the width of the distribution function. Moreover, we note here that the broadening caused by the diffusion term is roughly $\zeta = p_-^{*2}/\sigma_p^2 \gg 1$ times larger than $\delta h(\varphi, p_-^*)$ and thus dominates the broadening in the considered parameter regime. In addition, we emphasize that the approximated solution based on the Fokker-Planck equation is only justified at $\alpha\xi\zeta\Phi_L\chi^{*2} \ll 1$, with Φ_L being the total laser phase. Finally, we turn to a technical aspect of the use of the Fokker-Planck equation. Considering, e.g., an initial δ-like momentum distribution and a vanishing drift term, the Fokker-Planck equation predicts the occurrence of artificial particles with momentum larger than the initial one. This clearly unphysical feature implies that a completely consistent treatment of RR demands the evaluation of the full equation (3.17), which will be achieved numerically in the remainder of this thesis .

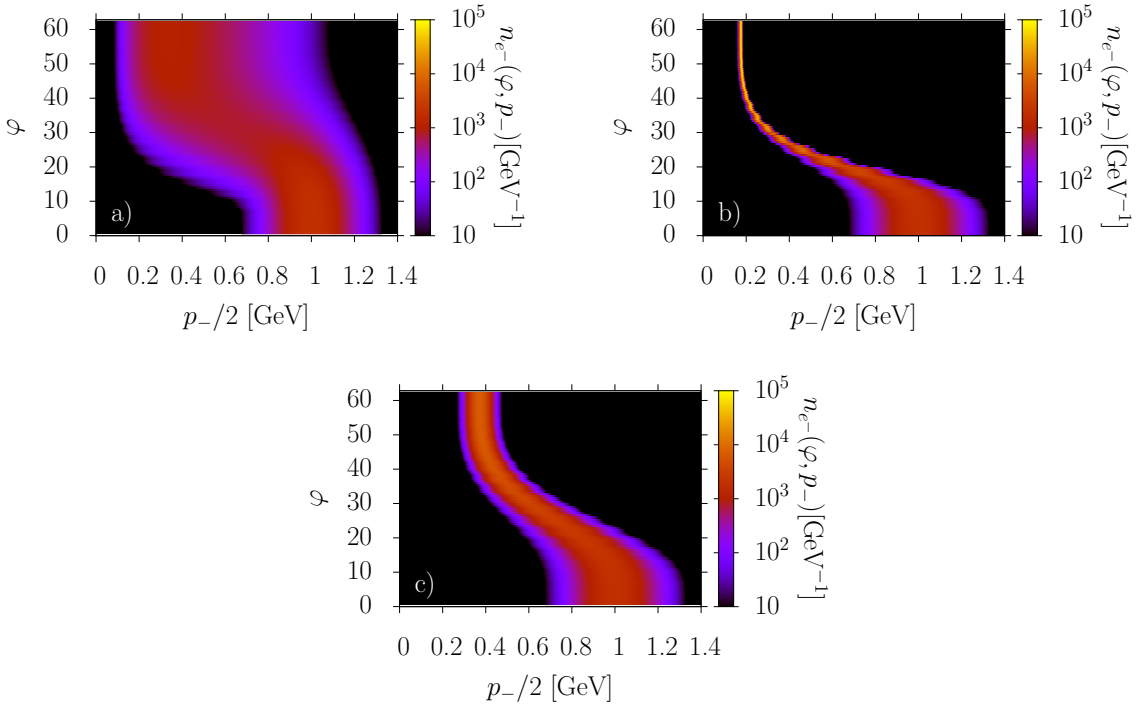

Figure 3.4: Phase evolution of the electron distribution as a function of $p_-/2 \approx \varepsilon$ for the shape function $f_2(\varphi)$ according to eq. (3.17) (part a)), to eq. (3.36) (part b)) and to eq. (3.30) with the replacement $I_{cl}(\varphi, p_-) \to I_q(\varphi, p_-)$ (part c)) [Neit 13].

In order to illustrate the effects discussed above and to show that they can in principle be experimentally verified with present-day technology, we consider a 10-cycle ($\varphi_f = 20\pi$), i.e., $f(\varphi) = f_2(\varphi) = \sin(\varphi)\sin^2(\varphi/20)$ ($\tau \approx 27$ fs), optical laser pulse with peak intensity $I_{0,2} = 2 \times 10^{22}$ W/cm^2 ($\xi_2 = 68$) [Yano 08] and

$\omega_0 = 1.55$ eV to collide with an initial Gaussian electron distribution with $p_-^* = 2$ GeV ($\varepsilon^* \approx 1$ GeV), such that $\chi_2^* = 0.8$, $\sigma_{p_-} = 0.2$ GeV, and a total number of 1000 electrons. Electron beams of such high energies are presently not only available in conventional accelerators but also by employing plasma-based electron accelerators [Leem 06, Wang 13], rendering an all-optical setup feasible in principle. The results of our numerical simulations are shown in fig. 3.4.

In agreement with our analysis above, the full quantum calculations based on eq. (3.17) displayed in fig. 3.4a) predicts a broadening of the electron distribution. On the other hand, a strong narrowing of the distribution is predicted in classical electrodynamics by employing the analytical solution in eq. (3.36) (see fig. 3.4b)). Moreover, in accordance with our findings in sec. 3.2.2 even the substitution $I_{cl}(\varphi, p_-) \to I_q(\varphi, p_-)$ would still lead to a narrowing of the distribution function (see fig. 3.4c)). Apparently these numerical results support the idea that the difference in the evolution of the electron beam in the classical and the nonlinear moderately quantum regime is due to the increasing importance of the stochasticity of photon emission in the quantum case. In addition, we mention that the condition ensuring the validity of our kinetic approach is fairly well-fulfilled, even in the most unfavorable classical treatment where the average energy of the final electron distribution is $\varepsilon_f^* = 173$ MeV corresponding to $\varepsilon_f^* \gg m\xi_2 = 35$ MeV.

Finally, we observe that the broadening of the electron momentum distribution caused by the inclusion of RR effects can also be interpreted in terms of the entropy of the distribution itself. Hence, we define the entropy (see sec. 2.2)

$$S(\varphi) := -\int_0^\infty \mathrm{d}p_-\, n_{e^-}(\varphi, p_-) \ln\left[\frac{n_{e^-}(\varphi, p_-)}{n_0}\right] \tag{3.44}$$

corresponding to the electron distribution, where we set the Boltzmann constant equal to unity and, in order to make the argument of the logarithm dimensionless, introduced the physically ineffective constant n_0, which can be chosen, for example, such that $S(0) = 0$ at initial phase φ_i. This definition implies the phase evolution of the entropy

$$\frac{\mathrm{d}S(\varphi)}{\mathrm{d}\varphi} = -\int_0^\infty \mathrm{d}p_-\, \frac{\partial n_{e^-}(\varphi, p_-)}{\partial\varphi} \ln\left[\frac{n_{e^-}(\varphi, p_-)}{n_0}\right] + \text{boundary terms}, \tag{3.45}$$

where the boundary terms can be assumed to vanish by virtue of physical considerations that the electron distribution as well as its derivative with respect to p_- vanish at the values $p_- \to 0$ and $p_- \to \infty$. Employing this definition and the approximated kinetic equation in eq. (3.27) results in

$$\frac{\mathrm{d}S(\varphi)}{\mathrm{d}\varphi} = -\frac{4\alpha m^2}{3\omega_0}\int_0^\infty \frac{\mathrm{d}p_-}{p_-}\chi^2(\varphi, p_-) n_{e^-}(\varphi, p_-)\Bigg\{1 - \frac{55\sqrt{3}}{32}\chi(\varphi, p_-) \times \left[1 + \frac{1}{6}\frac{p_-^2}{n_{e^-}^2(\varphi, p_-)}\left(\frac{\partial n_{e^-}(\varphi, p_-)}{\partial p_-}\right)^2\right]\Bigg\}. \tag{3.46}$$

This formula once more displays that the classical deterministic evolution of the electrons imply a "cooling" of the electron bunch, whereas the terms corresponding to quantum corrections induce a broadening of the distribution function.

3.3 Pulse-shape effects

Motivated by the fact that the final classical electron distribution $n_{e^-}(\varphi_f, p_-)$ given by eq. (3.36) depends only on the total fluence

$$\Phi = \frac{E_0^2}{\omega_0} \int_0^{\varphi_f} d\varphi f^2(\varphi), \tag{3.47}$$

we investigate in this section the influence of the laser pulse form $f(\varphi)$ on the electron and photon distributions at a given pulse fluence that can be modified in pulse shape and pulse duration via the various available pulse shaping techniques for laser pulses (see, e.g., [Wint 08] for a discussion of pulse shaping techniques in the context of High Harmonic Generation). Therefore, we solve the kinetic equations (3.17)-(3.18) numerically and consider a central angular frequency of the laser field corresponding to the laser photon energy $\omega_0 = 1.55\,\mathrm{eV}$ in the entire section.

3.3.1 Influence of the laser pulse shape

In the first numerical examples, we study the influence of two different shapes of the laser pulse at a given pulse fluence and pulse duration. The initial electron beam is assumed to be the Gaussian beam in eq. (3.35) with $N_{e^-} = 1000$, $p_-^* = 1.4\,\mathrm{GeV}$ corresponding to an average energy of $\varepsilon^* \approx 700\,\mathrm{MeV}$, and with $\sigma_{p_-} = 0.14\,\mathrm{GeV}$. Further, we choose two pulses of 20 cycles (final phase $\varphi_f = 40\pi$), the first one described by the function $f_3(\varphi) = \sin(\varphi)\sin^2(\varphi/40)$, with a peak intensity of $I_{0,3} = 10^{22}\,\mathrm{W/cm^2}$, and the second one by the function

$$f_4(\varphi) = \begin{cases} \sin(\varphi)\sin^2\left(\frac{\varphi}{4}\right) & \text{if } \varphi \in [0, 2\pi] \\ \sin(\varphi) & \text{if } \varphi \in [2\pi, 38\pi] \\ \sin(\varphi)\sin^2\left(\frac{\varphi - 36\pi}{4}\right) & \text{if } \varphi \in [38\pi, 40\pi], \end{cases} \tag{3.48}$$

corresponding to a pulse duration of 54 fs for both pulses. In order to achieve the same fluence $\Phi = 1.3 \times 10^9\,\mathrm{J/cm^2}$ for both pulses, the peak intensity of the second pulse is reduced to $I_{0,4} = 4 \times 10^{21}\,\mathrm{W/cm^2}$. The main difference between the two shape functions is that, while in the case of the first pulse the intensity increases and decreases smoothly over the entire pulse, the intensity is increased and decreased over just on cycle for the second pulse. The considered scenario yields the relativistic and the quantum nonlinearity parameters $\xi_3 = 48$ and $\chi_3^* = 0.40$ for the pulse shape $f_3(\varphi)$, and $\xi_4 = 31$ and $\chi_4^* = 0.25$ for the pulse shape $f_4(\varphi)$. As in both situations it is $\xi \gg 1$, we are allowed to apply the quasi-static approximation and we notice that we are slightly below the so-called quantum radiation dominated regime characterized by the conditions $R_Q = \alpha\xi \sim 1$ and $\chi^* \gtrsim 1$ [Di P 10] for the given parameters (see sec. 2.1.2).

In fig. 3.5 the phase evolution of the electron distributions $n_{e^-}(\varphi, p_-)$ and the photon spectra $n_\gamma(\varphi, k_-)k_-$ is shown for the pulse shape $f_3(\varphi)$ and in fig. 3.6 for the pulse shape $f_4(\varphi)$. fig. 3.5b) displays that for the pulse shape $f_3(\varphi)$, in the beginning less energy is emitted by the electrons and the main part of the energy is emitted at the peak of the pulse. On the contrary, in the case of the pulse shape $f_4(\varphi)$ (see fig. 3.6b)), the emission starts almost immediately after arrival of the pulse, which is due to the vast increase of the intensity to the maximum value over just one cycle. The same characteristic pattern can also be recognized in the evolution of the

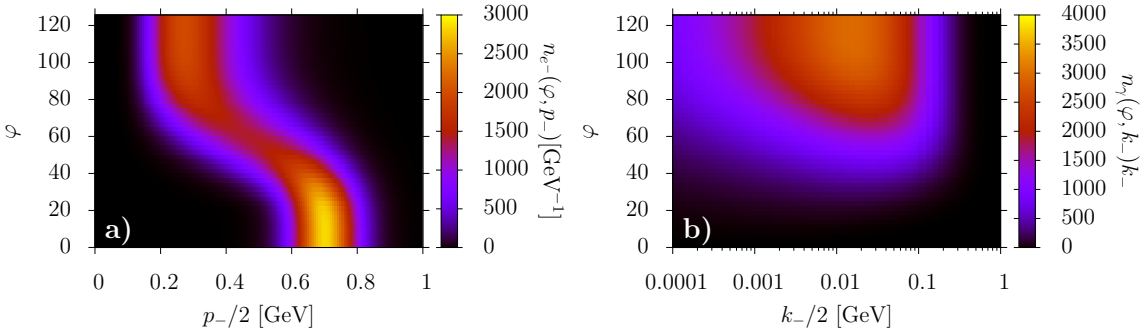

Figure 3.5: Phase evolution of the electron distribution (part a)) as a function of $p_-/2 \approx \varepsilon$ and the photon spectrum (part b)) as a function of $k_-/2 \approx \omega$ for the shape function $f_3(\varphi)$ [Neit 14].

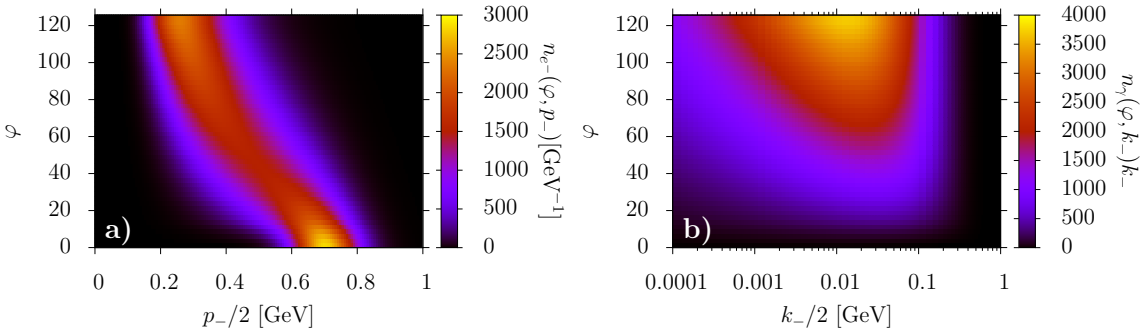

Figure 3.6: Phase evolution of the electron distribution (part a)) as a function of $p_-/2 \approx \varepsilon$ and the photon spectrum (part b)) as a function of $k_-/2 \approx \omega$ for the shape function $f_4(\varphi)$ [Neit 14].

electron distributions in fig. 3.5a) and fig. 3.6a). Further, in the case of the pulse shape $f_4(\varphi)$, we can identify a photon yield exceeding the one for the pulse shape $f_3(\varphi)$ (see also the final photon spectra in fig. 3.7b)) caused by the longer interaction time at a higher intensity, where the photon emission probability is enhanced.

Also, since the emission probability increases at higher intensities (see also the final photon spectra in fig. 3.7b)), the photon yield for the pulse shape $f_4(\varphi)$ exceeds the photon yield for the pulse shape $f_3(\varphi)$ due to the longer interaction time at a higher intensity. In turn, in the collision with the laser pulse with the shape function $f_4(\varphi)$, the electron bunch loses more energy. As already pointed out, the classical analytical solution in eq. (3.36) predicts the same final distribution function for both shape functions, i.e., the differences between the two final electron distributions (see fig. 3.7a)) are caused by the quantum effects in the interaction. As for both pulse shapes $f_3(\varphi)$ and $f_4(\varphi)$ the typical quantum nonlinearity parameters are not significantly smaller than unity ($\chi_3^* = 0.40$ and $\chi_4^* = 0.25$), a difference between the final distribution functions was expected. Although this difference is a signature of quantum RR, we note that the effect of the distribution function broadening discussed in sec. 3.2.3 is more prominent. Finally, anticipating a presently feasible total number of $N_{e^-} = 6 \times 10^8$ electrons (corresponding to a total charge of $Q = 100$ pC) [Wang 13], we can estimate the number of emitted photons N_γ. This results in $N_\gamma = 9.5 \times 10^9$ and $N_\gamma = 1.1 \times 10^{10}$ for the shape functions $f_3(\varphi)$ and $f_4(\varphi)$, respectively.

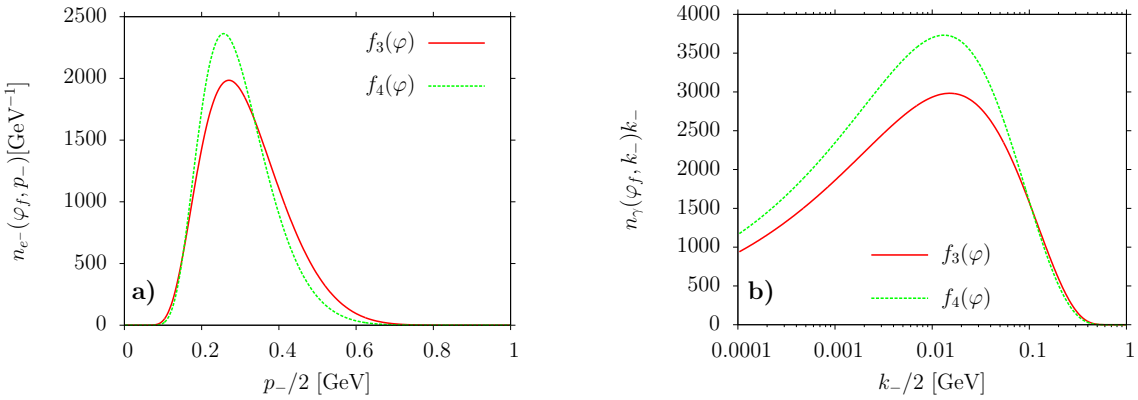

Figure 3.7: Comparison of the final electron distributions (part a)) as functions of $p_-/2 \approx \varepsilon$ and photon spectra (part b)) as functions of $k_-/2 \approx \omega$ for the shape functions $f_3(\varphi)$ (solid, red line) and $f_4(\varphi)$ (dashed, green line) [Neit 14].

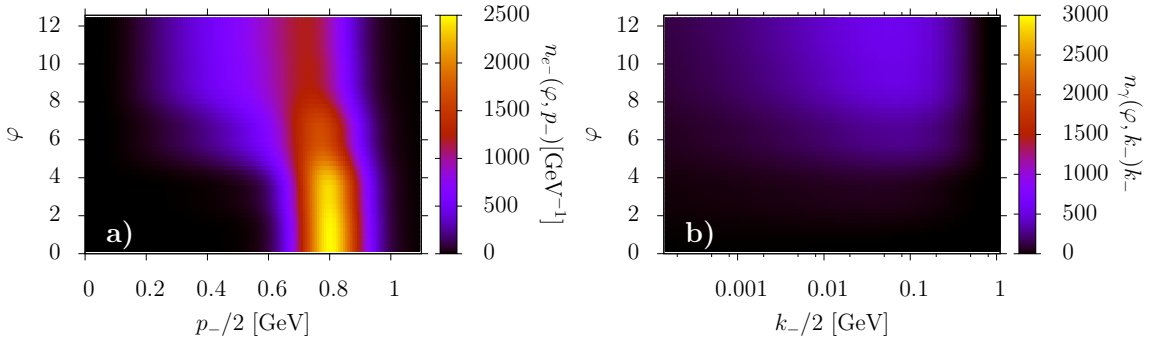

Figure 3.8: Phase evolution of the electron distribution (part a)) as a function of $p_-/2 \approx \varepsilon$ and the photon spectrum (part b)) as a function of $k_-/2 \approx \omega$ for the shape function $f_5(\varphi)$ [Neit 14].

3.3.2 Influence of the laser pulse duration

In the following paragraph, we now compare the impact of two different pulse durations for pulses with the same pulse shape at a given fluence. Keeping the $\sin^2$-pulse shape, we consider a two-cycle pulse ($\varphi_f = 4\pi$), i.e., $f(\varphi) = f_5(\varphi) = \sin(\varphi)\sin^2(\varphi/4)$, with peak intensity $I_{0,5} = 4 \times 10^{22}\,\mathrm{W/cm^2}$ and a 40-cycle pulse ($\varphi_f = 80\pi$), i.e., $f(\varphi) = f_6(\varphi) = \sin(\varphi)\sin^2(\varphi/80)$, with peak intensity $I_{0,6} = 2 \times 10^{21}\,\mathrm{W/cm^2}$, corresponding to pulse durations of 5 fs and 108 fs, respectively. The given parameters yield a fluence Φ that is equal to $5 \times 10^8\,\mathrm{J/cm^2}$. The initial Gaussian electron beam is centered around $p_-^* = 1.6\,\mathrm{GeV}$, corresponding to an average energy of $\varepsilon^* \approx 800\,\mathrm{MeV}$, and it has a standard deviation of $\sigma_{p_-} = 0.16\,\mathrm{GeV}$. The quantum nonlinearity parameter χ^* for such an electron beam is about unity for the shorter pulse, whereas for the longer pulse, the relativistic parameter is $\xi_5 = 97$ such that $R_Q \approx 0.7$, i.e., the process is considered to occur in the quantum radiation dominated regime (see sec. 2.1.2). In fig. 3.8 and fig. 3.9 the numerical results are shown for the pulse shape functions $f_5(\varphi)$ and $f_6(\varphi)$, respectively.

In comparison with the previous examples we identify, a completely different phase evolution of the electron distribution in case of the two-cycle pulse. In fig. 3.8a), we can observe that the electron distribution substantially spreads out as soon as the laser pulse intensity reaches its maximum and thereby loses its Gaussian shape.

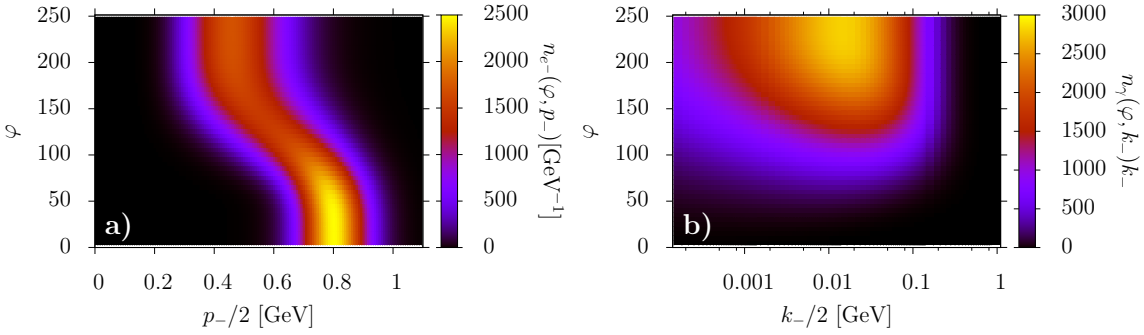

Figure 3.9: Phase evolution of the electron distribution (part a)) as a function of $p_-/2 \approx \varepsilon$ and the photon spectrum (part b)) as a function of $k_-/2 \approx \omega$ for the shape function $f_6(\varphi)$ [Neit 14].

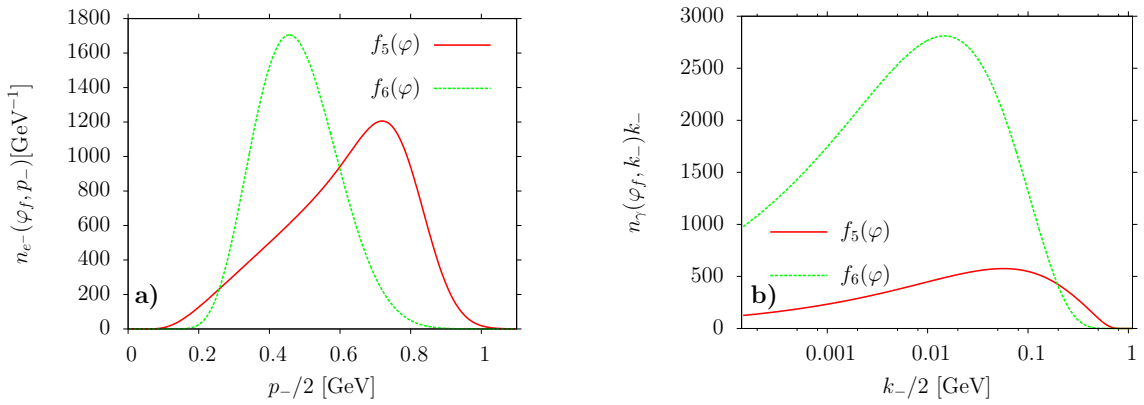

Figure 3.10: Comparison of the final electron distributions (part a)) as functions of $p_-/2 \approx \varepsilon$ and photon spectra (part b)) as functions of $k_-/2 \approx \omega$ for the shape functions $f_5(\varphi)$ (solid, red line) and $f_6(\varphi)$ (dashed, green line) [Neit 14].

On the other hand, for the longer pulse described by the shape function $f_6(\varphi)$, the electron distribution changes rather smoothly (see fig. 3.9a)) and the shape of the electron distribution remains approximately Gaussian. Even in the case of the shape function $f_6(\varphi)$, where $\chi_6^* \approx 0.2$ ($\xi_6 = 22$), the electron distributions appear to be very sensitive to quantum effects, corroborating the fact that the stochastic nature of the photon emission cannot be neglected in the nonlinear moderately quantum regime. As analyzed in sec. 3.2.3, the stochasticity of the photon emission process induces a drastic broadening as soon as quantum effects become important, whereas the classical analysis employing the LL equation predicts a strong narrowing of the electron distributions when taking into account RR effects [Neit 13]. As before, we consider the final electron distribution and photon spectrum in more detail, as they can be more relevant from an experimental point of view (see fig. 3.10).

Since the fluence of the laser field is the same for both pulse shapes, the classical solution (3.36) would again predict the same final electron distributions. This once more allows to conclude that, as in the previous example, the differences between the two final electron distributions in fig. 3.10a) arise due to quantum effects. We further mention that due to the longer interaction, although at lower laser intensity, the photon spectrum for the 40-cycle pulse has its maximum at lower energies and its photon yield is much higher than for the two-cycle pulse. Anticipating again a

nowadays feasible total number of $N_{e^-} = 6 \times 10^8$ electrons (corresponding to a total charge of $Q = 100$ pC) [Wang 13], we estimate the number of emitted photons N_γ for both pulses by integrating over the obtained photon distribution function. In the case of the shape function $f_5(\varphi)$, this yields $N_\gamma = 1.8 \times 10^9$ and for the shape function $f_6(\varphi)$, we obtain $N_\gamma = 8.5 \times 10^9$.

Finally, we point out that for the two-cycle pulse, where quantum effects are more significant, the photon spectrum is peaked at roughly $k_-^* \approx 0.2\,\mathrm{GeV}$. Recalling that the probability of pair creation contains a suppressing factor of approximately $\eta(k_-^*) = \exp(-8/3\varkappa^*)$, with $\varkappa^* = k_-^*\chi^*/p_-^*$ (see [Ritu 85]), we are able to conclude that for the peak of the photon spectrum, $\eta(k_-^*) \sim 10^{-12}$ and in turn that pair production is negligible, as it was initially presumed. Furthermore, we have also proven that numerical simulations including pair production (see ch. 4) yield the same final result.

4 Kinetic approach (2): Pair production

In this chapter, the kinetic approach derived and studied in the previous chapter is extended in such a way that the possible creation of electron-positron pairs is included in the kinetic equations describing the dynamics of the collision of the electron beam with the laser pulse (see, e.g., [Soko 10, Elki 11, Neru 11] for similar studies). After identifying the process dominating the production of pairs in the given parameter regime, we amend the corresponding pair production probabilities in the kinetic equations for photons and electrons. In addition, the kinetic equation for positrons is constituted analogously to the one for the electrons. The obtained fully coupled set of equations is then solved numerically and the interplay of the distribution functions is examined by the artificial neglect of some interdependencies. Finally, following the investigations of sec. 3.3, the influences of the laser pulse duration on the evolution of the distribution functions are studied at a given fluence of the laser field and different initial electron beam energies. Parts of this chapter have been presented in [Neit 14].

4.1 Derivation of the kinetic equations including pair creation

Considering the collision of highly-energetic electron bunches with ultra-strong laser fields as discussed in ch. 3 at even higher initial electron energies and field intensities invalidates the assumption that the production of electron-positron pairs can be neglected in the derivation of the kinetic equations. Although the other conditions required for the validity of the kinetic approach are not altered by an inclusion of pair creation, two major changes must be made to achieve an appropriate description of the interactions of the electrons with the laser field. Evidently, the distribution function describing the positrons can no longer be assumed to vanish identically. However, the kinetic equation for the positrons can be constructed analogously to the one corresponding to the electrons, since the probability of photon emission is the same for both species. Secondly, the collision terms occurring in eq. (3.1) and eq. (3.14) must not only take into account the expressions related to the process of photon emission, but must also include the probabilities for the creation of pairs. These electron-positron pairs are produced via the so-called trident process (see sec. 2.1.2) which describes the emission of a photon by an electron and the subsequent decay of the emitted photon into a pair of charged particles. The trident process itself can occur via two physical channels. In the first case, the

emitted photon is virtual and thereby the initial electron is considered to directly produce the electron-positron pair. In the second scenario, the emitted photon is real, which divides the trident process into two separate processes. As it was shown in [Hu 10, Ilde 11], the dominant process of pair creation in an intense laser plane-wave field ($\xi \gg 1$) is the separable subsequent process. In fact, this allows for an employment of the probability of laser-assisted pair production by a photon, where we again average all the probabilities over the initial photon polarization and sum over the final electron and positron spin. The probability per unit phase φ and per unit p_- that a pair with particles' momenta p_- and $k_- - p_-$ is produced by a photon with momentum k_- is given by (see [Ritu 85])

$$\frac{\mathrm{d}P_{k_-}}{\mathrm{d}\varphi \mathrm{d}p_-} = \frac{\alpha}{\sqrt{3}\pi}\frac{m^2}{\omega_0 k_-^2}\left[\frac{k_-^2}{p_-(k_- - p_-)}\,\mathrm{K}_{\frac{2}{3}}\left(\kappa(\varphi, k_-, p_-)\right) - \int_{\kappa(\varphi,k_-,p_-)}^{\infty} dx\,\mathrm{K}_{\frac{5}{3}}(x)\right], \tag{4.1}$$

where we introduced $\kappa(\varphi, k_-, p_-) = 2k_-^2/[3p_-(k_- - p_-)\varkappa(\varphi, k_-)]$, with $\varkappa(\varphi, k_-) = (k_-/m)|E(\varphi)|/F_{\mathrm{cr}}$. Introducing now the distribution function $n_{e^+}(\varphi, p_-)$ for the created positrons and applying the pair creation probability yields the set of kinetic equations (see [Baie 94])

$$\begin{aligned}\frac{\partial n_{e^-}(\varphi, p_-)}{\partial \varphi} &= \int_{p_-}^{\infty} \mathrm{d}p_{i,-}\, n_{e^-}(\varphi, p_{i,-})\frac{\mathrm{d}P_{p_{i,-}}}{\mathrm{d}\varphi \mathrm{d}p_-} - n_{e^-}(\varphi, p_-)\int_0^{p_-} \mathrm{d}k_- \frac{\mathrm{d}P_{p_-}}{\mathrm{d}\varphi \mathrm{d}k_-} \\ &\quad + \int_{p_-}^{\infty} \mathrm{d}k_-\, n_\gamma(\varphi, k_-)\frac{\mathrm{d}P_{k_-}}{\mathrm{d}\varphi \mathrm{d}p_-}, \end{aligned} \tag{4.2}$$

$$\begin{aligned}\frac{\partial n_{e^+}(\varphi, p_-)}{\partial \varphi} &= \int_{p_-}^{\infty} \mathrm{d}p_{i,-}\, n_{e^+}(\varphi, p_{i,-})\frac{\mathrm{d}P_{p_{i,-}}}{\mathrm{d}\varphi \mathrm{d}p_-} - n_{e^+}(\varphi, p_-)\int_0^{p_-} \mathrm{d}k_- \frac{\mathrm{d}P_{p_-}}{\mathrm{d}\varphi \mathrm{d}k_-} \\ &\quad + \int_{p_-}^{\infty} \mathrm{d}k_-\, n_\gamma(\varphi, k_-)\frac{\mathrm{d}P_{k_-}}{\mathrm{d}\varphi \mathrm{d}p_-}, \end{aligned} \tag{4.3}$$

$$\begin{aligned}\frac{\partial n_\gamma(\varphi, k_-)}{\partial \varphi} &= \int_{k_-}^{\infty} \mathrm{d}p_{i,-}\, \left[n_{e^-}(\varphi, p_{i,-}) + n_{e^+}(\varphi, p_{i,-})\right]\frac{\mathrm{d}P_{p_{i,-}}}{\mathrm{d}\varphi \mathrm{d}k_-} \\ &\quad - n_\gamma(\varphi, k_-)\int_0^{k_-} \mathrm{d}p_-\, \frac{\mathrm{d}P_{k_-}}{\mathrm{d}\varphi \mathrm{d}p_-}. \end{aligned} \tag{4.4}$$

At first we observe that the evolution of the electron distribution is no longer decoupled from the photon distribution and also the positron distribution function is coupled to the evolution of the photons. Even though the equations for the charged particles are not coupled directly, they can in principle be affected by each other through the linking equation of the photons, i.e., we obtain a fully coupled system of integro-differential equations. Further, we note that although the total number of particles is no longer conserved, the difference of eq. (4.2) and eq. (4.3) is conserved, which indicates the conservation of the total charge

$$\frac{\partial}{\partial \varphi}\left[\int_0^{\infty} \mathrm{d}p_-\, n_{e^-}(\varphi, p_-) - \int_0^{\infty} \mathrm{d}p_-\, n_{e^+}(\varphi, p_-)\right] = 0. \tag{4.5}$$

This can be explained by the fact that the expressions corresponding to pair creation cancel and that eq. (3.22) is valid independently for $n_{e^-}(\varphi, p_-)$ and $n_{e^+}(\varphi, p_-)$.

Moreover, we obtain the analogue of eq. (3.23)

$$\frac{\partial}{\partial\varphi}\left[\int_0^\infty \mathrm{d}p_-\, n_{e^-}(\varphi,p_-)p_- + \int_0^\infty \mathrm{d}p_-\, n_{e^+}(\varphi,p_-)p_- + \int_0^\infty \mathrm{d}k_-\, n_\gamma(\varphi,k_-)k_-\right] = 0, \tag{4.6}$$

ensuring the conservation of the total energy minus the total longitudinal momentum throughout to whole interaction. In addition, the numerically evaluated results of the kinetic equations (4.2)-(4.4) were found to coincide with results obtained for all the examples given in ch. 3, corroborating that the neglect of pair production was justified in these cases, as expected. Note that the investigations in the regime $\chi \gtrsim 1$ cannot be extended to arbitrary values of the quantum nonlinearity parameter in our approach, since the increased energy loss of the electrons via photon emission would lead to a violation of the required condition $p_-^* \gg m\xi$ that our approach is based on. Nevertheless, we ensured the validity of all our approximations throughout the whole numerical calculations. Finally, we mention that the generation of QED cascades is impossible in the setup under consideration [Soko 10], as the final particles for each RR effect taken into account (photon emission and pair creation) have values of the minus-momentum smaller than the initial particle.

4.2 The coupled dynamics of photon emission and pair production

In order to understand the mutual influence of the evolution of the particle distribution functions, we consider the collision of a 20-cycle $\sin^2$-pulse, i.e., $f(\varphi) = f_7(\varphi) = \sin(\varphi)\sin^2(\varphi/40)$, with laser peak intensity $I_{0,7} = 4.2\times10^{21}\,\mathrm{W/cm^2}$ with an initially Gaussian electron distribution with $p_-^* = 100\,\mathrm{GeV}$ ($\varepsilon^* \approx 50\,\mathrm{GeV}$) and $\sigma_{p_-} = 10\,\mathrm{GeV}$ that is normalized to unity. The given parameters yield the relativistic parameter $\xi_7 = 31$ and the quantum nonlinearity parameter $\chi_7^* = 19$.

The evolutions of the electron distribution, of the positron distribution and of the photon spectrum are shown in fig. 4.1. We observe that the emission of photons causes the electrons to lose a large amount of their initial momentum during the collision with the plane- wave field (see fig. 4.1a)). As expected, the thus-generated photons possess an energy sufficiently high to create electron-positron pairs. This evidently implies a loss in the yield of highly-energetic photons in the final photon spectrum as well as a rise in the number of charged particles. Here, we find that the ratio of the final and the initial number of electrons is approximately 1.56, i.e., the number of electrons is enhanced by more than 50%. In fig. 4.1b) we identify that the produced particles have a much smaller energy than the initial electrons. This can be understood by the fact that the photons creating the electron-positron pairs must have an energy smaller than the one of the emitting electron and, additionally, in the pair-production process this energy is subsequently distributed into two particles. The evolution of the distribution functions shown in fig. 4.1 already includes the fully-coupled dynamics of the electrons, positrons and photons making it difficult to identify how the evolution of each distribution function is affected by the radiation and pair-production processes. In order to obtain a deeper insight in the interdependencies of the interacting particles, we simulated the above considered collision again but excluded artificially either pair creation or the radiation of the created positrons. fig. 4.2 shows the final distributions corresponding to these calculations.

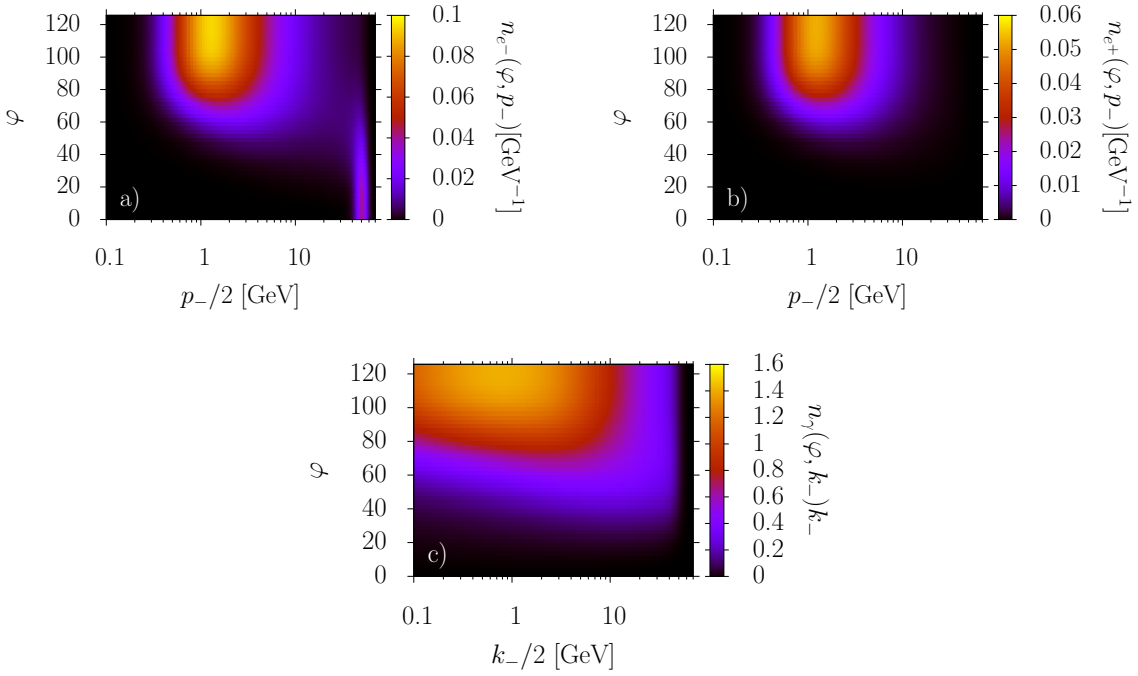

Figure 4.1: Phase evolution of the electron (part a)) and positron distribution (part b)) as functions of $p_-/2 \approx \varepsilon$ and of the photon spectrum (part c)) as a function of $k_-/2 \approx \omega$ for the shape function $f_7(\varphi)$ [Neit 14].

Fig. 4.2b) only displays the final distribution functions for the full dynamics and the one where radiation by positrons is excluded, since in the case of the exclusion of pair creation the distribution function describing the positrons has to vanish identically throughout the entire interaction of the electron bunch with the laser pulse. Further, we observe in fig. 4.2a) and fig. 4.2c) that the final electron distribution and the final photon spectrum are drastically altered if pair creation is taken into account. Apparently the high-energy part of the photon spectrum is substantially reduced by the inclusion of pair production, since the high-energetic photons can decay into pairs of charged particles. In turn, the total number of electrons is increased and we identify an enlarged gain in the low-energy part of the final energy distribution of the electrons (see fig. 4.2a)). On the other hand, the high-energy part of the final electron distribution remains unchanged, since the created particles occur mainly at energies much smaller than the initial energy of the electron bunch. As the number of particles is increased and these particles can emit radiation themselves, fig. 4.2c) exhibits an enhanced photon yield in the region of smaller photon energies. This is also apparent in case of the inclusion of RR for the produced positrons. In fig. 4.2b) it can be seen that the distribution is shifted to lower energies, implying that the created particles are able to interact with the external laser field and thus emit photons. Analogously, the incorporation of positron radiation enhances also the photon gain for smaller photon energies in comparison to the final spectrum where this radiation is not taken into account (see fig. 4.2c). Finally, we observe that the radiation emitted by the positrons hardly influences the evolution of the electrons and only leads to a marginally higher peak of the electron energy spectrum (see fig. 4.2a)). We can conclude that in this situation the created positrons do not only emit photons, but these photons still possess an energy sufficiently high to

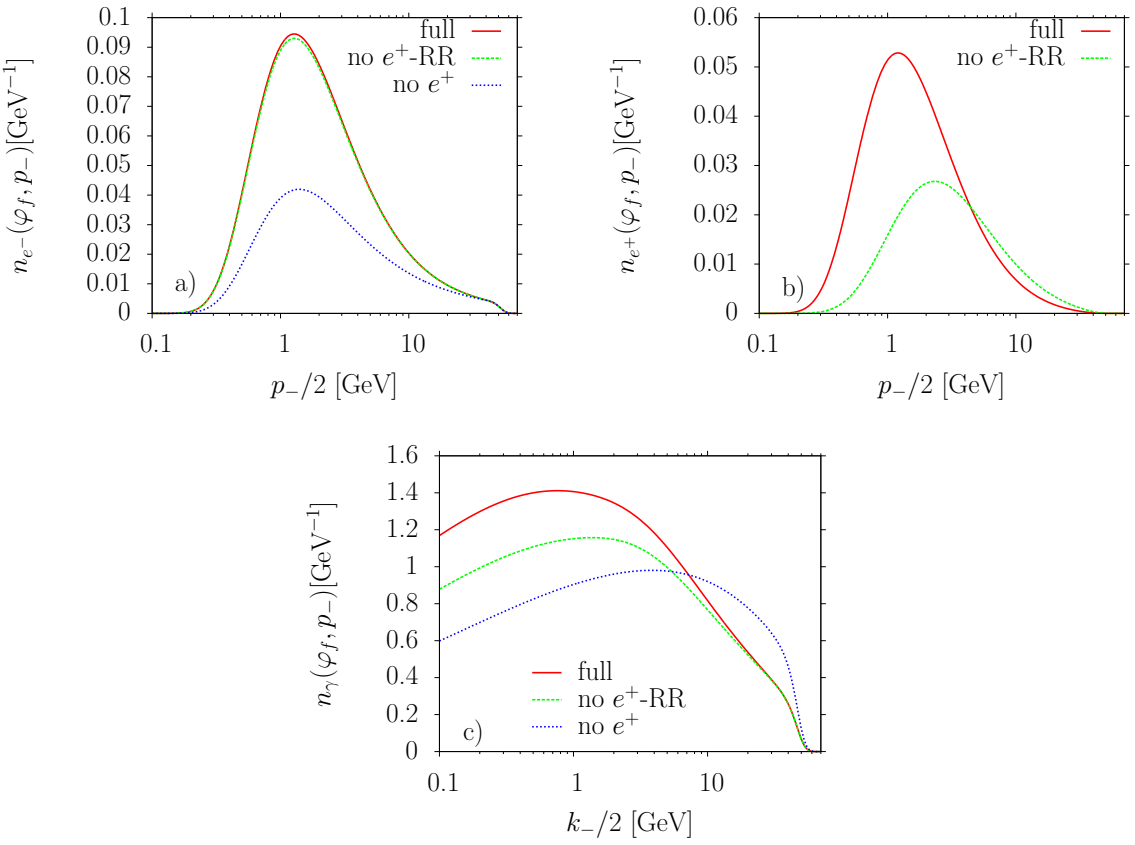

Figure 4.2: Comparison of the final electron (part a)) and positron distributions (part b)) as functions of $p_-/2 \approx \varepsilon$ and photon spectra (part b)) as functions of $k_-/2 \approx \omega$ for the full kinetic approach (solid, red line), without the radiation of positrons (dashed, green line) and without pair production (short dashed, blue line) for the initial Gaussian electron distribution with $p_-^* = 100\,\mathrm{GeV}$ ($\varepsilon^* \approx 50\,\mathrm{GeV}$) and the shape function $f_7(\varphi)$ [Neit 14].

produce a small amount of charged particles within the remaining interaction time with the laser pulse.

4.3 Dependence on the laser pulse shape and the initial electron energy

In comparison to our investigations in sec. 3.3, we now study the influences of the initial energy of the electrons and the laser peak intensities on the final electron and positron distributions and on the photon spectrum. To this end, we will again assume laser pulses at a given pulse fluence, which can be modified via pulse shaping in an actual experiment. In addition, we will examine how the dynamics is changed if the initial energy of the electron bunch is altered: We consider two initially Gaussian electron distributions, with the first one as before with $p_-^* = 100\,\mathrm{GeV}$ ($\varepsilon^* \approx 50\,\mathrm{GeV}$) and $\sigma_{p_-} = 10\,\mathrm{GeV}$ (see the previous section). Analogously, we choose the second one to be centered at $p_-^* = 10\,\mathrm{GeV}$ ($\varepsilon^* \approx 5\,\mathrm{GeV}$) with a width of $\sigma_{p_-} = 1\,\mathrm{GeV}$. Both distributions are normalized to unity. Each of the distributions is considered to collide with three different laser pulses in total, always featuring the fluence $\Phi = 5.2 \times 10^8\ \mathrm{J/cm^2}$ and a $\sin^2$-pulse form, i.e., $f(\varphi) = \sin(\varphi)\sin^2(\varphi/2N_L)$, but varying numbers of laser cycles N_L and laser peak intensities. For the first pulse we set, as in the previous numerical simulation, the peak intensity to be $I_{0,7} = 4.2 \times 10^{21}\,\mathrm{W/cm^2}$ for $f_7(\varphi) = \sin(\varphi)\sin^2(\varphi/40)$ ($\varphi_f = 40\pi$) corresponding to the parameters $\xi_7 = 31$ and $\chi_7^* = 19$. The second pulse is considered to be a five-cycle pulse, i.e., $f_8(\varphi) = \sin(\varphi)\sin^2(\varphi/10)$ ($\varphi_f = 10\pi$), with a peak intensity of $I_{0,8} = 1.7 \times 10^{22}\,\mathrm{W/cm^2}$ leading to the numerical values $\xi_8 = 63$ and $\chi_8^* = 37$. Finally, the third one-cycle pulse is chosen to have the shape function $f_9(\varphi) = \sin(\varphi)\sin^2(\varphi/2)$ ($\varphi_f = 2\pi$) and the peak intensity $I_{0,9} = 10^{23}\,\mathrm{W/cm^2}$ yielding $\xi_9 = 153$ and $\chi_9^* = 91$. The corresponding pulse durations are approximately 54 fs, 14 fs and 3 fs, respectively.

fig. 4.3 displays final electron and positron distributions as well as the photon spectra in case of the collision of the first electron distribution with the three different laser pulses. In accordance with our findings in sec. 3.3, we observe that the photon gain is smaller for the one-cycle pulse than the five-cycle pulse, which itself leads to a smaller photon yield than the 20-cycle pulse. This feature can again be explained by observing that the longer interaction time of the laser field and the electrons results in an enhanced radiation, even though the laser peak intensity is not as high as in the case of the shorter pulses. The number of electron-positron pairs created by the longer pulses also surmounts the number produced by the one-cycle pulse (see fig. 4.3), as both the laser intensities and the initial energy of the electrons are high enough to cause the emission of many photons with sufficiently high energy during the collision. In fact, in the case of the one-cycle pulse, the ratio of the final and the initial electron number is decreased to 1.06 in comparison to 1.56 for the 20-cycle pulse, although the intensity is larger by a factor of 24 for the former. Anticipating an experimental examination, we estimate the number of produced positrons N_{e^+} and photons N_γ considering a nowadays typical electron bunch with charge $Q \approx 100$ pC corresponding to a total initial number of $N_{e^-} = 6 \times 10^8$ [Wang 13]. Our numerical calculations indicate that the shape function $f_7(\varphi)$ results in $N_{e^+} = 3.3 \times 10^8$ and $N_\gamma = 5.5 \times 10^9$, $f_8(\varphi)$ yields $N_{e^+} = 1.3 \times 10^8$ and $N_\gamma = 1.7 \times 10^9$ and in case of $f_9(\varphi)$ one obtains $N_{e^+} = 3.4 \times 10^7$ and $N_\gamma = 5.5 \times 10^8$.

Considering now the second initial electron distribution, we expect pair creation

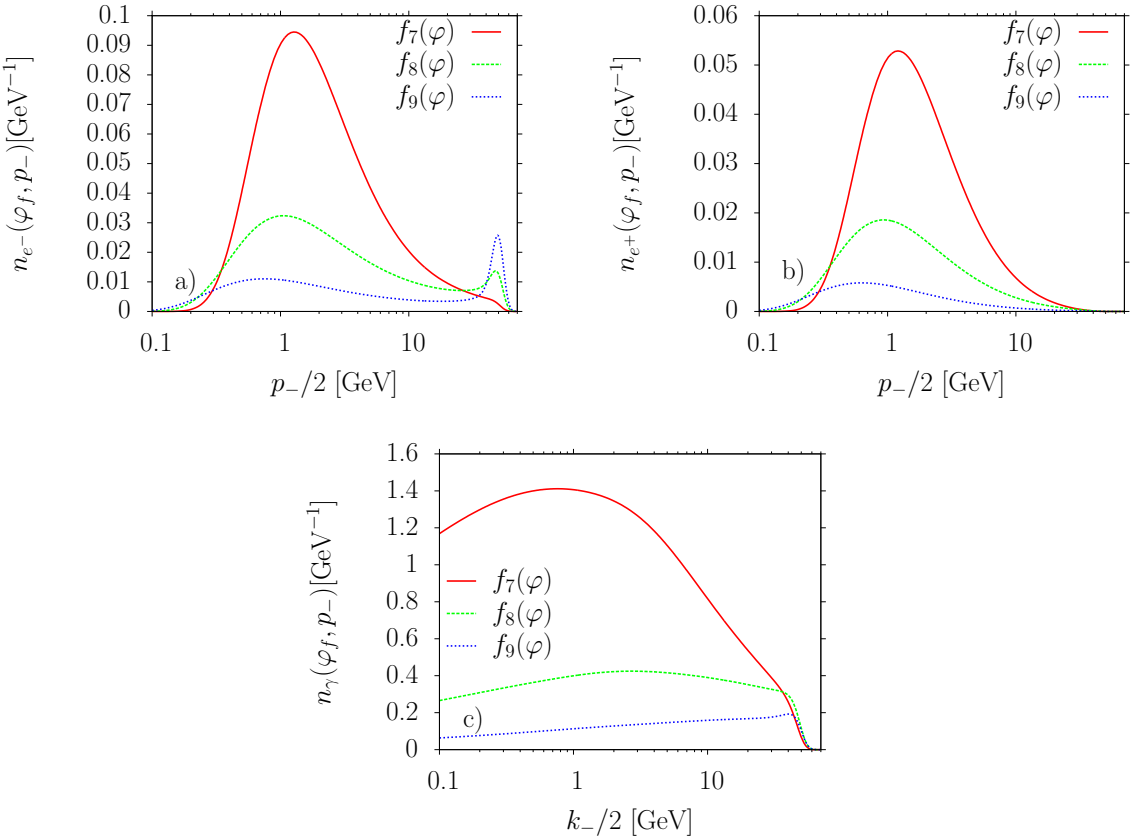

Figure 4.3: Comparison of the final electron (part a)) and positron distributions (part b)) as functions of $p_-/2 \approx \varepsilon$ and photon spectra (part c)) as functions of $k_-/2 \approx \omega$ for the shape functions $f_7(\varphi)$ (solid, red line), $f_8(\varphi)$ (dashed, green line) and $f_9(\varphi)$ (short dashed, blue line) for the initial Gaussian electron distribution with $p_-^* = 100\,\mathrm{GeV}$ ($\varepsilon^* \approx 50\,\mathrm{GeV}$) [Neit 14].

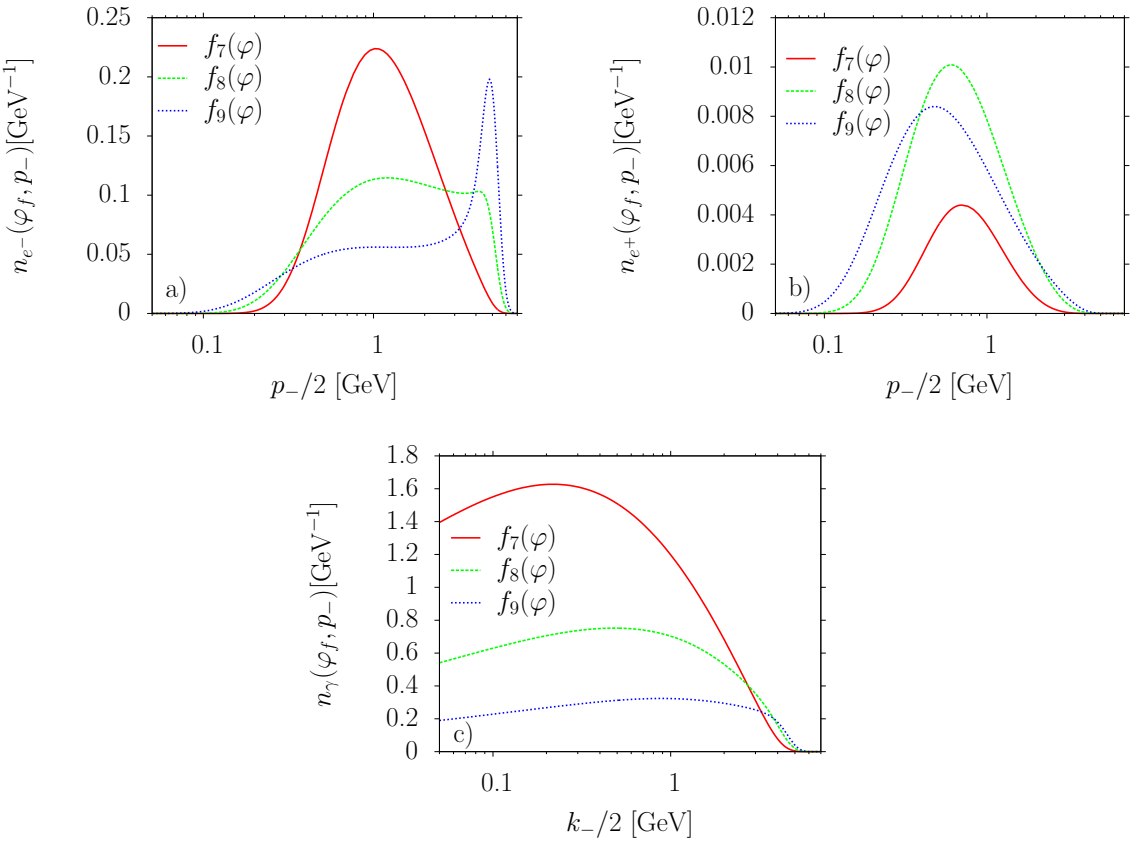

Figure 4.4: Comparison of the final electron (part a)) and positron distributions (part b)) as functions of $p_-/2 \approx \varepsilon$ and photon spectra (part c)) as functions of $k_-/2 \approx \omega$ for the shape functions $f_7(\varphi)$ (solid, red line), $f_8(\varphi)$ (dashed, green line) and $f_9(\varphi)$ (short dashed, blue line) for the initial Gaussian electron distribution with $p_-^* = 10\,\text{GeV}$ ($\varepsilon^* \approx 5\,\text{GeV}$) [Neit 14].

and quantum effects to be less prominent, as for $p_-^* = 10\,\mathrm{GeV}$ the value χ^* is decreased by a factor of 10 and in turn also the value $\varkappa^*$ will be reduced. In fig. 4.4 the final distribution functions are shown for the collision of the aforementioned three laser pulses with this electron distribution. As in the previous simulations, the collision with the 20-cycle pulse exhibits the largest loss in energy for the electrons. However, the collision of the laser pulses described by f_8 and f_9 result in much broader final electron distributions and in the case of the one-cycle pulse, the initial peak around $p_-^* = 10\,\mathrm{GeV}$ ($\varepsilon^* \approx 5\,\mathrm{GeV}$) can still be identified. In agreement with the analysis above, the long pulse still produces more photons, but in contrast to the previous example the maximum of the spectrum is shifted to smaller values of k_- (see fig. 4.4c)). Hence, the typical value $\varkappa^*$ is severely reduced resulting in a lower pair-production probability. In fact, the number of pairs created by the 20-cycle pulse is smaller than the one produced by the shorter pulses. This can be explained by the fact that, although the total photon yield is the highest for the longest pulse, the laser peak intensity and the energy of the emitted photons are not high enough to produce a large number of electron-positron pairs. On the other hand, in the case of the five-cycle pulse, the laser peak intensity is still sufficiently high to result in a slightly higher number of produced particles in comparison with the one-cycle pulse and thereby the beneficial effect of a longer interaction time is transferred onto the positron yield (see fig. 4.4b)). As before, we want to give estimates for the final N_{e^+} and N_γ produced by an electron bunch with total initial number of $N_{e^-} = 6 \times 10^8$ electrons. In the case of $f_7(\varphi)$, it results in $N_{e^+} = 5.8 \times 10^6$ and $N_\gamma = 5.6 \times 10^9$, whereas in the case of $f_8(\varphi)$ one obtains $N_{e^+} = 1.6 \times 10^7$ and $N_\gamma = 2.5 \times 10^9$, and in the case of $f_9(\varphi)$ one achieves $N_{e^+} = 1.4 \times 10^7$ and $N_\gamma = 1.0 \times 10^9$.

Finally, for presently available laser-accelerated electron beams [Wang 13], we give an estimation for the laser peak intensities at which electron-positron pairs should in principle be detectable. A Gaussian electron beam centered at $p_-^* = 4\,\mathrm{GeV}$ ($\varepsilon^* \approx 2\,\mathrm{GeV}$) and with $\sigma_{p_-} = 0.2\,\mathrm{GeV}$ with a total number of $N = 6 \times 10^8$ electrons (corresponding to a charge of $Q \approx 100$ pC as before) is considered to collide with 10-cycle $\sin^2$-shaped laser pulses differing in their peak intensities. Assuming that the detection of a few tens of positrons is practicable, we find detectable pair production at an intensity of $I_0 = 1.5 \times 10^{21}\,\mathrm{W/cm^2}$, which would yield a total number of 26 produced positrons. Considering also a slightly lower electron energy $p_-^* = 2\,\mathrm{GeV}$ ($\varepsilon^* \approx 1\,\mathrm{GeV}$), the creation of 19 pairs already demands an increased intensity of $I_0 = 5{\times}10^{21}\,\mathrm{W/\,cm^2}$. This implies that in order to study pair production experimentally, higher beam energies are more advantageous.

5

Numerical treatment of the kinetic equations

This chapter is dedicated to the numerical details of the evaluation of the kinetic equations (3.17)-(3.18) as well as (4.2)-(4.4). Since these kinetic equations constitute a coupled[I] system of linear partial integro-differential equations that has neither a known analytical solution nor can be simplified analytically via the common methods, e.g., by performing a Laplace transformation, the full system has to be treated numerically. Solving such a set of equations, however, can turn out to be vastly tedious depending on the actual structure of the formulas and the properties of the involved functions. In particular, strongly oscillating functions and functions with singularities in general render the numerical calculation of integrals and differentials troublesome. However, only removable singularities occur in the case of the kinetic equations due the analytical characteristics of the modified Bessel functions of the second kind (see app. A).

In order to overcome the numerical challenges of the kinetic equations, we recall the kinetic equation (3.17) for the electrons without the inclusion of pair creation

$$\begin{aligned}\frac{\partial n_{e^-}(\varphi,p_-)}{\partial\varphi} = &\int_{p_-}^{\infty} \mathrm{d}p_{i,-}\, n_{e^-}(\varphi,p_{i,-}) \frac{\alpha}{\sqrt{3}\pi}\frac{m^2}{\omega_0 p_{i,-}^2}\left[\left(\frac{p_{i,-}}{p_-}+\frac{p_-}{p_{i,-}}\right)\right.\\ &\left.\times \mathrm{K}_{\frac{2}{3}}\left(X(\varphi,p_-,p_{i,-})\right) - \int_{X(\varphi,p_-,p_{i,-})}^{\infty}\mathrm{d}x\,\mathrm{K}_{\frac{1}{3}}(x)\right]\\ &- n_{e^-}(\varphi,p_-)\int_0^{p_-}\mathrm{d}k_-\,\frac{\alpha}{\sqrt{3}\pi}\frac{m^2}{\omega_0 p_-^2}\left[\left(\frac{p_-}{p_- - k_-}+\frac{p_- - k_-}{p_-}\right)\right.\\ &\left.\times \mathrm{K}_{\frac{2}{3}}\left(X'(\varphi,p_-,k_-)\right) - \int_{X'(\varphi,p_-,k_-)}^{\infty}\mathrm{d}x\,\mathrm{K}_{\frac{1}{3}}(x)\right],\end{aligned} \tag{5.1}$$

[I] Recall that although (3.17) is completely decoupled from (3.18), the phase evolution of $n_\gamma(\varphi,k_-)$ is exclusively determined by the phase evolution of $n_{e^-}(\varphi,p_-)$.

where we employed the transformations (3.19) and (3.20), and introduced

$$X(\varphi, p_-, p_{i,-}) = \frac{2}{3\chi(\varphi, p_{i,-})}\left(\frac{p_{i,-}}{p_-} - 1\right), \quad X'(\varphi, p_-, k_-) = \frac{2}{3\chi(\varphi, p_-)}\left(\frac{k_-}{p_- - k_-}\right). \tag{5.2}$$

In order to calculate the evolution of the electron distribution function numerically, it is necessary to discretize the continuous phase and minus momentum variables and construct two grids with a finite number of points. Obviously, a finite grid is not able to cover the first integral in eq. (5.1) that extends to infinity, and the integrals have to be transformed in such a way that the integration interval can be covered by the grid. Furthermore, if the integration variable is equal to p_- (lower limit for the first integral and upper limit for the second one), both integrals exhibit a singularity due to the divergent part of the modified Bessel functions (see eq. (A.4)). These two singularities, however, are exactly compensating each other and for the purpose of numerical implementation it is favorable to make this cancellation more apparent. Therefore, we perform the following changes of variables $p_{i,-} = p_-/w$ ($\mathrm{d}p_{i,-}/\mathrm{d}w = -p_-/w^2$) and $k_- = p_-(1-w)$ ($\mathrm{d}k_-/\mathrm{d}w = -p_-$). Thus, we obtain

$$\begin{aligned}\frac{\partial n_{e^-}(\varphi, p_-)}{\partial \varphi} = &\int_0^1 \mathrm{d}w\, n_{e^-}(\varphi, p_-/w)\frac{\alpha}{\sqrt{3}\pi}\frac{m^2}{\omega_0 p_-}\left[\left(\frac{1}{w} + w\right)\mathrm{K}_{\frac{2}{3}}\left(\tilde{X}(\varphi, p_-, w)\right)\right. \\ &\left. - \int_{\tilde{X}(\varphi,p_-,w)}^{\infty}\mathrm{d}x\,\mathrm{K}_{\frac{1}{3}}(x)\right] \\ &- n_{e^-}(\varphi, p_-)\int_0^1 \mathrm{d}w\,\frac{\alpha}{\sqrt{3}\pi}\frac{m^2}{\omega_0 p_-}\left[\left(\frac{1}{w} + w\right)\mathrm{K}_{\frac{2}{3}}\left(\tilde{X}'(\varphi, p_-, w)\right)\right. \\ &\left. - \int_{\tilde{X}'(\varphi,p_-,w)}^{\infty}\mathrm{d}x\,\mathrm{K}_{\frac{1}{3}}(x)\right],\end{aligned} \tag{5.3}$$

with the transformed functions

$$\tilde{X}(\varphi, p_-, w) = \frac{2}{3\chi(\varphi, p_-)}(1-w) \quad \text{and} \quad \tilde{X}'(\varphi, p_-, w) = \frac{2}{3\chi(\varphi, p_-)}\left(\frac{1}{w} - 1\right), \tag{5.4}$$

where the cancellation of the terms on the right hand side for $w \to 1$ is evident due to the equal prefactors and the arguments of the modified Bessel functions. Analogously, we now transform eq. (3.18),

$$\begin{aligned}\frac{\partial n_\gamma(\varphi, k_-)}{\partial \varphi} = &\int_{k_-}^{\infty}\mathrm{d}p_{i,-}\, n_{e^-}(\varphi, p_{i,-})\frac{\alpha}{\sqrt{3}\pi}\frac{m^2}{\omega_0 (p_{i,-})^2}\left[\left(\frac{p_{i,-}}{p_{i,-} - k_-} + \frac{p_{i,-} - k_-}{p_{i,-}}\right)\right. \\ &\left. \times \mathrm{K}_{\frac{2}{3}}\left(X''(\varphi, k_-, p_{i,-})\right) - \int_{X''(\varphi,k_-,p_{i,-})}^{\infty}\mathrm{d}x\,\mathrm{K}_{\frac{1}{3}}(x)\right],\end{aligned} \tag{5.5}$$

where we defined

$$X''(\varphi, k_-, p_{i,-}) = \frac{2}{3\varkappa(\varphi, k_-)} \left(\frac{k_-^2}{p_{i,-}(p_{i,-} - k_-)} \right). \tag{5.6}$$

The substitution $p_{i,-} = k_-/w$ ($\mathrm{d}p_{i,-}/\mathrm{d}w = -k_-/w^2$) then yields

$$\begin{aligned} \frac{\partial n_\gamma(\varphi, k_-)}{\partial \varphi} = \int_0^1 \mathrm{d}w\, n_{e^-}(\varphi, k_-/w) \frac{\alpha}{\sqrt{3}\pi} \frac{m^2}{\omega_0 k_-} \Bigg[\left(1 - w + \frac{1}{1-w} \right) \\ \times \mathrm{K}_{\frac{2}{3}} \left(\tilde{X}''(\varphi, k_-, w) \right) - \int_{\tilde{X}''(\varphi, k_-, w)}^\infty \mathrm{d}x\, \mathrm{K}_{\frac{1}{3}}(x) \Bigg], \end{aligned} \tag{5.7}$$

with the changed expression

$$\tilde{X}''(\varphi, k_-, w) = \frac{2}{3\varkappa(\varphi, k_-)} \left(\frac{w^2}{1-w} \right). \tag{5.8}$$

For the inclusion of pair creation, the expressions corresponding to photon emission do not have to be altered and the radiation of positrons can be immediately incorporated with eq. (5.3) by the substitution $n_{e^-} \to n_{e^+}$, since the emission probabilities are identical for electrons and positrons. Thus, only the terms corresponding to pair production have to be transformed to facilitate a numerical treatment. An examination of the last part of eq. (4.4),

$$-\frac{\alpha m^2 n_\gamma(\varphi, k_-)}{\sqrt{3}\pi\omega_0} \int_0^{k_-} \frac{\mathrm{d}p_-}{k_-^2} \left[\frac{k_-^2}{p_-(k_- - p_-)} \mathrm{K}_{\frac{2}{3}} \left(\kappa(\varphi, k_-, p_-) \right) - \int_{\kappa(\varphi, k_-, p_-)}^\infty \mathrm{d}x\, \mathrm{K}_{\frac{5}{3}}(x) \right], \tag{5.9}$$

where we again made use of

$$\kappa(\varphi, k_-, p_-) = \frac{2}{3\varkappa(\varphi, k_-)} \frac{k_-^2}{p_-(k_- - p_-)}, \tag{5.10}$$

reveals that due to the integration path, the values corresponding to $\kappa \in (8/3\varkappa, \infty)$ are covered twice by the integration. Hence, we split the integral at the value $p_- = k_-/2$ and perform the transformations $p_- = k_- w/(1+w)$ ($\mathrm{d}p_-/\mathrm{d}w = k_-/(1+w)^2$) and $p_- = k_-/(1+w)$ ($\mathrm{d}p_-/\mathrm{d}w = -k_-/(1+w)^2$) in the first and second expressions, respectively. The resulting terms are identical and can be summed up again. Following the described procedure and employing also the identity eq. (A.9) yields

$$-\frac{2\alpha m^2 n_\gamma(\varphi, k_-)}{\sqrt{3}\pi\omega_0} \int_0^1 \frac{\mathrm{d}w}{(1+w)^2} \left[\left(w + \frac{1}{w} \right) \mathrm{K}_{\frac{2}{3}} \left(\tilde{\kappa}(\varphi, k_-, w) \right) + \int_{\tilde{\kappa}(\varphi, k_-, w)}^\infty \mathrm{d}x\, \mathrm{K}_{\frac{1}{3}}(x) \right], \tag{5.11}$$

with the transformed function

$$\tilde{\kappa}(\varphi, k_-, w) = \frac{2}{3\varkappa(\varphi, k_-)} \frac{(1+w)^2}{w}. \tag{5.12}$$

Finally, the formulas describing pair creation in the kinetic equations for the electrons and positrons are converted as in the procedures above. As the probabilities are once more the same for both species, just one term has to be modified,

$$\frac{\alpha m^2}{\sqrt{3}\pi\omega_0} \int_{p_-}^\infty \frac{\mathrm{d}k_-}{k_-^2} n_\gamma(\varphi, k_-) \left[\frac{k_-^2}{p_-(k_- - p_-)} \mathrm{K}_{\frac{2}{3}} \left(\kappa(\varphi, k_-, p_-) \right) - \int_{\kappa(\varphi, k_-, p_-)}^\infty \mathrm{d}x\, \mathrm{K}_{\frac{5}{3}}(x) \right]. \tag{5.13}$$

As before, we change the integration to a form that allows for a proper numerical calculation via $k_- = p_-/w$ ($\mathrm{d}k_-/\mathrm{d}w = -p_-/w^2$). With this we arrive at the last transformed part

$$\frac{\alpha m^2}{\sqrt{3}\pi\omega_0}\int_0^1 \frac{\mathrm{d}w}{p_-} n_\gamma\left(\varphi, \frac{p_-}{w}\right)\left[\frac{1-2u+2u^2}{u-u^2}\,\mathrm{K}_{\frac{2}{3}}\left(\tilde{\kappa}'(\varphi,p_-,w)\right) + \int_{\tilde{\kappa}'(\varphi,p_-,w)}^{\infty} \mathrm{d}x\,\mathrm{K}_{\frac{1}{3}}(x)\right], \tag{5.14}$$

with the altered function

$$\tilde{\kappa}'(\varphi,p_-,w) = \frac{2}{3\chi(\varphi,p_-)}\frac{1}{1-u}. \tag{5.15}$$

For the discretization of the phase and the minus momentum two static grids were constructed whereupon an equally spaced (like for the phase variable) or a logarithmic grid was built to cover the features of the distribution function adjusted to its range, e.g., a logarithmic spacing in case of the photon distribution $n_\gamma(\varphi,k_-)$. The phase evolution of the distribution functions was calculated by employing an explicit finite-difference method and the occurring integrals except for the one involving $\mathrm{K}_{\frac{1}{3}}(x)$ (see below) have been evaluated by the calculation of the corresponding Riemann sums, in which the momentum values not covered by the grid were computed via an interpolation of grid points.

Since the modified Bessel functions of the second kind are highly-nontrivial functions, the calculation of their values can be rather difficult and especially very time-consuming in a numerical simulation. Thus, a time-efficient numerical procedure is desirable and more easily calculable functions have been chosen as approximations for the occurring Bessel functions. By introducing the function (see [Baie 94])

$$\tilde{f}(x) = \sqrt{\frac{\pi}{2x}}\frac{\mathrm{e}^{-x}}{2}, \tag{5.16}$$

we can find the approximations

$$\mathrm{K}_{\frac{2}{3}}(x) \approx \tilde{f}(x)\left[\left(1+\frac{a_1}{x}\right)^{\frac{1}{6}} + \left(1+\frac{a_2}{x}\right)^{\frac{1}{6}}\right], \tag{5.17}$$

with the constants $a_1 = 0.1265$ and $a_2 = 1.040$, and likewise

$$\mathrm{K}_{\frac{1}{3}}(x) \approx \tilde{f}(x)\left[\left(1+\frac{b_1}{x}\right)^{-\frac{1}{6}} + \left(1+\frac{b_2}{x}\right)^{-\frac{1}{6}}\right], \tag{5.18}$$

with $b_1 = 0.054$ and $b_2 = 0.78$. Furthermore, an approximated expression was employed for the recurrent integral of the function $\mathrm{K}_{\frac{1}{3}}(x)$,

$$\int_x^\infty \mathrm{K}_{\frac{1}{3}}(y)\mathrm{d}y \approx 2f(x)\left[1+\frac{c_1}{x}+\frac{c_2}{x^2}\right]^{-\frac{1}{4}}, \tag{5.19}$$

where $c_1 = 2.53$ and $c_2 = 0.245$ [Baie 94][II]. The accuracy of these expressions was found to be better than 0.2% for (5.17), better than 1% for (5.18), and better than 2% for (5.19).

[II] Note that in [Baie 94], due to a typo, c_1 was mistaken for c_2 and vice versa.

In order to examine the validity of our numerical results, the conservation of the total charge (see eq. (3.22) and eq. (4.5)) and of the total energy minus the total longitudinal momentum (see eq. (3.23) and eq. (4.6)) has been monitored throughout the entire numerical simulation. On the other hand, the calculations have been compared with the existing results in the classical and quantum regime. In the case of the classical limit ($\chi \ll 1$), we guaranteed the consistency of the numerically obtained findings with the analytical limit of the kinetic equation (see fig. 3.3) which was shown to coincide with expression resulting from the LL equation in eq. (3.30). Furthermore, in the quantum regime our findings were in good agreement with the results achieved by a similar kinetic approach in [Soko 10] as well as with the results from alternative approaches, namely the microscopic approach in [Di P 10] (see app. E) and the stochastic model for RR in [Blac 14].

6 Summary and outlook

Summary

The aim of this thesis was to study the impact of radiation reaction on the dynamics of an electron beam colliding with a laser field. In particular, we wanted to compare the different characteristics of radiation reaction effects in the classical and the quantum regime.

To this end, we started in chapter 2 with a discussion of the dynamics of charged particles in an external electromagnetic field in the framework of classical electrodynamics. There, we identified the LL equation as the correct classical equation incorporating the energy and momentum loss due to radiation. Afterwards, this analysis of the interaction of charged particles with an external plane-wave field was transferred into the realm of QED. In the parameter regime under consideration, radiation reaction was shown to result from incoherent multiple photon emission and pair production. Finally, we reviewed some of the key aspects of the kinetic theory.

Following these remarks, we derived a kinetic approach characterizing the collision of an ultrarelativistic electron beam with an intense laser pulse in chapter 3. In the case of the nonlinear moderately quantum regime, the kinetic approach was reduced to a one-dimensional problem and the dynamics of electrons and photons were studied in terms of distribution functions. Whereas classical electrodynamics based on the LL equation predicts a narrowing of the electron energy distribution, radiation reaction was demonstrated to induce a broadening of energy distribution, when quantum effects become important. In order to understand the striking difference between quantum and classical radiation reaction, the classical limit of the kinetic equations was investigated employing an expansion in the quantum nonlinearity parameter χ. The details of this expansions were moved to the appendix B. As summarized in app. C, the resulting Fokker-Planck-like equation is equivalent to a stochastic single-particle equation. Considering an approximate solution of the kinetic equation derived in app. D, the leading-order quantum corrections are shown to render the final electron distributions broader than the initial ones. Hence, the increase of the electron energy width is caused by the stochastic nature of photon emission, which becomes substantial in the quantum regime. To further clarify the impact of radiation reaction on the dynamics of electrons and photons, we studied the influence of the laser pulse duration and shape at given total laser fluences. In

particular, the increase of the pulse duration at a given laser fluence was demonstrated to have a beneficial effect on the total photon yield. Since the classical analysis based on the LL equation depends exclusively on the total laser fluence, differences in the final electron energy distribution and the photon spectra must be due to the interplay of radiation reaction and quantum effects. Our numerical calculations indicated that the final electron and photon distributions are modified by quantum radiation reaction already at $\chi^* = 0.2 - 0.3$. Moreover, in app. E our approach was demonstrated to numerically coincide with the microscopic approach employed in [Di P 10].

In chapter 4, we extended our kinetic approach in order to incorporate the production of electron-positron pairs by photons emitted during the interaction. After the derivation of the kinetic equations, we investigated the nonlinear coupled evolution of the particles involved in the scattering process. To this end, the fully coupled dynamics were compared with those, where either the radiation of the produced positrons or pair production was artificially neglected. The high-energy part of the final photon spectrum was shown to be significantly decreased by the inclusion of pair creation. On the contrary, the increased number of charged particles resulted in a higher low-energy part of the electron and positron distribution in this case. Furthermore, the incorporation of photons emitted by positrons caused a slight modification in the electron distribution function pointing to the conclusion that there is a weak nonlinear coupling between all the particles' distribution functions. Analogously to the discussion in chapter 3, the influence of the pulse duration on the dynamics was studied for two initial electron distributions at a give total laser fluence. As it was demonstrated in chapter 3, longer pulse durations at a given fluence result in an increased final photon yield. On the one hand, considering sufficiently high initial electron beam energies, this beneficial effect of a longer pulse duration was shown to render a higher gain of produced pairs. On the other hand, if the initial beam energy is not high enough, the less energetic photons emitted cannot facilitate an enhanced number of created pairs. Anticipating an experimental investigation of pair production, this result hints that an increase in the energy of the electrons is more favorable than in increase the total laser fluence. In addition, the effect of pair creation was estimated to be in principle measurable for nowadays feasible laser intensities and electron bunch energies also in an all-optical setup.

Chapter 5 was devoted to the numerical treatment of the derived kinetic equations. In particular, it was shown how these equations can be rewritten into a form that allowed for a numerical evaluation via a finite-difference method. To this end, the specific discretization scheme was presented and the employed approximated expressions for the modified Bessel functions of the second kind were introduced.

In conclusion, a kinetic approach permitting the incorporation of radiation reaction effects has been investigated with special emphasis on a regime accessible with presently available high intensity laser pulses and ultrarelativistic electron beams.

Outlook

Motivated by the nowadays experimental feasible electron beam energies and laser pulse intensities, we considered several specific conditions in the derivation of our kinetic approach. In fact, some of these might point to a natural continuation of this work.

- The employed probabilities for photon emission and pair production were al-

ways averaged or summed over the spins of the charged particles and the polarization of the photons. Nevertheless, a description of the polarization characteristics of the quantum particles involved would be favorable, e.g., whether the emission of photons via spin-flip can result in a polarization or depolarization of the initial electron beam. Especially, it would be of interest if the final spins of the electrons and positrons as well as the polarization of the photons can be configured by an adequate choice of the laser parameters. However, it is not directly apparent whether a semi-classical kinetic approach facilitates the incorporation of the charged particles' spin or the photons' polarization.

- Considering laser pulses at even higher intensities, the production of a large amount of pairs might occur. If the number of pairs becomes sufficiently high the interaction between the produced particles have to be taken into account. In particular, an initial or created electron together with a positron can annihilate into a photon or one of the charged particles could reabsorb one of the emitted photons. The incorporation of these effects could render the treatment of collisions with larger laser pulse intensities feasible.

- A consequence of the implementation of larger total laser fluences would be the enhanced energy loss of the charged particles. This can in principle violate our assumption that the transverse momentum can be neglected in comparison to the longitudinal one. In this case, a kinetic approach has to account for all momentum components and cannot be reduced to a one-dimensional problem. Such an extended approach would allow for an increase in the total laser fluence, i.e., the consideration of higher laser peak intensities or longer laser pulse durations.

Appendices

A

Modified Bessel functions

In this appendix some of the characteristics of the modified Bessel functions used in this thesis are reviewed (see, e.g., [Abra 64, Jeff 07]).

The modified Bessel functions of the first kind $\mathrm{I}_{\pm\nu}(x)$ and of the second kind $\mathrm{K}_\nu(x)$, where ν indicates the order, are the solutions of the modified Bessel equation:

$$x^2\frac{\mathrm{d}^2y}{\mathrm{d}x^2} + x\frac{\mathrm{d}y}{\mathrm{d}x} - (x^2+\nu^2)y = 0. \tag{A.1}$$

The modified Bessel function of the second kind $\mathrm{K}_\nu(x)$ can be expressed in terms of $\mathrm{I}_{\pm\nu}(x)$:

$$\mathrm{K}_\nu(x) = \frac{\pi}{2}\frac{\mathrm{I}_{-\nu}(x) - \mathrm{I}_{+\nu}(x)}{\sin(\nu x)}, \tag{A.2}$$

where the right hand side has to be replaced by the limit

$$\mathrm{K}_\nu(x) = \lim_{\mu\to\nu}\mathrm{K}_\mu(x) \tag{A.3}$$

if ν is either an integer or equal to zero. In case of $\nu > -1$ and $x > 0$, the values of $\mathrm{I}_\nu(x)$ and $\mathrm{K}_\nu(x)$ are real and positive. As in the context of photon emission and pair creation investigated in this work there occur solely the modified Bessel functions of the second kind, the following discussion will be focused on $\mathrm{K}_\nu(x)$. For arguments $x \to 0$, the function $\mathrm{K}_\nu(x)$ exhibits a divergence according to

$$\mathrm{K}_\nu(x) \propto \frac{1}{2}\left(\Gamma(\nu)\left(\frac{x}{2}\right)^{-\nu} + \Gamma(-\nu)\left(\frac{x}{2}\right)^{\nu}\right) \qquad (x \to 0), \tag{A.4}$$

with $\Gamma(\nu)$ being the gamma function. For large arguments $|x| \to \infty$, it decreases exponentially,

$$\mathrm{K}_\nu(x) \propto \sqrt{\frac{\pi}{2x}}\mathrm{e}^{-x} \qquad (|x| \to \infty). \tag{A.5}$$

Furthermore, the modified Bessel functions of the second kind are symmetric in the order ν,

$$\mathrm{K}_{-\nu}(x) = \mathrm{K}_\nu(x), \tag{A.6}$$

and fulfill the following recurrence relations

$$\mathrm{K}_{\nu-1}(x) + \mathrm{K}_{\nu+1}(x) = -2\frac{\mathrm{d}}{\mathrm{d}x}\mathrm{K}_\nu(x), \tag{A.7}$$

$$x\frac{\mathrm{d}}{\mathrm{d}x}\mathrm{K}_\nu(x) - \nu\,\mathrm{K}_\nu(x) = -x\,\mathrm{K}_{\nu+1}(x). \tag{A.8}$$

Employing eq. (A.6) and eq. (A.7), we obtain the helpful identity

$$\int_y^\infty \mathrm{d}x\,\mathrm{K}_{\frac{5}{3}}(x) = 2\mathrm{K}_{\frac{2}{3}}(y) - \int_y^\infty \mathrm{d}x\,\mathrm{K}_{\frac{1}{3}}(x). \tag{A.9}$$

In addition, for constants a and μ, the definite integral

$$\int_0^\infty \mathrm{d}x\,x^\mu\,\mathrm{K}_\nu(ax) = 2^{\mu-1}a^{-\mu-1}\Gamma\left(\frac{1+\mu+\nu}{2}\right)\Gamma\left(\frac{1+\mu-\nu}{2}\right) \tag{A.10}$$

can be employed if $\mathrm{Re}(a) > 0$ and $\mathrm{Re}(\mu + 1 \pm \nu > 0)$.

B

Calculation of the expansion of eq. (3.17)

In sec. 3.2 we studied the classical limit and the leading order quantum corrections of the kinetic equation describing the electron distribution function, where we employed a perturbative expansion of eq. (3.17). This appendix is devoted to some of the calculation details of this expansion.

In order to arrive at the approximation (3.27) to eq. (3.17), it is favorable to change the integration variables in eq. (3.17) (see also eq. (5.1) and eq. (5.2)). Hence, we perform the transformations $p_{i,-} = p_-(1 + \mathrm{v}\chi(\varphi, p_-))$, with $\mathrm{d}p_{i,-}/\mathrm{dv} = p_-\chi(\varphi, p_-)$, and $k_- = p_-\mathrm{v}\chi(\varphi, p_-)/(1 + \mathrm{v})$, with $\mathrm{d}k_-/\mathrm{dv} = p_-\chi(\varphi, p_-)/[1 + \mathrm{v}\chi(\varphi, p_-)]^2$, in the first integral and second integral, respectively. By rearranging the terms and dropping for the moment the quantum nonlinearity parameter's explicit dependency of on the phase and the momentum $\chi = \chi(\varphi, p_-)$, we obtain

$$\frac{\partial n_{e^-}^{p_-}}{\partial \varphi} = \frac{\alpha m^2}{\sqrt{3}\pi\omega_0}\frac{\chi}{p_-}\int_0^\infty \mathrm{dv}\left\{\left[\frac{1}{\tilde{\mathrm{v}}_\chi} + \frac{1}{\tilde{\mathrm{v}}_\chi^3}\right]\left[n_{e^-}^{\tilde{\mathrm{v}}_\chi p_-}\mathrm{K}_{\frac{2}{3}}\left(\frac{2\mathrm{v}}{3\tilde{\mathrm{v}}_\chi}\right) - n_{e^-}^{p_-}\mathrm{K}_{\frac{2}{3}}\left(\frac{2\mathrm{v}}{3}\right)\right]\right.$$
$$\left. - \frac{1}{\tilde{\mathrm{v}}_\chi^2}\left[n_{e^-}^{\tilde{\mathrm{v}}_\chi p_-}\int_{2\mathrm{v}/3\tilde{\mathrm{v}}_\chi}^\infty \mathrm{d}x\,\mathrm{K}_{\frac{1}{3}}(x) - n_{e^-}^{p_-}\int_{2\mathrm{v}/3}^\infty \mathrm{d}x\,\mathrm{K}_{\frac{1}{3}}(x)\right]\right\}, \tag{B.1}$$

where we introduced the symbols $\tilde{\mathrm{v}}_\chi = 1 + \mathrm{v}\chi$, $n_{e^-}^{p_-} = n_{e^-}(\varphi, p_-)$ and $n_{e^-}^{\tilde{\mathrm{v}}_\chi p_-} = n_{e^-}(\varphi, \tilde{\mathrm{v}}_\chi p_-)$ for the sake of compact writing. We aim for an expansion up to cubic order in the quantum nonlinearity parameter and start by pointing out that there is no term corresponding to the zero-th order, since there is a factor of χ in front of the integral and the expression in the curly brackets vanishes in the limit $\chi \to 0$, as well. Furthermore, there is no contribution proportional to χ in the Taylor series due to the very same reason. On the one hand, the occurring derivative with respect to χ acts on the factor χ in front of the integral leaving the term in the curly brackets unaffected, which in turn vanishes by evaluating it at the point $\chi = 0$. On the other hand, the derivative acts on the integral leaving the factor χ in front of the integral unaffected and therefore gives again no contribution to the expansion.

Thus, the lowest-order contribution of the perturbative expansion is of the order of χ^2 and it is given by

$$\frac{\partial n_{e^-}^{p_-}}{\partial \varphi} = \frac{\alpha m^2}{\sqrt{3}\pi\omega_0}\frac{\chi^2}{p_-}\int_0^\infty \mathrm{dv}\left[\mathrm{v}p_-\mathfrak{F}\left(\frac{2\mathrm{v}}{3}\right)\frac{\partial n_{e^-}^{p_-}}{\partial p_-} - \frac{2\mathrm{v}^2}{3}\mathfrak{F}'\left(\frac{2\mathrm{v}}{3}\right)n_{e^-}^{p_-}\right] + \mathcal{O}\left(\chi^3\right), \tag{B.2}$$

where we defined the function

$$\mathfrak{F}(x) := 2\mathrm{K}_{\frac{2}{3}}(x) - \int_x^\infty \mathrm{d}y\, \mathrm{K}_{\frac{1}{3}}(y) \tag{B.3}$$

and the prime notation $\mathfrak{F}'(x)$ indicates the derivate with respect to the argument x. Like in eq. (B.2) and in the following terms of the Taylor series the calculation of integrals of $\mathfrak{F}(x)$ and its derivatives is required. We exemplify the principal procedure by explicitly evaluating the first integral on the right hand side of eq. (B.2). By employing the definition of $\mathfrak{F}(x)$ and integrating by parts, we achieve an expression whose value can be determined with the help of the formula (A.10):

$$\begin{aligned}\int_0^\infty \mathrm{dv}\,\mathrm{v}\,\mathfrak{F}\left(\frac{2\mathrm{v}}{3}\right) &= \int_0^\infty \mathrm{dv}\,\mathrm{v}\left[2\mathrm{K}_{\frac{2}{3}}\left(\frac{2\mathrm{v}}{3}\right) - \int_{2\mathrm{v}/3}^\infty \mathrm{d}x\,\mathrm{K}_{\frac{1}{3}}(x)\right] \\ &= \int_0^\infty \mathrm{dv}\,2\mathrm{v}\,\mathrm{K}_{\frac{2}{3}}\left(\frac{2\mathrm{v}}{3}\right) - \int_0^\infty \mathrm{dv}\,\frac{\mathrm{v}^2}{3}\,\mathrm{K}_{\frac{1}{3}}\left(\frac{2\mathrm{v}}{3}\right) \\ &\overset{(A.10)}{=} \frac{2\pi}{\sqrt{3}}.\end{aligned} \tag{B.4}$$

All the remaining integrations occurring in the expansion of eq. (3.17) up to the order of χ^3 can be obtained following this outline of analysis, and without displaying further details, we list here only the final results:

$$\int_0^\infty \mathrm{dv}\,\mathrm{v}^2\mathfrak{F}\left(\frac{2\mathrm{v}}{3}\right) = \frac{55\pi}{24}, \tag{B.5}$$

$$\int_0^\infty \mathrm{dv}\,\mathrm{v}^2\mathfrak{F}'\left(\frac{2\mathrm{v}}{3}\right) = -2\sqrt{3}\pi, \tag{B.6}$$

$$\int_0^\infty \mathrm{dv}\,\mathrm{v}^3\mathfrak{F}'\left(\frac{2\mathrm{v}}{3}\right) = -\frac{165\pi}{16}, \tag{B.7}$$

$$\int_0^\infty \mathrm{dv}\,\mathrm{v}^4\mathfrak{F}''\left(\frac{2\mathrm{v}}{3}\right) = \frac{495\pi}{8}. \tag{B.8}$$

Therefore, by only taking into account terms proportional to χ^2, eq. (3.17) reads

$$\begin{aligned}\frac{\partial n_{e^-}^{p_-}}{\partial\varphi} &= \frac{2\alpha m^2}{3\omega_0}\chi^2\left(\frac{2n_{e^-}^{p_-}}{p_-} + \frac{\partial n_{e^-}^{p_-}}{\partial p_-}\right) \\ &= -\frac{2\alpha m^2}{3\omega_0}\frac{\partial}{\partial p_-}\left[-\chi^2(\varphi,p_-)n_{e^-}(\varphi,p_-)\right],\end{aligned} \tag{B.9}$$

where the explicit dependency on the phase and the momentum was included again in the last line. As intended, this result yields the first term in eq. (3.28) coinciding with the classical electrodynamics result obtained by employing the LL equation.

Analogously, the perturbative expansion up to the order χ^3 allows for an identification of the leading-order quantum corrections to the kinetic equation, which we

indicate by $\left(\partial n_{e^-}^{p_-}/\partial\varphi\right)_{\chi^3}$,

$$\begin{aligned}\left(\frac{\partial n_{e^-}^{p_-}}{\partial\varphi}\right)_{\chi^3} =& \frac{\alpha m^2}{\sqrt{3}\pi\omega_0}\frac{\chi^3}{18p_-}\int_0^\infty \mathrm{d}\mathrm{v}\,\mathrm{v}^2\left\{\left[36\mathrm{v}\mathfrak{F}'\left(\frac{2\mathrm{v}}{3}\right)+4\mathrm{v}^2\mathfrak{F}''\left(\frac{2\mathrm{v}}{3}\right)\right]n_{e^-}^{p_-}\right.\\ &\left.-\left[36p_-\mathfrak{F}\left(\frac{2\mathrm{v}}{3}\right)+12\mathrm{v}p_-\mathfrak{F}'\left(\frac{2\mathrm{v}}{3}\right)\right]\frac{\partial n_{e^-}^{p_-}}{\partial p_-}+9p_-^2\mathfrak{F}\left(\frac{2\mathrm{v}}{3}\right)\frac{\partial^2 n_{e^-}^{p_-}}{\partial p_-^2}\right\}\\ =&\frac{\alpha m^2}{3\omega_0}\chi^3\left[-\frac{55\sqrt{3}}{8}\frac{n_{e^-}^{p_-}}{p_-}+\frac{55}{8\sqrt{3}}\frac{\partial n_{e^-}^{p_-}}{\partial p_-}+\frac{55p_-}{16\sqrt{3}}\frac{\partial^2 n_{e^-}^{p_-}}{\partial p_-^2}\right].\end{aligned} \tag{B.10}$$

Anticipating the final Fokker-Planck-like structure of the approximated kinetic equation and writing again the explicit dependency on the phase and the momentum, the expressions occurring in eq. (B.10) can be artificially rearranged in the formula

$$\begin{aligned}\left(\frac{\partial n_{e^-}(\varphi,p_-)}{\partial\varphi}\right)_{\chi^3} =& -\frac{\partial}{\partial p_-}\left[\frac{\alpha m^2}{\sqrt{3}\omega_0}\frac{55}{8}\chi^3(\varphi,p_-)n_{e^-}(\varphi,p_-)\right]\\ &+\frac{1}{2}\frac{\partial^2}{\partial p_-^2}\left[\frac{\alpha m^2}{3\omega_0}\frac{55}{8\sqrt{3}}p_-\chi^3(\varphi,p_-)n_{e^-}(\varphi,p_-)\right].\end{aligned} \tag{B.11}$$

Finally, we conclude that the combination of eq. (B.9) and eq. (B.11) leads exactly to the Fokker-Planck-like equation investigated in the main text:

$$\frac{\partial n_{e^-}(\varphi,p_-)}{\partial\varphi} = -\frac{\partial}{\partial p_-}\left[A(\varphi,p_-)n_{e^-}(\varphi,p_-)\right]+\frac{1}{2}\frac{\partial^2}{\partial p_-^2}\left[B(\varphi,p_-)n_{e^-}(\varphi,p_-)\right] \tag{B.12}$$

with

$$A(\varphi,p_-) = -\frac{2\alpha m^2}{3\omega_0}\chi^2(\varphi,p_-)\left[1-\frac{55\sqrt{3}}{16}\chi(\varphi,p_-)\right], \tag{B.13}$$

$$B(\varphi,p_-) = \frac{\alpha m^2}{3\omega_0}\frac{55}{8\sqrt{3}}p_-\chi^3(\varphi,p_-). \tag{B.14}$$

C

Connection between the Fokker-Planck and the Langevin equation

In this appendix it is shown how the Langevin equation describing the stochastic motion of a single particle can be related to the Fokker-Planck equation describing the deterministic evolution of a macroscopic distribution of these particles. Therefore, some parts of the theory of stochastic differential equations are recapitulated here. However, this is only intended to be a short overview and does not include complete mathematical proofs of the equations and properties given below. A more detailed discussion of the topics related to stochastic differential processes can be found, e.g., in [Gard 09].

C.1 From the Langevin to the Fokker-Planck equation

Instead of the usual notations for stochastic processes we will here employ the same variables as in the main text, e.g., we use the phase φ as evolution variable and not the common t as symbol for the time. Considering now a stochastic process, i.e., a random variable $\hat{P}_-(\varphi)$[I] that evolves in phase and corresponds to the measurable values $p_-(\varphi)$, the Langevin equation can be written as

$$\mathrm{d}p_-(\varphi) = A[\varphi, p_-(\varphi)]\mathrm{d}\varphi + \sqrt{B[\varphi, p_-(\varphi)]}\mathrm{d}W(\varphi), \tag{C.1}$$

where the square-root is due to the anticipation of the final form of the related Fokker-Plank equation. The functions $A[\varphi, p_-(\varphi)]$ and $B[\varphi, p_-(\varphi)]$ are the so-called drift coefficient and diffusion coefficient, respectively. The names already hint at the influence of these functions on the evolution of a particle distribution, and will be justified in sec. C.2.

The expression $\mathrm{d}W(\varphi)$ indicates an infinitesimal stochastic function, namely the Wiener process. The Wiener process is a stochastic process fulfilling the Markov condition, i.e., the stochastic evolution of the events is only influenced by the values at the last phase step and not by those before that. The conditional probability $P(w, \varphi|w_0, \varphi_0)$ to find the value w at phase φ under the assumption that it had the

[I] The notation $\hat{P}_-(\varphi)$ for the random variable is chosen to avoid confusion with the probabilities occurring in the text indicated by P.

initial value w_0 at initial phase φ_0[II] is then given by the expression

$$P(w,\varphi|w_0,\varphi_0) = \frac{1}{\sqrt{2\pi(\varphi-\varphi_0)}}\exp\left[-\frac{(w-w_0)^2}{2(\varphi-\varphi_0)}\right], \tag{C.2}$$

with the initial condition $P(w,\varphi_0|w_0,\varphi_0)=\delta(w-w_0)$. The Wiener process is continuous everywhere[III] but differentiable nowhere. By means of a Riemann-Stieltjes integral, the Ito stochastic integral of an arbitrary function $G(t)$ is defined as

$$\int_{\varphi_0}^{\varphi} G(\varphi')\mathrm{d}W(\varphi') := \underset{L\to\infty}{\text{ms-lim}}\left\{\sum_{l=1}^{L} G(\varphi_{l-1})\left[W(\varphi_l)-W(\varphi_{l-1})\right]\right\}, \tag{C.3}$$

where ms-lim indicates the mean square limit and convergence under this limit is equivalent to the vanishing of the mean square deviation. Note that an alternative but nevertheless equivalent way to define stochastic integration is given by the Stratonovich integral which differs from the Ito integral by the choice of the intermediate evaluation points for the subintervals. Furthermore, this definition can be proven to imply the identities $\mathrm{d}W(\varphi)^2=\mathrm{d}t$ and $\mathrm{d}W(\varphi)^{2+M}=0$ for $M>0$.

Facilitating these properties for a function $G[p_-(\varphi)]$ depending on the stochastically evolving variable $p_-(\varphi)$, we can expand $\mathrm{d}G[p_-(\varphi)]$ up to second order in $\mathrm{d}W(\varphi)$,

$$\begin{aligned}
\mathrm{d}G[p_-(\varphi)] =& G[p_-(\varphi)+\mathrm{d}p_-(\varphi)] - G[p_-(\varphi)] \\
=& \frac{\partial G[p_-(\varphi)]}{\partial p_-(\varphi)}\mathrm{d}p_-(\varphi) + \frac{1}{2}\frac{\partial^2 G[p_-(\varphi)]}{\partial p_-(\varphi)^2}\mathrm{d}p_-(\varphi)^2 \\
=& \frac{\partial G[p_-(\varphi)]}{\partial p_-(\varphi)}\left\{A[\varphi,p_-(\varphi)]\mathrm{d}\varphi + \sqrt{B[\varphi,p_-(\varphi)]}\mathrm{d}W(\varphi)\right\} \\
&+ \frac{1}{2}\frac{\partial^2 G[p_-(\varphi)]}{\partial p_-(\varphi)^2}B[\varphi,p_-(\varphi)]\mathrm{d}W(\varphi)^2 \\
=& \left\{A[\varphi,p_-(\varphi)]\frac{\partial G[p_-(\varphi)]}{\partial p_-(\varphi)} + \frac{1}{2}B[\varphi,p_-(\varphi)]\frac{\partial^2 G[p_-(\varphi)]}{\partial p_-(\varphi)^2}\right\}\mathrm{d}\varphi \\
&+ \sqrt{B[\varphi,p_-(\varphi)]}\frac{\partial G[p_-(\varphi)]}{\partial p_-(\varphi)}\mathrm{d}W(\varphi),
\end{aligned} \tag{C.4}$$

where all higher-order terms have been discarded. eq. (C.4) is known as Ito's formula and by applying it to the phase derivative of the mean value of an arbitrary function $G[p_-(\varphi)]$, we now connect the Langevin with the Fokker-Planck equation:

$$\begin{aligned}
\frac{\mathrm{d}}{\mathrm{d}\varphi}\left\langle G[p_-(\varphi)]\right\rangle =& \frac{\left\langle \mathrm{d}G[p_-(\varphi)]\right\rangle}{\mathrm{d}\varphi} \\
=& \left\langle A[\varphi,p_-(\varphi)]\frac{\partial G[p_-(\varphi)]}{\partial p_-(\varphi)} + \frac{1}{2}B[\varphi,p_-(\varphi)]\frac{\partial^2 G[p_-(\varphi)]}{\partial p_-(\varphi)^2}\right\rangle.
\end{aligned} \tag{C.5}$$

Since the process $p_-(\varphi)$ with initial value $p_{-,0}$ has the conditional probabilities $P(\varphi,p_-|\varphi_0,p_{-,0})$, we rewrite eq. (C.5) by employing the definition of the mean value.

[II] In this appendix, the subscript 0 is used to indicate the initial phase value instead of i as in the main text, since it allows to write the sequences and sums in an easily accessible way.

[III] Mathematically strictly speaking, the Wiener process is *almost surely* continuous, i.e., it is a continuous function of phase with probability one.

This yields

$$\begin{aligned}\frac{\langle \mathrm{d}G[p_-(\varphi)]\rangle}{\mathrm{d}\varphi} &= \int \mathrm{d}p_-\, G(p_-)\partial_\varphi P(\varphi, p_-|\varphi_0, p_{-,0}) \\ &= \int \mathrm{d}p_- \left[A(\varphi,p_-)\partial_{p_-}G(p_-) + \frac{1}{2}B(\varphi,p_-)\partial^2_{p_-}G(p_-)\right] P(\varphi,p_-|\varphi_0,p_{-,0}) \\ &= \int \mathrm{d}p_-\, G(p_-)\left\{-\partial_{p_-}\left[A(\varphi,p_-)P(\varphi,p_-|\varphi_0,p_{-,0})\right]\right. \\ &\qquad \left. +\frac{1}{2}\partial^2_{p_-}\left[B(\varphi,p_-)P(\varphi,p_-|\varphi_0,p_{-,0})\right]\right\},\end{aligned} \tag{C.6}$$

where we integrated by parts to obtain the last line and the integration path includes all values corresponding to the set of possible events. As the function $G(p_-)$ was chosen to be arbitrary, the conditional probability $P(\varphi, p_-|\varphi_0, p_{-,0})$ has to fulfill the Fokker-Planck equation

$$\begin{aligned}\partial_\varphi P(\varphi,p_-|\varphi_0,p_{-,0}) = &-\partial_{p_-}\left[A(\varphi,p_-)P(\varphi,p_-|\varphi_0,p_{-,0})\right] \\ &+\frac{1}{2}\partial^2_{p_-}\left[B(\varphi,p_-)P(\varphi,p_-|\varphi_0,p_{-,0})\right].\end{aligned} \tag{C.7}$$

The Fokker-Planck equation, however, describes the evolution of the probability density function, which in our case complies with the momentum distribution functions for the considered particles, e.g., the momentum distribution for the electrons $n_{e^-}(\varphi, p_-)$. Finally, by substituting the conditional probability by the electron distribution function, we achieve the Fokker-Planck equation of the main text (see eq. (3.27)):

$$\frac{\partial n_{e^-}(\varphi,p_-)}{\partial\varphi} = -\frac{\partial}{\partial p_-}\left[A(\varphi,p_-)n_{e^-}(\varphi,p_-)\right] + \frac{1}{2}\frac{\partial^2}{\partial p_-^2}\left[B(\varphi,p_-)n_{e^-}(\varphi,p_-)\right]. \tag{C.8}$$

C.2 Interpretation of $A(\varphi, p_-)$ and $B(\varphi, p_-)$

For the purpose of comprehending the functions' $A(\varphi, p_-)$ and $B(\varphi, p_-)$ influence on the phase evolution of the momentum distribution of the electrons, we investigate two simplified versions of eq. (C.7) in this section. Since there is no general solution to the Fokker-Planck equation involving arbitrary complex functions $A(\varphi, p_-)$ and $B(\varphi, p_-)$, we will only consider the cases in which the one function is a constant and the other one is vanishing to get a principal understanding of their meaning. However, in app. D an approximate solution to eq. (3.27) of the main text including more complex structured functions is derived displaying the same properties as in the far simpler cases discussed here.

At first, by setting $A(\varphi, p_-) \equiv A$ and $B(\varphi, p_-) \equiv 0$, we reduce eq. (C.8) to

$$\frac{\partial n_{e^-}(\varphi,p_-)}{\partial\varphi} = -A\frac{\partial}{\partial p_-}\left[n_{e^-}(\varphi,p_-)\right], \tag{C.9}$$

and with the initial electron distribution $n_{e^-}(0, p_-)$ chosen to be a normalized Gaussian centered around p_-^* and width σ_{p_-}, we obtain the result

$$n_{e^-}(\varphi,p_-) = \frac{1}{\sqrt{\pi/2}\sigma_{p_-}[1+\mathrm{erf}(p_-^*/\sqrt{2}\sigma_{p_-})]}\exp\left[-\frac{(p_- - p_-^* - A\varphi)^2}{2\sigma_{p_-}^2}\right], \tag{C.10}$$

where we also set $\varphi_0 = 0$ and introduced the error function $\mathrm{erf}(x)$.[IV] From eq. (C.10) it becomes immediately apparent why the function $A(\varphi, p_-) \equiv A$ is called drift coefficient. In this special scenario the Gaussian distribution - without changing its shape - shifts to higher values of p_-^* for increasing phase and $A > 0$. On the other hand, for $A < 0$, the distribution drifts into the other direction.

Secondly, we now assume $A(\varphi, p_-) \equiv 0$ and $B(\varphi, p_-) \equiv B$ transforming eq. (C.8) into

$$\frac{\partial n_{e^-}(\varphi, p_-)}{\partial \varphi} = \frac{1}{2} B \frac{\partial^2}{\partial p_-^2} \left[n_{e^-}(\varphi, p_-) \right], \tag{C.11}$$

which is the well-known heat equation. Employing the initial condition $n_{e^-}(0, p_-) = \delta(p_- - p_-^*)$, we find the solution

$$n_{e^-}(\varphi, p_-) = \frac{1}{\sqrt{B\varphi\pi/2}[1 + \mathrm{erf}(p_-^*/\sqrt{2B\varphi})]} \exp\left[-\frac{(p_- - p_-^*)^2}{2B\varphi} \right]. \tag{C.12}$$

Although the width σ_{p_-} is missing due to the choice of a delta peak as initial condition, a brief comparison with eq. (C.10) shows that the term $B\varphi$ occurs in the same positions and thus can be easily interpreted as a time-evolving width. If $B < 0$, there exist no bounded solutions to eq. (C.12) and an interpretation of the solutions as distribution function is impossible. With that we are able to conclude that the appearance of the term including B leads to a broadening of the width of the distribution for increasing phase.

[IV] Note that we employed $p_- \in (0, \infty)$, as always.

D

Approximated solution of eq. (3.27)

In sec. 3.2.3, the influence of the quantum corrections on the evolution of the electron distribution was discussed with a special emphasis on the aspect whether the initial width of the distribution σ_{p_-} is increased or decreased. There, an approximate solution of the Fokker-Planck-like equation (3.27) was employed which assumed an initial Gaussian distribution to evolve in such a way that, on the one hand, the Gaussian shape was preserved but, on the other hand, allowed for a shift of the peak as well as an alteration of the width. Here, we derive this approximate solution and its resulting properties used in the main text.

We begin by writing down again the expanded kinetic equation (3.27),

$$\frac{\partial n_{e^-}(\varphi, p_-)}{\partial \varphi} = -\frac{\partial}{\partial p_-}\left[A(\varphi, p_-) n_{e^-}(\varphi, p_-)\right] + \frac{1}{2}\frac{\partial^2}{\partial p_-^2}\left[B(\varphi, p_-) n_{e^-}(\varphi, p_-)\right], \quad \text{(D.1)}$$

and separate the dependencies on the phase and the momentum included in the definition of $\chi(\varphi, p_-)$ for the drift coefficient $A(\varphi, p_-)$,

$$\begin{aligned} A(\varphi, p_-) &= -\frac{2\alpha}{3\omega_0}\frac{E^2(\varphi)}{F_{\mathrm{cr}}^2} p_-^2 + \frac{55\alpha}{8\sqrt{3}\omega_0 m}\frac{|E^3(\varphi)|}{F_{\mathrm{cr}}^3} p_-^3 \\ &= \mathfrak{a}(\varphi) p_-^2 + \mathfrak{b}(\varphi) p_-^3, \end{aligned} \quad \text{(D.2)}$$

and for the diffusion coefficient $B(\varphi, p_-)$,

$$B(\varphi, p_-) = \frac{\alpha 55}{24\sqrt{3}\omega_0 m}\frac{|E^3(\varphi)|}{F_{\mathrm{cr}}^3} p_-^4 = \mathfrak{c}(\varphi) p_-^4. \quad \text{(D.3)}$$

The explicit separation of phase and momentum permits the rescaling of the originally assumed electron distribution by $\bar{n}_{e^-}(\varphi, p_-) := p_-^2 n_{e^-}(\varphi, p_-)$ and by employing the newly defined phase dependent functions $\mathfrak{a}(\varphi)$, $\mathfrak{b}(\varphi)$ and $\mathfrak{c}(\varphi)$, we achieve

$$\begin{aligned} \frac{\partial \bar{n}_{e^-}(\varphi, p_-)}{\partial \varphi} = p_-^2 \Bigg(&-\frac{\partial}{\partial p_-}\left\{\bar{n}_{e^-}(\varphi, p_-)\left[\mathfrak{a}(\varphi) + \mathfrak{b}(\varphi) p_-\right]\right\} \\ &+\frac{1}{2}\frac{\partial^2}{\partial p_-^2}\left[\mathfrak{c}(\varphi) p_-^2 \bar{n}_{e^-}(\varphi, p_-)\right]\Bigg). \end{aligned} \quad \text{(D.4)}$$

Considering the further course of derivation, it is convenient to search for a solution of the partial differential equation depending on $x = 1/p_-$ instead of p_-. Thus, by

introducing a new electron distribution $\tilde{n}_{e^-}(\varphi, x)$ and in addition performing the change $\partial/\partial p_- = -x^2\partial/\partial x$, we obtain

$$\begin{aligned}\frac{\partial \tilde{n}_{e^-}(\varphi,x)}{\partial\varphi} =& -\frac{\partial}{\partial x}\left\{\tilde{n}_{e^-}(\varphi,x)\left[-\mathfrak{a}(\varphi)-\frac{\mathfrak{b}(\varphi)}{x}\right]\right\}\\ &+\frac{1}{2}\frac{\partial}{\partial x}\left\{x^2\frac{\partial}{\partial x}\left[\frac{\mathfrak{c}(\varphi)}{x^2}\tilde{n}_{e^-}(\varphi,x)\right]\right\},\end{aligned} \tag{D.5}$$

where we artificially inserted additional minus signs in order to preserve the Fokker-Planck-like structure of the formula. Presuming a distribution function well-peaked at $x^*(\varphi)$, the terms arising from the derivatives not acting on the distribution function itself are negligible and the differential equation is reduced to

$$\frac{\partial \tilde{n}_{e^-}(\varphi,x)}{\partial\varphi} \approx -\left[-\mathfrak{a}(\varphi)-\frac{\mathfrak{b}(\varphi)}{x^*(\varphi)}\right]\frac{\partial \tilde{n}_{e^-}(\varphi,x)}{\partial x}+\frac{\mathfrak{c}(\varphi)}{2}\frac{\partial^2 \tilde{n}_{e^-}(\varphi,x)}{\partial x^2}. \tag{D.6}$$

The movement of the peak position is approximately determined by the differential equation

$$\frac{\partial x^*(\varphi)}{\partial\varphi} \approx -\mathfrak{a}(\varphi)-\frac{\mathfrak{b}(\varphi)}{x^*(\varphi)}. \tag{D.7}$$

Since the Fokker-Planck equation (D.1) is the result of a perturbative expansion of the original kinetic equation (3.17), its validity is restricted to a parameter regime with $\chi(\varphi, p_-) \ll 1$ and in turn, the terms proportional to $\mathfrak{b}(\varphi)$ and $\mathfrak{c}(\varphi)$ have to be understood as corrections of higher order. Therefore, the phase evolution of the peak position $x^*(\varphi)$ must be governed by the expression proportional to $\mathfrak{a}(\varphi)$ within this framework. Hence, the shift of the peak position is approximately given by

$$x^*(\varphi, x_0^*) \approx x_0^* - \int_0^\varphi \mathrm{d}\varphi'\,\mathfrak{a}(\varphi') - \int_0^\varphi \mathrm{d}\varphi'\,\frac{\mathfrak{b}(\varphi')}{x_0^* - \int_0^{\varphi'}\mathrm{d}\varphi''\,\mathfrak{a}(\varphi'')}, \tag{D.8}$$

where we set again the initial phase $\varphi_i = 0$ and introduced the initial peak position $x^*(0) = x_0^*$.

Analogously, the motion of the momentum value at which the original Gaussian distribution is centered is obtained by employing the relation between x and p_- and defining the initial condition for the peak position $p_-^*(0) = p_{0,-}^* = 1/x_0^*$,

$$\begin{aligned}p_-^*(\varphi, p_{0,-}^*) \approx& \left[\frac{1}{p_{0,-}^*} - \int_0^\varphi \mathrm{d}\varphi'\,\mathfrak{a}(\varphi') - \int_0^\varphi \mathrm{d}\varphi'\,\frac{\mathfrak{b}(\varphi')}{\frac{1}{p_{0,-}^*} - \int_0^{\varphi'}\mathrm{d}\varphi''\,\mathfrak{a}(\varphi'')}\right]^{-1}\\ =:& \frac{p_{0,-}^*}{h^{(q)}(\varphi, p_{0,-}^*)}.\end{aligned} \tag{D.9}$$

In order to illustrate the structural similarity, we defined in the last line the function $h^{(q)}(\varphi, p_{0,-}^*)$ as the counterpart to the change in momentum given by $p_-^{*(c)}(\varphi, p_{0,-}) = p_{0,-}^*/h^{(c)}(\varphi, p_{0,-}^*)$ (see eq. (3.32)) in classical electrodynamics. To further clarify the connection between $h^{(c)}(\varphi, p_{0,-}^*)$ and $h^{(q)}(\varphi, p_{0,-}^*)$, the part corresponding to the

classical dynamics is separated,

$$\begin{aligned} h^{(q)}(\varphi, p^*_{0,-}) &\approx 1 - p^*_{0,-} \int_0^\varphi \mathrm{d}\varphi'\, \mathfrak{a}(\varphi') - p^{*\,2}_{0,-} \int_0^\varphi \mathrm{d}\varphi' \, \frac{\mathfrak{b}(\varphi')}{1 - p^*_{0,-} \int_0^{\varphi'} \mathrm{d}\varphi''\, \mathfrak{a}(\varphi'')} \\ &= h^{(c)}(\varphi, p^*_{0,-}) - p^{*\,2}_{0,-} \int_0^\varphi \mathrm{d}\varphi' \, \frac{\mathfrak{b}(\varphi')}{h^{(c)}(\varphi', p^*_{0,-})} \\ &= h^{(c)}(\varphi, p^*_{0,-}) - \frac{55\sqrt{3}}{16} \int_0^\varphi \mathrm{d}\varphi'\, \chi(\varphi', p^*_{0,-}) \frac{\partial}{\partial \varphi'} \left\{ \ln \left[h^{(c)}(\varphi', p^*_{0,-}) \right] \right\} \\ &=: h^{(c)}(\varphi, p^*_{0,-}) \left[1 - \delta h(\varphi, p^*_{0,-}) \right], \end{aligned} \tag{D.10}$$

and the deviation $\delta h(\varphi, p^*_{0,-})$ of the function describing the approximated quantum process from the classical one is defined. We note here that $\delta h(\varphi, p^*_{0,-})$ only occurs due to the quantum correction in the drift term $A(\varphi, p_-)$ of eq. (D.1) and is strictly positive for all phases $\varphi > 0$.

Returning to the problem of finding a solution to the Fokker-Planck-like equation, the combination of eq. (D.6) and eq. (D.8) allows for an analytical solution by means of the method of characteristics. Setting the initial distribution function to be a Gaussian centered at x^*_0 and with width σ_x yields

$$\tilde{n}_{e^-}(\varphi, x) \approx \frac{\mathcal{N}_x}{\sqrt{\sigma_x^2 + \int_0^\varphi \mathrm{d}\varphi'\, \mathfrak{c}(\varphi')}} \exp\left\{ - \frac{\left[x - x^*(\varphi, x^*_0) \right]^2}{2 \left[\sigma_x^2 + \int_0^\varphi \mathrm{d}\varphi'\, \mathfrak{c}(\varphi') \right]} \right\}, \tag{D.11}$$

where $\mathcal{N}_x$ is a normalization constant.[I] In turn, eq. (D.11) can be reformulated in terms of the momentum p_- as intended in the beginning,

$$\begin{aligned} n_{e^-}(\varphi, p_-) &\approx \frac{\mathcal{N}_{p_-}}{\sqrt{\sigma_x^2 + \int_0^\varphi \mathrm{d}\varphi'\, \mathfrak{c}(\varphi')\, p_-^2}} \exp\left\{ - \frac{\left[\frac{1}{p_-} - \frac{1}{p^*_-(\varphi, p^*_{0,-})} \right]^2}{2 \left[\sigma_x^2 + \int_0^\varphi \mathrm{d}\varphi'\, \mathfrak{c}(\varphi') \right]} \right\} \\ &= \frac{\mathcal{N}_{p_-}}{\sqrt{\sigma_x^2 + \int_0^\varphi \mathrm{d}\varphi'\, \mathfrak{c}(\varphi')\, p_-^2}} \exp\left\{ - \frac{\left[h^{(q)}(\varphi, p^*_{0,-}) \right]^2 \left[p_- - \frac{p^*_{0,-}}{h^{(q)}(\varphi, p^*_{0,-})} \right]^2}{2 p_-^2 p^{*\,2}_{0,-} \left[\sigma_x^2 + \int_0^\varphi \mathrm{d}\varphi'\, \mathfrak{c}(\varphi') \right]} \right\}, \end{aligned} \tag{D.12}$$

where we employed eq. (D.9) and $\mathcal{N}_{p_-}$ indicates the normalization factor. As in the derivation we assumed the approximate solution to be well-peaked, we can further simplify the distribution function,

$$n_{e^-}(\varphi, p_-) \approx \frac{\mathcal{N}_{p_-} \left[h^{(q)}(\varphi, p^*_{0,-}) \right]^2}{\sqrt{\sigma_x^2 + \int_0^\varphi \mathrm{d}\varphi'\, \mathfrak{c}(\varphi')\, p^{*\,2}_{0,-}}} \exp\left\{ - \frac{\left[h^{(q)}(\varphi, p^*_{0,-}) \right]^4 \left[p_- - \frac{p^*_{0,-}}{h^{(q)}(\varphi, p^*_{0,-})} \right]^2}{2 p^{*\,4}_{0,-} \left[\sigma_x^2 + \int_0^\varphi \mathrm{d}\varphi'\, \mathfrak{c}(\varphi') \right]} \right\}, \tag{D.13}$$

[I] The normalization "constant" evolves, however, itself in phase, since the mean value and the width of the distribution function are varying. Explicitly, for a distribution normalized to unity, we obtain $\mathcal{N}_x = \left(\sqrt{\frac{\pi}{2}} \left\{ 1 + \mathrm{erf}\left[\frac{x^*(\varphi, x^*_0)}{\sqrt{2\sigma_x^2 + 2\int_0^\varphi \mathrm{d}\varphi'\, \mathfrak{c}(\varphi')}} \right] \right\} \right)^{-1}$.

where we made use of the property $p_- \approx p^*_{0,-}/h^{(q)}(\varphi, p^*_{0,-})$.[II] Finally, we give an approximate formula describing the evolution of the distribution width including quantum corrections, where we return from $\mathfrak{c}(\varphi)$ to the function $B(\varphi, p_-)$ and employ the substitution $\sigma_x = p^{*\,2}_{0,-}\sigma_{p_-}$. From eq. (D.13), we can identify the expression corresponding to the standard deviation of a Gaussian distribution and can expand the result in the small parameters $B(\varphi, p_-)$ and $\delta h(\varphi, p_-)$,

$$\begin{aligned}
\sigma^{(q)}_{p_-}(\varphi, p^*_{0,-}) &\approx \sqrt{\frac{\sigma^2_{p_-} + \int_0^\varphi \mathrm{d}\varphi'\, B(\varphi', p^*_{0,-})}{\left[h^{(q)}(\varphi, p^*_{0,-})\right]^4}} \\
&= \sqrt{\frac{\sigma^2_{p_-}}{\left[h^{(c)}(\varphi, p^*_{0,-})\right]^4}} \sqrt{\frac{1 + \int_0^\varphi \mathrm{d}\varphi' \, \frac{B(\varphi', p^*_{0,-})}{\sigma^2_{p_-}}}{\left[1 - \delta h(\varphi, p^*_{0,-})\right]^4}} \\
&\approx \sigma^{(c)}_{p_-}(\varphi, p^*_{0,-}) \left[1 + 2\delta h(\varphi, p^*_{0,-}) + \frac{1}{2\sigma^2_{p_-}} \int_0^\varphi \mathrm{d}\varphi'\, B(\varphi', p^*_{0,-})\right],
\end{aligned} \tag{D.14}$$

with the definition of the classically evolving width $\sigma^{(c)}_{p_-}(\varphi, p^*_{0,-})$ given in eq. (3.38). We recall here that in order for this approximation to be valid, the distribution function must be well-peaked, i.e., $\sigma \ll p^*_-$, throughout the whole interaction and the corrections have to be much smaller than the leading-order contribution. In the case of eq. (D.14), this implies that $\alpha\xi\zeta\Phi_\mathrm{L}\chi^{*\,2} \ll 1$ has to be fulfilled, with the total laser phase Φ_L and the ratio $\zeta = p^{*\,2}_-/\sigma^2_p$. In addition, the term proportional to $\delta h(\varphi, p^*_{0,-})$ in eq. (D.14) is much smaller than the term proportional to $B(\varphi', p^*_{0,-})$ which contains the additional factor ζ.

[II] For the sake of completeness, we give here the explicit form of the normalization factor: $\mathcal{N}_{p_-} = \left(\sqrt{\frac{\pi}{2}}\left\{1 + \mathrm{erf}\left[\frac{h^{(q)}(\varphi, p^*_{0,-})}{p^*_{0,-}\sqrt{2\sigma^2_x + 2\int_0^\varphi \mathrm{d}\varphi'\, \mathfrak{c}(\varphi')}}\right]\right\}\right)^{-1}$.

E

Microscopic approach

In this appendix the agreement of the "macroscopic" kinetic approach with the so-called microscopic approach developed in [Di P 10] is investigated by the comparison of the results for the emitted photon spectra. In order to calculate the photon spectrum in the framework of the microscopic approach, the probability of the incoherent emission of more than one photon by a single electron is determined. By an integration over all but one degrees of freedom, the single-photon spectrum can be obtained. Although the microscopic approach has the advantage of circumventing the problem of finding a solution to the kinetic integro-differential equations (3.17) and (3.18), multi-dimensional integrals have to be evaluated, whose dimensionality rise with an increase in the number of emitted photons. In [Di P 10] the multidimensional integrals were calculated via the Monte Carlo method and the inclusion of up to 16 emitted photons was found to be sufficient for convergence of the spectrum at the given parameters.

In order to obtain a comparable photon spectrum to this numerical result, we set the peak intensity to $I_0 = 10^{23}\,\mathrm{W/cm^2}$ [I] and consider a two-cycle sinusoidal pulse, i.e., $f(\varphi) = \sin(\varphi)$ ($\varphi_f = 4\pi$, $\xi = 154$), with a pulse duration of about 5 fs and central angular frequency $\omega_0 = 1.55\,\mathrm{eV}$. Furthermore, we have chosen an initial Gaussian electron distribution centered at $p_-^* \approx 2$ GeV (corresponding to $\varepsilon^* = 1\,\mathrm{GeV}$ considered in [Di P 10]) and a standard deviation of $\sigma_{p_-} = 0.1\,\mathrm{GeV}$. For the sake of comparison with the single-particle approach in [Di P 10], we normalized the electron distribution to unity ($N = 1$) and the photon spectra are plotted against the normalized quantity $\varpi = k_-/p_-^*$. In fig. E.1 the numerical result for the final photon spectrum is shown and the solid, red line corresponds to the quantum photon spectrum taking into account RR effects, i.e., the incoherent emission of multiple photons.

By averaging the single-photon emission spectrum (see Eq. (3.16)) with respect to the initial electron distribution, we can calculate the quantum spectrum without the inclusion of RR effects. Moreover, the classical spectra without RR can be obtained in the limit of negligible photon recoil, i.e., $k_- \ll p_-$, by substituting $1 + u \approx 1$ and $u \approx k_-/p_-$ in the single-photon emission probability in eq. (3.16) multiplied by k_-. The analytical solution of $p_-(\varphi)$ in eq. (3.32) can be employed, to take into account RR effects via the LL equation in the classical spectrum. Comparing the quantum spectrum including RR effects in fig. E.1 (solid, red line) with the solid black line

[I] Note that in [Di P 10] the value of the average intensity is given instead of the peak intensity.

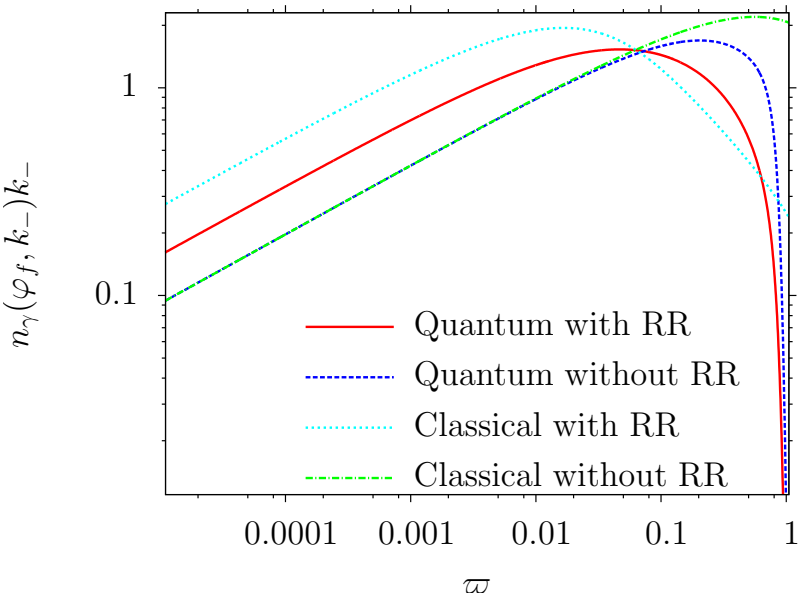

Figure E.1: Photon emission spectra: quantum spectrum with RR effects (solid, red line), quantum spectrum without RR effects (long-dashed, dark blue line), classical spectrum with RR effects (short dashed, light blue line) and classical spectrum without RR effects (dot-dashed, green line) [Neit 14].

in Fig. 2 in [Di P 10] reveals that the numerical simulations achieved by the two different approaches are in excellent agreement [Neit 14].

Bibliography

[Abra 04] M. Abraham and A. Föppl. *Theorie der Elektrizität: bd. Einführung in die Maxwellsche Theorie der Elektrizität, von A. Föppl. 2. vollständig umgearb.aufl., hrsg. von M. Abraham. Theorie der Elektrizität*, B.G. Teubner, 1904.

[Abra 64] M. Abramowitz and I. A. Stegun. *Handbook of Mathematical Functions with Formulas, Graphs, and Mathematical Tables*. Dover, New York, 1964.

[Agos 04] P. Agostini and L. F. DiMauro. "The physics of attosecond light pulses". *Rep. Prog. Phys.*, Vol. 67, No. 6, 813, 2004.

[Baie 94] V. N. Baier, V. M. Katkov, and V. M. Strakhovenko. *Electromagnetic Processes at High Energies in Oriented Single Crystals*. World Scientific, Singapore, 1994.

[Bell 08] A. R. Bell and J. G. Kirk. "Possibility of Prolific Pair Production with High-Power Lasers". *Phys. Rev. Lett.*, Vol. 101, 200403, 2008.

[Bere 82] V. Berestetskii, E. Lifshitz, and L. P. Pitaevskiĭ. *Quantum Electrodynamics. Course of theoretical physics*, 1982.

[Blac 14] T. G. Blackburn, C. P. Ridgers, J. G. Kirk, and A. R. Bell. "Quantum Radiation Reaction in LaserElectron-Beam Collisions". *Phys. Rev. Lett.*, Vol. 112, 015001, 2014.

[Boca 09] M. Boca and V. Florescu. "Nonlinear Compton scattering with a laser pulse". *Phys. Rev. A*, Vol. 80, 053403, 2009.

[Boca 10] M. Boca and V. Florescu. "The completeness of Volkov spinors". *Rom. J. Phys.*, Vol. 55, No. 5, 511, 2010.

[Boni 84] R. Bonifacio and F. Casagrande. "Instabilities and quantum initiation in the free-electron laser". *Opt. Commun.*, Vol. 50, No. 4, 251, 1984.

[Boni 85] R. Bonifacio and F. Casagrande. "Instability threshold, quantum initiation and photonstatistics in high-gain free electron lasers". *Nucl. Instrum. Methods Phys. Res., Sec. A*, Vol. 237, No. 12, 168, 1985.

[Brow 64] L. S. Brown and T. W. B. Kibble. "Interaction of Intense Laser Beams with Electrons". *Phys. Rev.*, Vol. 133, No. 3A, A705, 1964.

[Chen 11] M. Chen, A. Pukhov, T.-P. Yu, and Z.-M. Sheng. "Radiation reaction effects on ion acceleration in laser foil interaction". *Plasma Phys. Controlled Fusion*, Vol. 53, No. 1, 014004, 2011.

[Di P 08] A. Di Piazza. "Exact solution of the Landau-Lifshitz equation in a plane wave". *Lett. Math. Phys.*, Vol. 83, No. 3, 305, 2008.

[Di P 09] A. Di Piazza, K. Z. Hatsagortsyan, and C. H. Keitel. "Strong Signatures of Radiation Reaction below the Radiation-Dominated Regime". *Phys. Rev. Lett.*, Vol. 102, 254802, 2009.

[Di P 10] A. Di Piazza, K. Z. Hatsagortsyan, and C. H. Keitel. "Quantum Radiation Reaction Effects in Multiphoton Compton Scattering". *Phys. Rev. Lett.*, Vol. 105, 220403, 2010.

[Di P 12] A. Di Piazza, C. Müller, K. Z. Hatsagortsyan, and C. H. Keitel. "Extremely high-intensity laser interactions with fundamental quantum systems". *Rev. Mod. Phys.*, Vol. 84, 1177, 2012.

[Dira 28] P. A. M. Dirac. "The Quantum Theory of the Electron". *P. Roy. Soc. Lond. A Mat.*, Vol. 117, No. 778, 610, 1928.

[Elki 11] N. V. Elkina, A. M. Fedotov, I. Y. Kostyukov, M. V. Legkov, N. B. Narozhny, E. N. Nerush, and H. Ruhl. "QED cascades induced by circularly polarized laser fields". *Phys. Rev. ST Accel. Beams*, Vol. 14, 054401, 2011.

[Esar 09] E. Esarey, C. B. Schroeder, and W. P. Leemans. "Physics of laser-driven plasma-based electron accelerators". *Rev. Mod. Phys.*, Vol. 81, 1229, 2009.

[Fedo 10] A. M. Fedotov, N. B. Narozhny, G. Mourou, and G. Korn. "Limitations on the Attainable Intensity of High Power Lasers". *Phys. Rev. Lett.*, Vol. 105, 080402, 2010.

[Fran 61] P. A. Franken, A. E. Hill, C. W. Peters, and G. Weinreich. "Generation of Optical Harmonics". *Phys. Rev. Lett.*, Vol. 7, 118, 1961.

[Furr 51] W. H. Furry. "On Bound States and Scattering in Positron Theory". *Phys. Rev.*, Vol. 81, No. 1, 115, 1951.

[Gard 09] C. Gardiner. *Stochastic Methods: A Handbook for the Natural and Social Sciences. Springer Series in Synergetics*, Springer, 2009.

[Gree 14] G. Green, D. and N. Harvey, C.˙ "Transverse Spreading of Electrons in High-Intensity Laser Fields". *Phys. Rev. Lett.*, Vol. 112, 164801, 2014.

[Gupt 72] N. D. S. Gupta. "Comments on Relativistic Motion with Radiation Reaction". *Phys. Rev. D*, Vol. 5, 1546, 1972.

[Haff 00] H. Häffner, T. Beier, N. Hermanspahn, H.-J. Kluge, W. Quint, S. Stahl, J. Verdú, and G. Werth. "High-Accuracy Measurement of the Magnetic Moment Anomaly of the Electron Bound in Hydrogenlike Carbon". *Phys. Rev. Lett.*, Vol. 85, 5308, 2000.

[Hamm 10] R. T. Hammond. "Relativistic Particle Motion and Radiation Reaction in Electrodynamics". *Electron. J. Theor. Phys.*, Vol. 7, No. 23, 221, 2010.

[Hann] D. Hanneke, S. Fogwell, and G. Gabrielse. "New Measurement of the Electron Magnetic Moment and the Fine Structure Constant". *Phys. Rev. Lett.*, Vol. 100, 120801.

[Hart 10] F. Hartemann. *High-Field Electrodynamics. Pure and Applied Physics*, Taylor & Francis, 2010.

[Harv 11] C. Harvey, T. Heinzl, and M. Marklund. "Symmetry breaking from radiation reaction in ultra-intense laser fields". *Phys. Rev. D*, Vol. 84, 116005, 2011.

[Hein 13] T. Heinzl, C. Harvey, A. Ilderton, M. Marklund, S. S. Bulanov, S. Rykovanov, C. B. Schroeder, E. Esarey, and W. P. Leemans. "Detecting radiation reaction at moderate laser intensities". *ArXiv e-prints*, Oct. 2013.

[Heis 36] W. Heisenberg and H. Euler. "Consequences of Dirac Theory of the Positron". *Z. Phys.*, Vol. 98, 714, 1936.

[Herr 73] J. C. Herrera. "Relativistic Motion in a Uniform Magnetic Field". *Phys. Rev. D*, Vol. 7, 1567, 1973.

[Hu 10] H. Hu, C. Müller, and C. H. Keitel. "Complete QED Theory of Multiphoton Trident Pair Production in Strong Laser Fields". *Phys. Rev. Lett.*, Vol. 105, 080401, 2010.

[Ilde 11] A. Ilderton. "Trident Pair Production in Strong Laser Pulses". *Phys. Rev. Lett.*, Vol. 106, 020404, 2011.

[Ilde 13a] A. Ilderton and G. Torgrimsson. "Radiation reaction from QED: Light-front perturbation theory in a plane wave background". *Phys. Rev. D*, Vol. 88, 025021, 2013.

[Ilde 13b] A. Ilderton and G. Torgrimsson. "Radiation reaction in strong field QED". *Phys. Lett. B*, Vol. 725, 481, 2013.

[Jack 75] J. D. Jackson. *Classical Electrodynamics*. John Wiley & Sons, New York, 2nd Ed., 1975.

[Jeff 07] A. Jeffrey and D. Zwillinger. *Table of Integrals, Series, and Products. Table of Integrals, Series, and Products Series*, Elsevier Science, 2007.

[Kazi 11] P. O. Kazinski and M. A. Shipulya. "Asymptotics of physical solutions to the Lorentz-Dirac equation for planar motion in constant electromagnetic fields". *Phys. Rev. E*, Vol. 83, 066606, 2011.

[Khok 04] M. Khokonov. "Cascade processes of energy loss by emission of hard phonons". *Sov. Phys. JETP*, Vol. 99, No. 4, 690, 2004.

[King 13] B. King and H. Ruhl. "Trident pair production in a constant crossed field". *Phys. Rev. D*, Vol. 88, 013005, 2013.

[Koga 05] J. Koga, T. Z. Esirkepov, and S. V. Bulanov. "Nonlinear Thomson scattering in the strong radiation damping regime". *Phys. Plasmas*, Vol. 12, No. 9, 093106, 2005.

[Land 75] L. Landau and E. Lifshitz. *The Classical Theory of Fields. Course of theoretical physics*, Butterworth Heinemann, 1975.

[Leem 06] W. P. Leemans, B. Nagler, A. J. Gonsalves, C. Toth, K. Nakamura, C. G. R. Geddes, E. Esarey, C. B. Schroeder, and S. M. Hooker. "GeV electron beams from a centimetre-scale accelerator". *Nature Phys.*, Vol. 2, No. 10, 696, 2006.

[Mack 11] F. Mackenroth and A. Di Piazza. "Nonlinear Compton scattering in ultrashort laser pulses". *Phys. Rev. A*, Vol. 83, 032106, 2011.

[Maim 60] T. H. Maiman. "Stimulated optical radiation in ruby". *Nature*, Vol. 187, 493, 1960.

[Malk 12] V. Malka. "Laser plasma accelerators". *Phys. Plasmas*, Vol. 19, No. 5, 055501, 2012.

[Muls 10] P. Mulser and D. Bauer. *High Power Laser-Matter Interaction. Springer Tracts in Modern Physics*, Springer, 2010.

[Naum 09] N. Naumova, T. Schlegel, V. T. Tikhonchuk, C. Labaune, I. V. Sokolov, and G. Mourou. "Hole Boring in a DT Pellet and Fast-Ion Ignition with Ultraintense Laser Pulses". *Phys. Rev. Lett.*, Vol. 102, 025002, 2009.

[Neit 13] N. Neitz and A. Di Piazza. "Stochasticity Effects in Quantum Radiation Reaction". *Phys. Rev. Lett.*, Vol. 111, 054802, 2013.

[Neit 14] N. Neitz and A. Di Piazza. "Electron-beam dynamics in a strong laser field including quantum radiation reaction". *ArXiv e-prints*, March 2014.

[Neru 11] E. N. Nerush, I. Y. Kostyukov, A. M. Fedotov, N. B. Narozhny, N. V. Elkina, and H. Ruhl. "Laser Field Absorption in Self-Generated Electron-Positron Pair Plasma". *Phys. Rev. Lett.*, Vol. 106, 035001, 2011.

[Niki 64] A. Nikishov and V. Ritus. "Quantum processes in the field of a plane electromagnetic wave and in a constant field". *Sov. Phys. JETP*, Vol. 19, No. 2, 529, 1964.

[Niki 96] A. I. Nikishov. "The Lorentz-Dirac equation in light of quantum theory". *J. Exp. Theor. Phys.*, Vol. 83, 274, 1996.

[Nobe 65] Nobel Prize in Physics. `http://www.nobelprize.org/nobel\_prizes/physics/laureates/1965/index.html`, 1965.

[Pita 81] L. Pitaevskii and E. Lifshitz. *Physical Kinetics*. Elsevier Science, 1981.

[Prot 97] M. Protopapas, C. H. Keitel, and P. L. Knight. "Atomic physics with super-high intensity lasers". *Rep. Prog. Phys.*, Vol. 60, No. 4, 389, 1997.

[Ritu 85] V. Ritus. "Quantum effects of the interaction of elementary particles with an intense electromagnetic field". *J. Russ. Laser Res.*, Vol. 6, No. 5, 497, 1985.

[Rohr 02] F. Rohrlich. "Dynamics of a classical quasi-point charge". *Phys. Lett. A*, Vol. 303, No. 56, 307, 2002.

[Rohr 07] F. Rohrlich. *Classical Charged Particles*. World Scientific, Singapore, 2007.

[Rohr 08] F. Rohrlich. "Dynamics of a charged particle". *Phys. Rev. E*, Vol. 77, 046609, 2008.

[Saut 31a] F. Sauter. "Über das Verhalten eines Elektrons im homogenen elektrischen Feld nach der relativistischen Theorie Diracs". *Z. Phys.*, Vol. 69, No. 11, 742, 1931.

[Saut 31b] F. Sauter. "Zum 'Kleinschen Paradoxon"'. *Z. Phys.*, Vol. 73, No. 7, 547, 1931.

[Schw 51] J. Schwinger. "On Gauge Invariance and Vacuum Polarization". *Phys. Rev.*, Vol. 82, No. 5, 664, 1951.

[Seip 11] D. Seipt and B. Kämpfer. "Nonlinear Compton scattering of ultrashort intense laser pulses". *Phys. Rev. A*, Vol. 83, 022101, Feb 2011.

[Sen 71a] N. Sen Gupta. "On the motion of a charged particle in a uniform electric field with radiation reaction". *Int. J. Theor. Phys.*, Vol. 4, No. 3, 179, 1971.

[Sen 71b] N. Sen Gupta. "Synchrotron motion with radiation reaction". *Int. J. Theor. Phys.*, Vol. 4, No. 5, 389, 1971.

[Sen 73] N. Sen Gupta. "On the motion of a charged particle with radiation reaction". *Int. J. Theor. Phys.*, Vol. 8, No. 4, 301, 1973.

[Shen 70] C. S. Shen. "Synchrotron Emission at Strong Radiative Damping". *Phys. Rev. Lett.*, Vol. 24, 410, 1970.

[Soko 10] I. V. Sokolov, N. M. Naumova, J. A. Nees, and G. A. Mourou. "Pair Creation in QED-Strong Pulsed Laser Fields Interacting with Electron Beams". *Phys. Rev. Lett.*, Vol. 105, 195005, 2010.

[Spoh 00] H. Spohn. "The critical manifold of the Lorentz-Dirac equation". *Europhys. Lett.*, Vol. 50, No. 3, 287, 2000.

[Spoh 04] H. Spohn. *Dynamics of Charged Particles and their Radiation Field*. Cambridge University Press, Cambridge, 2004.

[Stri 85] D. Strickland and G. Mourou. "Compression of amplified chirped optical pulses". *Opt. Comm.*, Vol. 56, No. 3, 219, 1985.

[Stur 11] S. Sturm, A. Wagner, B. Schabinger, J. Zatorski, Z. Harman, W. Quint, G. Werth, C. H. Keitel, and K. Blaum. "g Factor of Hydrogenlike $^{28}Si^{13+}$". *Phys. Rev. Lett.*, Vol. 107, 023002, 2011.

[Stur 14] S. Sturm, F. Khler, J. Zatorski, A. Wagner, Z. Harman, *et al.* "High-precision measurement of the atomic mass of the electron". *Nature*, Vol. 506, No. 7489, 467, 2014.

[Tamb 10] M. Tamburini, F. Pegoraro, A. Di Piazza, C. H. Keitel, and A. Macchi. "Radiation reaction effects on radiation pressure acceleration". *New J. Phys.*, Vol. 12, No. 12, 123005, 2010.

[Tamb 11] M. Tamburini, F. Pegoraro, A. D. Piazza, C. Keitel, T. Liseykina, and A. Macchi. "Radiation reaction effects on electron nonlinear dynamics and ion acceleration in lasersolid interaction". *Nucl. Instrum. Meth. A*, Vol. 653, No. 1, 181, 2011.

[Tamb 14] M. Tamburini, C. H. Keitel, and A. D. Piazza. "Electron dynamics controlled via self-interaction". *Phys. Rev. E*, Vol. 89, 021201, 2014.

[Thom 12] A. G. R. Thomas, C. P. Ridgers, S. S. Bulanov, B. J. Griffin, and S. P. D. Mangles. "Strong Radiation-Damping Effects in a Gamma-Ray Source Generated by the Interaction of a High-Intensity Laser with a Wakefield-Accelerated Electron Beam". *Phys. Rev. X*, Vol. 2, 041004, 2012.

[Vask 05] F. T. Vasko and O. E. Raichev. *Quantum Kinetic Theory and Applications.* Springer, 2005.

[Verd 04] J. Verdú, S. Djekić, S. Stahl, T. Valenzuela, M. Vogel, G. Werth, T. Beier, H.-J. Kluge, and W. Quint. "Electronic g Factor of Hydrogenlike Oxygen $^{16}O^{7+}$". *Phys. Rev. Lett.*, Vol. 92, 093002, 2004.

[Volk 35] D. Volkov. "Class of solutions of Dirac's equation". *Z. Phys.*, Vol. 94, No. 3, 250, 1935.

[Wang 13] X. Wang, R. Zgadzaj, N. Fazel, Z. Li, S. A. Yi, X. Zhang, W. Henderson, Y. Y. Chang, R. Korzekwa, H. E. Tsai, C. H. Pai, H. Quevedo, G. Dyer, E. Gaul, M. Martinez, A. C. Bernstein, T. Borger, M. Spinks, M. Donovan, V. Khudik, G. Shvets, T. Ditmire, and M. C. Downer. "Quasi-monoenergetic laser-plasma acceleration of electrons to 2 GeV". *Nat. Commun.*, Vol. 4, 2013.

[Wint 08] C. Winterfeldt, C. Spielmann, and G. Gerber. "Colloquium: Optimal control of high-harmonic generation". *Rev. Mod. Phys.*, Vol. 80, 117, 2008.

[Yano 08] V. Yanovsky, V. Chvykov, G. Kalinchenko, P. Rousseau, T. Planchon, T. Matsuoka, A. Maksimchuk, J. Nees, G. Cheriaux, G. Mourou, and K. Krushelnick. "Ultra-high intensity- 300-TW laser at 0.1 Hz repetition rate". *Opt. Express*, Vol. 16, No. 3, 2109, 2008.

[Zako 05] S. Zakowicz. "Square-integrable wave packets from the Volkov solutions". *J. Math. Phys.*, Vol. 46, No. 3, 2005.

[Zhid 02] A. Zhidkov, J. Koga, A. Sasaki, and M. Uesaka. "Radiation Damping Effects on the Interaction of Ultraintense Laser Pulses with an Overdense Plasma". *Phys. Rev. Lett.*, Vol. 88, 185002, 2002.

Acknowledgements

At the end of this work, I would like to say thanks to the many people that helped me throughout the last years making this work possible.

First of all, I am deeply indebted to my supervisor PD Antonino Di Piazza, without whom this thesis would not exist. He did not only provide his profound physical insights in countless discussions, but also encouraged me not to capitulate in the face of seemingly unsurmountable difficulties.

Moreover, I want to thank Prof. Christoph H. Keitel for giving me the opportunity to be a PhD student in his theory division. This allowed me to work with excellent physicists from all over the world.

To Prof. Joerg Jaeckel I am grateful for writing the second review for this thesis.

I had the great pleasure to have many fruitful discussion with my coworkers as well as scientists from other institutes. Therefore, I thank amongst others Felix Mackenroth, Sebastian Meuren, Matteo Tamburini, Naveen Kumar, Jörg Evers, John Kirk, Tom Blackburn, and Gianluca Sarri.

A special thanks goes to the proofreaders, whose remarks helped me to improve the manuscript significantly: Felix Mackenroth, Sarah Müller, Stefano Cavaletto, and Naveen Kumar.

For the creation of a great working environment, I want to thank my current and former office mates, namely Huayu Hu, Qurrat-ul-Ain Gulfam, Sarah Müller, Omri Har-Shemesh, Fernando Oster, Stefano Cavaletto, Sebastian Meuren, Oleg Skoromnik, Nikolay Belov, Ekaterina Berseneva, Fabian Lauble, Sebastian Lautz, Johannes Dombrowsky, and Robin Weis.

To all my roommates, but especially to Cosima Lawall, I want to say thank you for making my time in Heidelberg so delightful and for cheering me up again, whenever I was in a bad mood.

Finally, I want to thank all my friends and my family for supporting me not only in the last years, but also from the very beginning.